

The Role of Germicidal Ultraviolet Light in the Formation of Secondary Organic Aerosols

by

Eureka Choi

A thesis

presented to the University Of Waterloo

in fulfilment of the

thesis requirement for the degree of

Master of Applied Science

in

Chemical Engineering

Waterloo, Ontario, Canada, 2017

© Eureka Choi 2017

Author's Declaration

I hereby declare that I am the sole author of this thesis. This is a true copy of the thesis, including any required final revisions, as accepted by my examiners.

I understand that my thesis may be made electronically available to the public.

Abstract

Ultraviolet (UV) light with a wavelength of 254 nm has proven to be effective at inactivating microorganisms, and thus has been increasingly employed as a method of disinfection of indoor environments. UV light with wavelengths of over 300 nm is known to promote the formation of secondary organic aerosol (SOA) particles. The portion of UV light produced by the sun that penetrates into the Earth's atmosphere has wavelengths of over 300 nm, and is observed to promote SOA formation within the Earth's atmosphere. The majority of SOA particles can be classified as fine particulate matter, or particles with diameters of 2.5 μm or smaller. The particles of fine particulate matter are of particular concern for human health, as they are associated with enhancing infectious diseases, causing allergic effects, and promoting respiratory and cardiovascular conditions.

Germicidal UV treatment, using UV light with a wavelength of 254 nm, is commonly used for the purpose of improving air quality and reducing the transmission of infectious microorganisms. Thus, it is often used in environments such as hospitals, where there are individuals with weaker or compromised immune systems, and thus more susceptible to a variety of negative health effects. As such, these individuals would also be at higher risk for the health effects associated with exposure to fine particulate matter. Therefore, it is of importance to determine if the use of germicidal UV treatment in indoor environments will promote significant SOA formation.

SOA particles are formed as a result of gas phase oxidation of volatile organic compounds (VOCs), and various types of VOCs are commonly found in almost all indoor environments. In this work, toluene was selected as the representative VOC to be tested. In the experiments, mixtures of air and toluene were exposed to 254 nm UV light, varying the conditions of the air, the amounts of toluene added, the duration of UV exposure, and the duration of post-UV recirculation. The amount of particles formed in the fine particulate matter size range were measured for each experiment. Significant levels of particle formation were observed for UV exposure periods of as short as 5 minutes. The particle formation levels ranged from 2.383 particles/cm³ for 5 minutes of UV exposure, to 1449.76 particles/cm³ for 15 minutes of UV exposure. Particle formation was found to increase with increasing concentrations of gas phase

toluene, as well as increasing durations of UV irradiation. Higher levels of relative humidity also resulted in increased particle formation and growth. However, the amount of recirculation time after UV exposure did not appear to have a significant effect on the level of particle formation. The initial amount of ambient particles present prior to UV exposure varied from 3.781 particles/cm³ to 27.082 particles/cm³, and was found to correlate positively with the relative humidity of the air. Variations in the initial amount of particles present over this range did not have an effect on the amount of particle formation. Overall, in this work, it was determined that exposure of toluene to 254 nm germicidal UV light does result in SOA particle formation.

Acknowledgements

I would like to thank my supervisor Professor William Anderson for suggesting the topic of this project, as well as for all his help and support throughout this project.

I would also like to thank my co-supervisor Professor Zhongchao Tan for his support and for the use of his equipment in the work done.

In addition, I would like to express my gratitude to Dr. Carol Moralejo for training me on the use of the lab equipment, as well as her assistance and input on various aspects of this project.

I am also grateful for Professor Xianshe Feng for acting as a reader, and reviewing my thesis.

As well, I would like to recognize the Ontario Graduate Scholarship (OGS) for their financial support.

Most of all, I would like to thank everyone who supported me through the duration of this project.

Dedication

This thesis is dedicated to all my friends and family who helped and supported me through this journey to make a dream come true.

Especially to Nyx, for being there every step of the way.

Table of Contents

Author's Declaration	ii
Abstract.....	iii
Acknowledgements	v
Dedication	vi
Table of Contents	vii
List of Figures	x
List of Tables.....	xiii
List of Abbreviations	xv
Chapter 1 – Introduction.....	1
1.1 Objective.....	4
1.2 Hypothesis	5
Chapter 2 - Background	6
2.1 Germicidal UV.....	6
2.2 Volatile Organic Compounds.....	13
2.2.1 VOC UV Absorbance.....	17
2.3 Secondary Organic Aerosols	21
2.3.1 SOA Formation from Toluene.....	25
2.4 Photocatalytic Oxidation.....	27
2.5 Related Existing Work.....	28
Chapter 3 - Equipment	31
3.1 Experimental Setup.....	31
3.2 Gas Chromatography	37
3.3 Aerosol Particle Sizer.....	38
3.4 Data Analysis Software	40
Chapter 4 - Methods and Experiments	41
4.1 Experimental Conditions	41
4.1.1 Parameters Tested.....	41
4.1.2 Other System Variables.....	44
4.2 Experimental Procedure.....	47
4.2.1 Gas Chromatography Calibration	47

4.2.2 UV Irradiation Experiments	47
4.2.3 Unfiltered Air Experiments	51
4.2.4 Room Air Experiments.....	51
4.2.5 Above-door Germicidal UV System Experiment	52
Chapter 5 - Results and Discussion	53
5.1 Complete Degradation Experiment.....	53
5.2 Controls	55
5.2.1 UV Light	55
5.2.2 Toluene	56
5.3 Minimal Exposure Experiment	57
5.3.1 Constant Recirculation Time	57
5.3.2 Constant Total Time	59
5.4 Factorial Experiment.....	61
5.4.1 Statistical Analysis	65
5.5 Unfiltered Air Experiment.....	68
5.6 Room Air Experiments.....	71
5.7 Replicate Experiments.....	77
5.8 Toluene Mass Balance	80
5.9 Comparison of Results	82
Chapter 6 - Extended Experiments.....	87
6.1 Above-door Germicidal UV System Experiment	87
6.2 185 nm UV with Ozone	89
6.3 Other VOCs.....	91
Chapter 7 – Conclusions and Recommendations.....	96
7.1 Conclusions.....	96
7.2 Recommendations.....	97
7.1.1 Smaller Size Fraction	97
7.1.2 Expanding on Variables	97
7.1.3 Other VOCs.....	98
7.1.4 Particle Composition	98
7.1.5 Modelling SOA Particle Formation and Growth.....	99

References	100
Appendices	105
Appendix A: Data Sets and Graphs	105
A-1 Minimal Exposure Experiments	105
A-2 Factorial Experiment	109
A-3 Unfiltered Air Experiment	121
A-4 Room Air Experiments	122
A-5 Toluene Mass Balances	126
Appendix B: Supplemental Information	128
B-1 VOC Concentrations in Indoor Environments.....	128
B-2 UV Irradiance Rate in Reactor Calculation.....	132

List of Figures

Figure 1: Absorption spectrum for toluene; the second graph shown is a selected portion of the first graph, focusing on the area around 254 nm (Data from Serralheiro et al. (2015)).....	19
Figure 2: Mechanism of UV photooxidation of VOCs, where R is the portion of the compound structure not involved in this reaction mechanism (Xue et al., 2013).....	22
Figure 3: Proposed SOA formation mechanism from toluene, where X represents non-particle products from all gas phase loss.....	26
Figure 4: Diagram of experimental setup.....	31
Figure 5: Front view photo of experimental setup.....	32
Figure 6: Side view photos of experimental setup.....	33
Figure 7: Diagram of reactor vessel.....	34
Figure 8: Photo of APS attached to reactor vessel.....	35
Figure 9: TSI 3321 aerosol particle sizer.....	38
Figure 10: Graph of gas phase concentrations of toluene at varying liquid additions.....	42
Figure 11: Vessel temperature profile taken from vessel sample port.....	45
Figure 12: Temperature profile at vessel exit port.....	46
Figure 13: Particle size distribution for complete degradation experiment of toluene.....	54
Figure 14: Particle size distribution for blank experiment with no toluene.....	55
Figure 15: Fine particulate matter formation vs. UV exposure time in minimal exposure experiments with constant recirculation time.....	57
Figure 16: Particle size distribution for minimal exposure experiment with constant post-UV recirculation, with 5 minutes of UV exposure and 5 minutes of post-UV recirculation.....	58
Figure 17: Fine particulate matter formation vs. UV exposure time in minimal exposure experiments with constant total time.....	59
Figure 18: Particle size distribution for minimal exposure experiment with constant post-UV recirculation, with 5 minutes of UV exposure and 1 minute of post-UV recirculation.....	60
Figure 19: Particle size distribution for the factorial experiment with the lowest fine particulate matter formation (55-85 ng/mL toluene, 5 minutes UV, 15 minutes recirculation).....	64
Figure 20: Particle size distribution for the factorial experiment with the lowest fine particulate matter formation (100-125 ng/mL toluene, 15 minutes UV, 1 minute recirculation).....	64
Figure 21: Initial toluene concentration vs. initial fine particulate matter concentration for compressed air experiments.....	68
Figure 22: UV exposure time vs. fine particulate matter formation for compressed air experiments.....	69
Figure 23: Particle increase for filtered and unfiltered compressed air experiments with 55-85 ng/mL toluene, 5 minutes UV exposure, 1 minute post-UV recirculation.....	70
Figure 24: Initial fine particulate matter levels for unfiltered and filtered room air experiments.....	72
Figure 25: Fine particulate matter production for unfiltered and filtered room air experiments.....	73
Figure 26: Particle increase values for unfiltered room air experiments.....	74
Figure 27: Particle increase values for filtered room air experiments.....	75

Figure 28: Comparison of particle increase values between unfiltered and filtered room air experiments.....	76
Figure 29: Initial fine particulate matter concentration vs fine particulate matter formation for replicate experiments.....	78
Figure 30: Initial toluene concentration vs fine particulate matter formation for replicate experiments.....	78
Figure 31: Comparison of particle increase in for filtered and unfiltered experiments using compressed and room air	84
Figure 32: Particle size distribution for above-door UV system experiment	87
Figure 33: Particle size distribution for toluene degradation under 185 nm ozone-producing UV	90
Figure 34: Absorption spectrum for toluene (Data from Serralheiro et al. (2015))	92
Figure 35: Absorption spectrum for limonene (Data from Smialek et al. (2012))	92
Figure 36: Toluene particle size distribution (Experiment 2).....	94
Figure 37: Limonene particle size distribution (Experiment 2)	95
Figure A-1: 55-85 ng/mL toluene, 1 minute UV irradiation, 5 minutes post-UV recirculation ..	106
Figure A-2: 55-85 ng/mL toluene, 2 minutes UV irradiation, 5 minutes post-UV recirculation.	106
Figure A-3: 55-85 ng/mL toluene, 3 minutes UV irradiation, 5 minutes post-UV recirculation.	107
Figure A-4: 55-85 ng/mL toluene, 4 minutes UV irradiation, 5 minutes post-UV recirculation.	107
Figure A-5: 55-85 ng/mL toluene, 5 minutes UV irradiation, 1 minute post-UV recirculation ..	110
Figure A-6: 55-85 ng/mL toluene, 5 minutes UV irradiation, 5 minutes post-UV recirculation.	110
Figure A-7: 55-85 ng/mL toluene, 5 minutes UV irradiation, 15 minutes post-UV recirculation	111
Figure A-8: 55-85 ng/mL toluene, 10 minutes UV irradiation, 1 minute post-UV recirculation.	111
Figure A-9: 55-85 ng/mL toluene, 10 minutes UV irradiation, 5 minutes post-UV recirculation (Experiment 1)	112
Figure A-10: 55-85 ng/mL toluene, 10 minutes UV irradiation, 5 minutes post-UV recirculation (Experiment 2)	112
Figure A-11: 55-85 ng/mL toluene, 10 minutes UV irradiation, 5 minutes post-UV recirculation (Experiment 3)	113
Figure A-12: 55-85 ng/mL toluene, 10 minutes UV irradiation, 15 minutes post-UV recirculation	113
Figure A-13: 55-85 ng/mL toluene, 15 minutes UV irradiation, 1 minute post-UV recirculation	114
Figure A-14: 55-85 ng/mL toluene, 15 minutes UV irradiation, 5 minutes post-UV recirculation	114
Figure A-15: 55-85 ng/mL toluene, 15 minutes UV irradiation, 15 minutes post-UV recirculation	115

Figure A-16: 100-125 ng/mL toluene, 5 minutes UV irradiation, 1 minute post-UV recirculation	115
Figure A-17: 100-125 ng/mL toluene, 5 minutes UV irradiation, 5 minutes post-UV recirculation	116
Figure A-18: 100-125 ng/mL toluene, 5 minutes UV irradiation, 15 minutes post-UV recirculation	116
Figure A-19: 100-125 ng/mL toluene, 10 minutes UV irradiation, 1 minute post-UV recirculation	117
Figure A-20: 100-125 ng/mL toluene, 10 minutes UV irradiation, 5 minutes post-UV recirculation	117
Figure A-21: 100-125 ng/mL toluene, 10 minutes UV irradiation, 15 minutes post-UV recirculation	118
Figure A-22: 100-125 ng/mL toluene, 15 minutes UV irradiation, 1 minute post-UV recirculation	118
Figure A-23: 100-125 ng/mL toluene, 15 minutes UV irradiation, 5 minutes post-UV recirculation	119
Figure A-24: 100-125 ng/mL toluene, 15 minutes UV irradiation, 15 minutes post-UV recirculation	119
Figure A-25: Unfiltered compressed air, 55-85 ng/mL toluene, 5 minutes UV irradiation, 1 minute post-UV recirculation.....	121
Figure A-26: Filtered room air, 15.9% RH, 55-85 ng/mL toluene, 5 minutes UV irradiation, 1 minute post-UV recirculation.....	122
Figure A-27: Filtered room air, 16.0% RH, 55-85 ng/mL toluene, 5 minutes UV irradiation, 1 minute post-UV recirculation.....	123
Figure A-28: Filtered room air, 43.2% RH, 55-85 ng/mL toluene, 5 minutes UV irradiation, 1 minute post-UV recirculation.....	123
Figure A-29: Filtered room air, 22.7% RH, 55-85 ng/mL toluene, 5 minutes UV irradiation, 1 minute post-UV recirculation.....	124
Figure A-30: Unfiltered room air, 23.8% RH, 55-85 ng/mL toluene, 5 minutes UV irradiation, 1 minute post-UV recirculation.....	124
Figure A-31: Unfiltered room air, 33.4% RH, 55-85 ng/mL toluene, 5 minutes UV irradiation, 1 minute post-UV recirculation.....	125
Figure A-32: Unfiltered room air, 18.6% RH, 55-85 ng/mL toluene, 5 minutes UV irradiation, 1 minute post-UV recirculation.....	125

List of Tables

Table 1: Irradiance levels in germicidal UV setups	9
Table 2: UV dosages required for inactivation of microorganisms	10
Table 3: Possible indoor VOCs and their sources (Huang et al., 2016).....	14
Table 4: Indoor VOC compound concentrations as reported by Cometto-Muñiz and Abraham (2015).....	15
Table 5: Concentrations of some common indoor VOCs, obtained from Salonen et al. (2009), and Cometto-Muñiz and Abraham (2015)	16
Table 6: Comparison of SOA formation experiments in literature	29
Table 7: GC Specifications.....	37
Table 8: Gas phase concentrations of toluene at varying liquid additions	42
Table 9: Gas chromatography calibration sequence.....	47
Table 10: Variations of the experimental procedure	50
Table 11: Complete degradation experiment data	53
Table 12: Results of t-test for air blank and air blank with toluene samples	56
Table 13: Summary of levels of factors in factorial experiment.....	61
Table 14: Fine particulate matter production in factorial experiments	62
Table 15: Comparison of specifications of select factorial experiments	63
Table 16: Design of experiment ANOVA analysis in Statistica 11	66
Table 17: Factorial ANOVA analysis in Statistica 11	67
Table 18: Analysis of replicate experiments	77
Table 19: Toluene mass balances.....	80
Table 20: Comparison of particle formation in experiments using compressed air from the building supply	82
Table 21: Comparison of particle formation in for filtered and unfiltered experiments using compressed and room air	84
Table 22: Specification for toluene degradation experiment with 185 nm ozone-producing lamp	89
Table 23: Comparison of properties of toluene and limonene	91
Table 24: Comparison of long exposure experiment results for toluene and limonene	93
Table A-1: Fine particulate matter formation in minimal exposure experiment with constant recirculation time	105
Table A-2: Fine particulate matter Formation in minimal exposure experiment with constant total time.....	105
Table A-3: Data for analysis of significant particle formation.....	108
Table A-4: Data set for factorial experiments.....	109
Table A-5: Data for Analysis in Statistica 11	120

Table A-6: Initial toluene concentration and initial fine particulate matter levels for compressed air experiments	121
Table A-7: Data for Room Air Experiments	122
Table A-8: Data for toluene mass balances.....	126
Table A-9: Statistics of VOC concentrations in home or school environments (Cometto-Muñiz and Abraham, 2015).....	128
Table A-10: Statistics of VOC concentrations in commercial environments (Cometto-Muñiz and Abraham, 2015)	130
Table A-11: Overview of calculations of UV irradiance in reactor	132
Table A-12: Calculations for UV irradiance in reactor.....	132

List of Abbreviations

ANOVA	Analysis of variance
APS	Aerosol particle sizer
BVDV	Bovine viral diarrhea virus
DOE	Design of experiment
GC	Gas chromatography
OH	Hydroxyl (radical)
RH	Relative humidity
SOA	Secondary organic aerosol
UV	Ultraviolet
VOC	Volatile organic compound

Chapter 1 – Introduction

In recent years, ultraviolet (UV) light has been increasingly used for disinfection of indoor environments. UV light with a wavelength of 254 nm has been shown to be effective at inactivating microorganisms, such as bacteria and viruses (Katara et al., 2008) (Lau et al., 2008). However, UV light with wavelengths of over 300 nm are also known to promote the formation of aerosol particles (Presto et al., 2005) (Kroll et al., 2006), which can cause or enhance negative health effects in humans (Poschl, 2005) (Hallaquist et al., 2009) (Wolkoff, 2012). Thus, it is plausible that irradiation using germicidal UV light with a wavelength of 254 nm may also promote the formation of aerosol particles.

A significant portion of all atmospheric aerosol particles are secondary organic aerosols (SOAs). SOAs are formed as a result of oxidation reactions when volatile organic compounds (VOCs) react to produce products of lower volatility (Hallaquist et al., 2009) (Ng, et al., 2007). These lower volatility products are more likely to condense to form aerosol particles (Hallaquist et al., 2009). There are a vast number of types of VOCs found in the both the atmosphere, as well as in indoor environments. Each type of VOC has the potential to undergo a number of different reaction pathways, depending on the conditions. Each of these reaction pathways will produce a different distribution of products. The degree to which any particular oxidation product contributes to SOA formation depends on the equilibrium established between the gas and particle phases for that compound at the given conditions (Kroll and Seinfeld, 2008). This means that some oxidation products will contribute more significantly to the formation of SOAs than others, while some may not contribute at all (Hallaquist et al., 2009). Since there are many different types of VOCs and possible products, all of which contribute differently to SOA formation, there are many factors that need to be considered in determining the extent and rate of formation of SOAs (Kroll and Seinfeld, 2008).

Of particular concern with regards to particle formation is fine particulate matter, or particles with diameters of 2.5 μm and smaller. With recent research, it has become increasingly evident that fine particulate matter has negative health impacts on humans. This includes the potential to

enhance infectious or allergic conditions, as well as cause damaging respiratory and cardiovascular diseases (Poschl, 2005) (Hallaquist et al., 2009) (Wolkoff, 2012). Disinfection using germicidal UV light is often used in sensitive environments, such as hospitals and other healthcare buildings (Katara et al., 2008). In these environments, there is a greater chance for people at higher risk for detrimental effects to be exposed to any aerosol particles that may form, and thus be more seriously affected by the related health effects. Consequently, it is important to establish how UV light with a wavelength of 254 nm will contribute to the production of fine particulate matter.

In existing research, it has been shown that UV light produced by the sun, with wavelengths of 300 nm and longer, plays a significant role in atmospheric formation of SOA particles. Although the sun also produces UV light with shorter wavelengths, the shorter wavelengths are not able to penetrate Earth's ozone layer to reach the lower atmosphere. In the atmosphere, the 300+ nm UV light promotes the formation of hydroxyl (OH) radicals through the photolytic reaction of other compounds present in the system, such as ozone or nitrous acid (Presto et al., 2005) (Kroll et al., 2006). These OH radicals react readily with VOCs, causing an increase in oxidation reactions compared to conditions without UV light (Kroll et al., 2005). These oxidation reactions then proceed to form the lower volatility products, some of which will condense to form SOA (Hallaquist et al., 2009). However, existing research has not determined whether the particle formation mechanism observed in the atmosphere is also relevant in UV-treated indoor environments. Germicidal UV light has a wavelength of 254 nm, shorter than the 300+ nm UV sunlight that promotes atmospheric SOA formation. While the mechanism through which 300+ nm UV light produced by the sun contributes to SOA formation is understood, there are uncertainties as to how 254 nm UV light compares.

The culmination of this research will determine whether SOA formation can occur when germicidal UV light is used for indoor disinfection. This knowledge can be applied to future work to determine if any additional air quality control measures are required in conjunction with UV light disinfection. In addition, the particle size distribution will be known, which will aid in determining what type of air quality control would be best suited for eliminating the sizes of

particles that would be present. Overall, this knowledge will aid in minimizing any unnecessary detrimental health effects resulting from the use of germicidal UV treatment.

1.1 Objective

The aim of this project was to investigate the amount of SOA formation with respect to a number of variables. These variables included the initial VOC concentrations, conditions of the air, duration of UV exposure, and duration of post-UV recirculation. Since there is such a wide variety of types of VOCs that may be found in indoor environments, these experiments focussed on a single type of VOC, and developed an understanding of how particle formation varied under different conditions. This knowledge was then later expanded by testing other types of VOCs with different properties, and comparing the SOA formation results. The experiments were performed in a closed chamber environment, allowing for control and measurement of the variables of interest, such as the concentration of VOC present in the gas phase, and the particle size distribution in the gas. In addition, samples were taken from the chamber throughout the duration of each experiment, which allowed for the observation of any changes that occurred over time. The goal was to analyze the particle size distributions that resulted from germicidal UV irradiation under different sets of conditions, in order to determine the extent of SOA formation. Comparison of the change in VOC levels and particle size distribution over varying conditions allowed for the determination of how UV light and other ambient factors affected SOA formation from the particular VOC tested.

The following are the objectives of this work:

1. To determine if SOA particles are formed upon exposure of gas phase VOCs to 254 nm UV light.
2. To determine the effects of the initial VOC concentrations, duration of UV exposure, and duration of post-UV recirculation on the amount of particle formation observed.
3. To determine if variations in the initial amount of ambient particles present and relative humidity of the air affect the amount of particle formation observed.

1.2 Hypothesis

Indoor air UV treatment systems use germicidal UV light with a wavelength of 254 nm, which has been thoroughly studied for its germicidal properties, but less so for possible related particle formation. The UV light produced by the sun that penetrates into Earth's atmosphere has wavelengths of around 300 nm and greater, and is known to promote SOA formation in the atmosphere through the photooxidation of VOCs. Since germicidal UV has a similar wavelength to the atmospheric sunlight known to promote VOC formation, it is plausible that it will react with VOCs by similar mechanisms. Therefore, it is hypothesized that the use of germicidal UV light to treat indoor air will promote SOA formation from VOCs present in the environment.

Chapter 2 - Background

2.1 Germicidal UV

Treatment of indoor air using UV light is a common engineering control for the reduction of transmission of airborne infectious agents (Kujundzic et al., 2007). Certain wavelengths of UV light are capable of disinfecting air by inactivating the microorganisms that may be present (Ke et al., 2009) (Lim and Blatchley III, 2009) (Dumyahn and First, 1999). The wavelengths of UV light typically employed for inactivation of microorganisms range from 200-320 nm (Kowalski, 2009). Work as early as studies in 1936 by Wells, and 1938 by Sharp have investigated the use of germicidal UV lamps for the purpose of inactivation of microorganisms. Since then, it has been determined that germicidal UV is effective at inactivating a wide range of pathogens, including both bacteria and viruses (Lim and Blatchley III, 2009) (Daryany et al., 2009). This includes the ability to inactivate one of the most resilient enveloped viruses, the bovine viral diarrhea virus (Daryany et al., 2009).

Germicidal UV encompasses a range of wavelengths of UV light due to the fact that different wavelengths act on different parts of the microorganisms. Absorbance of UV light induces photobiochemical changes in the various parts of bacterial cells, causing the cell to become inactivated (Lim and Blatchley III, 2009). For example, nucleic acids are most significantly degraded by UV-C, with wavelengths ranging from 100-280 nm, while proteins most significantly break down due to absorption of UV light with wavelengths longer than 300 nm (Daryany et al., 2009) (Kowalski, 2009). Degradation of the genetic material, in the form of nucleic acids, is the most effective method of ensuring microbial inactivation. Although the exact wavelength that is most effective for inactivation varies slightly between different types and species of microorganisms, wavelengths that are similar are still effective at inactivation (Kowalski, 2009). Thus, the most common form of germicidal UV light used has a wavelength of 254 nm, which is part of the spectrum effective at degrading genetic material in essentially all microorganisms (Lim and Blatchley III, 2009). In this work, germicidal UV will refer to UV light with a wavelength of 254 nm, as this is the wavelength that germicidal UV systems typically employ.

Disinfection of indoor air using germicidal UV has been widely accepted as an effective method of indoor air quality control, and is commonly recommended as an engineering control of reduction of airborne disease transmission (Dumyahn and First, 1999) (Ke et al., 2009) (Kujundzic et al., 2007). It is most commonly used in environments where there is a high risk of disease transmission, especially from undiagnosed but potentially infectious individuals, such as hospital waiting areas, emergency rooms, and jails (Dumyahn and First, 1999). Germicidal UV is also commonly used to treat higher traffic confined spaces with shared air, such as airplane cabins and classrooms (Lim and Blatchley III, 2009). UV air treatment systems can be designed to work effectively in a wide variety of indoor environments. There also exist portable modular systems, as well as smaller non-specific systems commercially available for purchase. Most UV air treatment systems consist of low-pressure mercury vapour lamps that emit UV radiation at a wavelength of 254 nm (Kujundzic et al., 2007) (Kowalski, 2009).

UV treatment systems for larger rooms and buildings are most commonly installed in either the ventilation air ducts, or in the upper air portion of the room. Different types of environments may be better suited to a particular type of system, or it may not be feasible to install a specific type of system in a given environment (Kowalski, 2009). Thus, there are a number of factors that need to be considered in selecting a germicidal UV treatment system for any particular environment.

Upper air UV systems are installed in the upper portions of the room, above eye level. They usually consist of multiple lamps installed on the upper walls or ceiling. Since these systems are installed in the occupied area of the room, there is the risk of UV exposure to people in the room. Sometimes, these types of systems will use louvers to direct the light and minimize exposure to the occupants (Kowalski, 2009). In order to further minimize the exposure of any room occupants to UV light, UV-absorbing paints may be used on the wall or ceiling (Kowalski, 2009). In addition, UV treatments can be scheduled for times when the room is vacant. Upper air systems are typically more cost effective than in-duct systems, however they may be less ideal for use in some highly occupied spaces due to the possibility of UV exposure (Kowalski, 2009) (Dumyahn and First, 1999) (Lim and Blatchley III, 2009).

More commonly, UV systems can be installed in the ventilation air ducts of the building (Dumyahn and First, 1999) (Lim and Blatchley III, 2009). This allows for increased irradiance and circulation of the treated air, resulting in improved rates of microbial inactivation. In addition, this type of system can also be used while the room is occupied without fear of UV exposure (Kujundzic et al., 2007). Most in-duct germicidal UV systems are designed to be effective with the typical duct air velocity of 2-3 m/s in most building air systems (Kowalski, 2009). Additionally, there are a number of other design considerations that can be implemented to increase the amount of UV dosage that the air passing through receives. Some in-duct systems utilize recirculation in order to dose the air multiple times, or the ductwork can be constructed of reflective material, such as polished aluminum, to increase irradiance (Kowalski, 2009). In-duct systems are often designed specifically for each room or building, in order to account for the size and shape of the room, and ensure that the air being is sufficiently treated.

It has been determined that the degree of microbial inactivation depends on the UV dosage received by the microorganisms. In addition, higher levels of UV dosage also result in increased rates of VOC degradation (Shen and Yu, 1999). In order to evaluate the effectiveness of UV systems that have setups using different exposure times, lamps with different wattage, or varying lamp orientation in the room, measurements of UV irradiance and dosage can be used. UV irradiance is a measure of the flux of UV radiant energy an area is exposed, and UV dosage is the total amount of UV radiant energy an area is exposed to over a certain period of time. With the irradiance level measured, the UV dosage can be determined for any amount of exposure time employed with the following equation:

$$UV \text{ dosage } \left[\frac{mJ}{cm^2} \right] = Irradiance \left[\frac{mW}{cm^2} \right] \times time [s]$$

Table 1 below shows a comparison of the irradiance levels of some different germicidal UV systems.

Table 1: Irradiance levels in germicidal UV setups

Setup	Irradiance (mW/cm ²)
Pilot-scale chamber <ul style="list-style-type: none"> • 0.93 m x 0.93 m x 0.93 m (0.8 m³) • 4 UV lamps in corners • full chamber irradiation 	0.0098 - 0.0114
Upper-air UV in room <ul style="list-style-type: none"> • 87 m³ • 5 UV lamps; 4 in corners, 1 in centre • upper air irradiation 	0.025 – 0.027
Above-door UV in room <ul style="list-style-type: none"> • approximately 7.5 m³ floor space • hospital patient bathroom • 1 lamp • full room irradiation 	0.013 – 0.108
In-duct UV <ul style="list-style-type: none"> • 0.6 m x 0.6 m duct • single lamp • length of 0.5 m 	0.73

Note: Irradiance levels for the pilot-scale chamber, upper-air UV, and in-duct UV obtained from Kujundzic et al. (2007), irradiance levels for above-door UV obtained from Hunt and Anderson (2016)

As seen in Table 1, the irradiance level for the in-duct UV system is much higher than those of all the room systems. Since the in-duct system treats flowing air, the air has a much shorter exposure time compared to in a room system. The higher irradiance level over a shorter period of time allows the air being treated by the in-duct system to receive an adequate UV dose, comparable to those delivered by the room systems. The UV dosages and equivalent exposure time requirements for inactivation for a number of different types of airborne microorganisms are shown below in Table 2.

Table 2: UV dosages required for inactivation of microorganisms

Microorganism	Log reduction	UV dosage required ($\mu\text{J}/\text{cm}^2$)	Time required at 0.013 mW/cm ² (secs)
Bacteria	1	600	0.046
<i>Bacillus subtilis</i>	1	1400	0.108
<i>Escherichia coli</i>	1	200-1500	0.015-0.115
	2	1017-2356	0.078-0.181
<i>Mycobacterium tuberculosis</i>	1	500	0.038
<i>Pseudomonas aeruginosa</i>	1	400	0.031
<i>Serratia indica</i>	1	20900	1.608
<i>Staphylococcus aureus</i>	1	200-2000	0.015-0.154
Bacterial spores	1	9000	0.692
<i>Bacillus subtilis</i>	1	8500-14900	0.654-1.146
	2	15949-19345	1.227-1.488
<i>Penicillium citrinum</i>	2	47984-89419	3.691-6.878
Fungal cells and yeast	1	2300	0.177
<i>Aspergillus versicolor</i>	1	9600	0.738
<i>Candida famata</i> var. <i>flareri</i>	2	12917-17497	0.994-1.346
Fungal spores	1	31500	2.423
<i>Aspergillus niger</i>	1	398400	30.646
<i>Aspergillus versicolor</i>	1	13900-76800	1.069-5.908
<i>Penicillium chrysogenum</i>	1	53100-164500	4.085-12.654
<i>Rhizopus nigricans</i>	1	26700	2.054
Viruses*	1	600	0.046
Adenovirus (dsDNA)	1	5900	0.454
Bacteriophage - MS2 (ssRNA)	1	339-423	0.026-0.032
	2	803-909	0.062-0.070
Bovine viral diarrhea virus**	1.75	530000	40.769
	Complete	1600000	123.077
Coliphage - Phi X174 (ssDNA)	1	444-494	0.034-0.038
	2	974-1031	0.075-0.079
Coliphage -T7 (dsDNA)	1	910-1196	0.070-0.092
	2	1906-2005	0.417-0.154
Coronavirus	1	300	0.023
Coxsackievirus	1	2100	0.162
Influenza A virus	1	1900	0.146
Phage - Phi 6 (dsRNA)	1	662-863	0.051-0.066
	2	1388-1771	0.107-0.136
Sindbis virus	1	2200	0.169

*Abbreviations of the types of viruses: single-stranded RNA (ssRNA), single-stranded DNA (ssDNA), double-stranded RNA (dsRNA), double-stranded DNA (dsDNA)

**The dosage data provided is for BVDV in liquid media, but is included for comparison as one of the most UV-resistant microorganisms

Note: Dosages for 2 log reduction of *E.coli*, *B. subtilis* spores, *P. citrinum* spores, and *C. famata* obtained from Lin and Li (2002); dosages for MS2, Phi X174, Phi 6, and T7 viruses obtained from Tseng and Li (2005); dosages for BVDV obtained from (Daryany et al., 2009); all other dosages obtained from Kowalski (2009).

Human exposure to UV rays, such as sunlight, is commonly known to be associated with negative health effects. All UV light with wavelengths below 320 nm are known to cause significant health effects, including skin burns and eye damage (Kowalski, 2009). In addition, UV rays are also known to be carcinogenic, causing skin cancer (Daryany et al., 2009). The most serious UV related health effect is eye damage. Since UV light is invisible to human eyes, unintentional exposure can go undetected for extended periods of time. Symptoms of overexposure of eyes to UV light include blurred vision, sensitization to light, eye pain, and teary eyes (Kowalski, 2009). Overexposure of the skin to UV light can cause erythema (skin reddening, similar to sunburn), photosensitivity, skin aging, immune system damage, and skin cancer (Kowalski, 2009).

However, with indoor UV air treatment, these risks can be minimized or eliminated with the placement of the system, and management of the treatment schedule. The American Conference of Governmental Industrial Hygienists (ACGIH) states that exposure to doses below 60 J/m² of 254 nm UV light is safe for humans (Kowalski, 2009). That is equivalent to 7.692 minutes of full exposure to the germicidal UV system with an irradiance level of 0.013 mW/cm² used for comparison above. Since most UV treatment systems are shielded to avoid full exposure, or are run when the room is vacant, it is unlikely that room occupants will receive a dose considered to be dangerous from a germicidal UV system. Upper air systems are installed close to the ceiling, which maximizes the distance between the UV lamps and any occupants of the room, thus minimizing their UV exposure levels (Dumyahn and First, 1999). In-duct UV systems are located in an area completely separate from the occupants of the room, and thus there are no exposure risks associated with this type of system.

In addition to being effective at disinfecting indoor environments, there are a number of other benefits that make the use of UV air treatment systems favourable. Germicidal UV systems are suitable for most types of indoor environments, as they tend to be customizable to various different environments, and have low equipment costs (Kowalski, 2009). They are also easy and convenient to use, are noise free with no moving parts, and require only relatively short contact times in order to be effective, as demonstrated by the inactivation times shown above in Table 2 (Dumyahn and First, 1999) (Lim and Blatchley III, 2009). A small system consisting of one upper

air lamp is capable of achieving a 40% overall reduction in airborne microbes with five minutes of UV exposure (Hunt and Anderson, 2016). Finally, UV disinfection also lacks any negative residual effects after the treatment is completed, and thus is a medically endorsed method of air treatment (Katara et al., 2008).

2.2 Volatile Organic Compounds

VOCs are defined as organic compounds with boiling points of between 50-260°C at room temperature and standard atmospheric pressure (Huang et al., 2016). The relatively low boiling points of these compounds mean that they also have high vapour pressures at normal conditions, and will partition significantly into the gas phase. VOCs are commonly found in all types of indoor environments. There are over 100 000 possible VOCs that can be found in an environment, and their concentrations depend on the types of emission sources that may be present (Hallaquist et al., 2009). Many VOCs can be categorized as low molecular weight pollutants, including aromatic-, fatty-, halogenated-, and oxygenated-hydrocarbons, terpenes, aldehydes, ketones, and esters (Huang et al., 2016).

VOCs are known to reduce indoor air quality, as well as being associated with negative health effects (Quici et al., 2010) (Salonen et al., 2009). This is a concern, as the US Environmental Protection Agency estimates the indoor VOC levels can be 5 to 10 times higher than outdoor levels (Huang et al., 2016) (Salonen et al., 2009). Outdoors, VOC can originate from anthropogenic or natural sources, however natural sources are relatively minor in comparison (Huang et al. 2016). The primary outdoor sources of VOCs are motor vehicle exhaust and industrial by-products (Huang et al., 2016) (Zou et al., 2006). In indoor environments, there are many more possible sources of VOCs. In addition, it is more difficult for VOCs to disperse from indoor environments, therefore sources that would easily disperse outdoors will tend to be more significant indoors. Ventilation rate has a significant effect on the concentrations of indoor VOCs. However, in addition to dispersing VOCs generated indoors, ventilation is also capable of bringing VOCs generated outdoors into the indoor environment, especially in areas with higher levels of pollutants outdoors, such as industrial areas (De Blas et al., 2012).

There is a wide variety of possible VOCs that may be found in indoor environments. The types and concentrations of indoor VOCs depend on factors such as the emission sources present, the efficiency of the ventilation system, and the age and purpose of the room and building (Huang et al., 2016) (Salonen et al., 2009) (De Blas et al., 2012). Some possible sources of indoor VOCs include building materials and furnishings with adhesive or solvents, electronic equipment, household

cleaning products, air fresheners, combustion products, and human metabolism (Huang et al., 2016) (Quici et al., 2010) (Salonen et al., 2009) (De Blas et al., 2012). It is difficult to quantify the VOC generation effect of intermittent sources such as use of electronic equipment, cleaning products, and human metabolism, as they will vary significantly over time in the same environment, and even more so between different buildings (Salonen et al., 2009). Table 3 below shows a list of some possible indoor VOCs and their sources.

Table 3: Possible indoor VOCs and their sources (Huang et al., 2016)

VOCs	Possible Sources
Formaldehyde	Pesticides, flooring materials, insulating materials, wood-based materials, machine, coatings and paints
Toluene	Pesticides, flooring materials, insulating materials, wood-based materials, paints, adhesives, gasoline, combustion sources
Acetaldehyde	Wood-based materials, flooring materials, HVAC system
Paradichlorobenzene	Ceiling materials, wood-based materials, pesticides
Ethylbenzene	Furniture, paints, adhesives, gasoline, combustion sources
Methylene chloride	Flooring materials, furniture, HVAC system, coatings and paints
Chloroethylene	Flooring materials, coatings and paints, dry-cleaned clothes
Carbon tetrachloride	Coatings and paints, industrial strength cleaners
Chloroform	Pesticide, glue
Naphthalene	Insulating materials, mixed materials, wall painting
Other VOCs (e.g., esters and ketones)	Plastics, resins, plasticizers, solvents usage, flavors, perfumes, paints, disinfectants, adhesives

There are over 900 different VOCs that have been identified at detectable levels in typical indoor environments, with typically 20-150 types of VOCs in a single environment (Salonen et al., 2009). However, despite the large number of possible VOCs, as few as 20-30 compounds at higher concentrations will typically represent 50-75% of the total VOCs present (Salonen et al., 2009). The total concentration of all the VOCs in a typical nonindustrial environment is normally found to be below 1 mg/m³, but in most cases, it is much lower, with a typical level of around 70 µg/m³ (Salonen et al., 2009). Typically, a single VOC will have a concentration under 10 µg/m³ in an indoor environment (Salonen et al., 2009). Cometto-Muñiz and Abraham (2015) conducted an overview of the most commonly reported indoor VOCs in literature, comparing the concentrations measured in different studies. The various indoor environments reported were divided into two categories, home or school, and commercial. The findings from this literature review distribution of the compound concentrations are summarized below in Table 4.

Table 4: Indoor VOC compound concentrations as reported by Cometto-Muñiz and Abraham (2015)

	Concentration	Number of compounds
Home or school environments	All	152
	10-200 µg/m ³	22
	3-10 µg/m ³	44
	0.55-3 µg/m ³	44
	0.01-0.55 µg/m ³	42
Commercial environments	All	96
	8-1000 µg/m ³	22
	2-7 µg/m ³	44
	0.3-2 µg/m ³	29

There are some common compounds that are found in many samples of different indoor locations. A summary of the most commonly found compounds and their typical concentrations in indoor environments is listed below in Table 5. The full table of VOC compounds found and their respective indoor concentration ranges can be found in Appendix B-1 VOC Concentrations in Indoor Environments.

Table 5: Concentrations of some common indoor VOCs, obtained from Salonen et al. (2009), and Cometto-Muñiz and Abraham (2015)

Compound	Concentration range ($\mu\text{g}/\text{m}^3$)
Toluene	1.60 – 776.5
Styrene	0.04 – 64.0
α -pinene	0.20 – 269.0
Benzene	0.09 – 43.7
p-dichlorobenzene	0.3 – 144.6
n-heptane	1.20 – 295.4
o-xylene	0.2 – 29
Ethylbenzene	0.2 – 61
Limonene	1.90 – 49.3
n-decane	2.20 – 41.8
p- and m-xylene	0.4 – 190
Formaldehyde	5.6 – 134.0
1-butanol	0.3 – 147.6
Nonanal	0.2 – 30
Benzaldehyde	0.3 – 12
1,2-propandiol	0.2 – 280
Decanal	0.2 – 13
Decamethylcyclopentasiloxane	0.4 – 150
Tetrachloroethylene	0.02 – 432.0
Trichloroethylene	0.02 – 8.8

Thus, since UV light promotes VOC degradations, a positive side effect of the use of germicidal UV systems is the reduction of VOC levels and thus improvement of indoor air quality in that aspect. There also exist UV photocatalytic systems, similar in design to germicidal UV systems, used for the purpose of eliminating indoor VOCs (Quici et al., 2010). However, at the same time, SOAs are formed from the oxidation products of VOCs, and therefore the degradation of the VOCs may result in the formation of fine particulate matter.

The type of VOCs present in a certain environment plays a major role in SOA formation. Many VOCs emitted into the atmosphere can be inefficient at SOA generation (Hallaquist et al., 2009). There are certain types of VOCs that are more effective at forming lower volatility SOA precursor compounds, while the products from the oxidation reactions of other VOCs will not significantly

contribute to particle formation. In particular, toluene and other light aromatic compounds have been found to form dominant SOA precursors (Hildebrant et al., 2009).

Since there is such a wide variety of VOCs, their associated health effects can vary just as greatly. Some VOCs, such as benzene and 1,3-butadiene, are known to be toxic, carcinogenic, or mutagenic (De Blas et al., 2012) (Zou et al., 2006). As well, aromatics, such as toluene and alkenes, are thought to contribute significantly to cardiovascular conditions (Zou et al., 2006) (Mauderly and Chow, 2008). In general, it is common of many VOCs to be associated with negative health effects in humans. The inhalation of VOCs can cause symptoms such as respiratory irritation, difficulty breathing, nausea, and damage to the central nervous system and other organs (Huang et al., 2016). In addition, conditions such as asthma, allergies, and cardiovascular effects may be promoted or aggravated by the presence of VOCs (Quici et al., 2010) (Mauderly and Chow, 2008). Some VOCs can also be easily absorbed through the skin and mucous membranes, which allows them to more easily affect organs and metabolic systems (Huang et al., 2016).

2.2.1 VOC UV Absorbance

The interaction between a VOC and UV light depends largely on the absorbance properties of the particular VOC at the given wavelength of UV light. Absorbance is the amount of light of a particular wavelength taken in by a substance. The absorbance of monochromatic light of a specific wavelength by a substance is governed by the Beer-Lambert law, where A represents the absorbance, T represents the transmittance, I represents the light flux transmitted by the substance, and I_0 represents the light flux received by the sample:

$$A = \log\left(\frac{1}{T}\right) = \log\left(\frac{I_0}{I}\right)$$

The absorbance of a particular wavelength of light by a substance is affected by the properties of the substance itself, the concentration of the substance in the medium, and the distance that the light travels through the medium.

The level of absorbance will vary for different wavelengths of light, and can be measured using a UV-Vis Spectrometer. In this case, the absorption spectrum for toluene was measured, and is shown below in Figure 1.

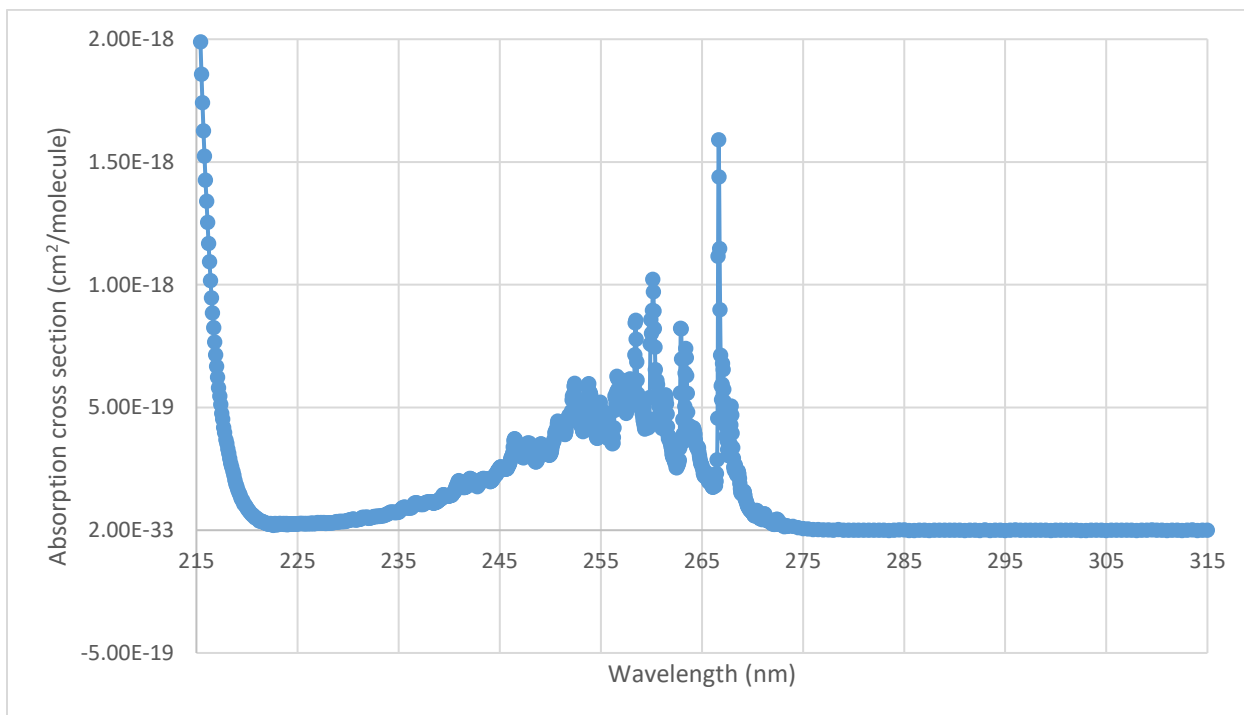
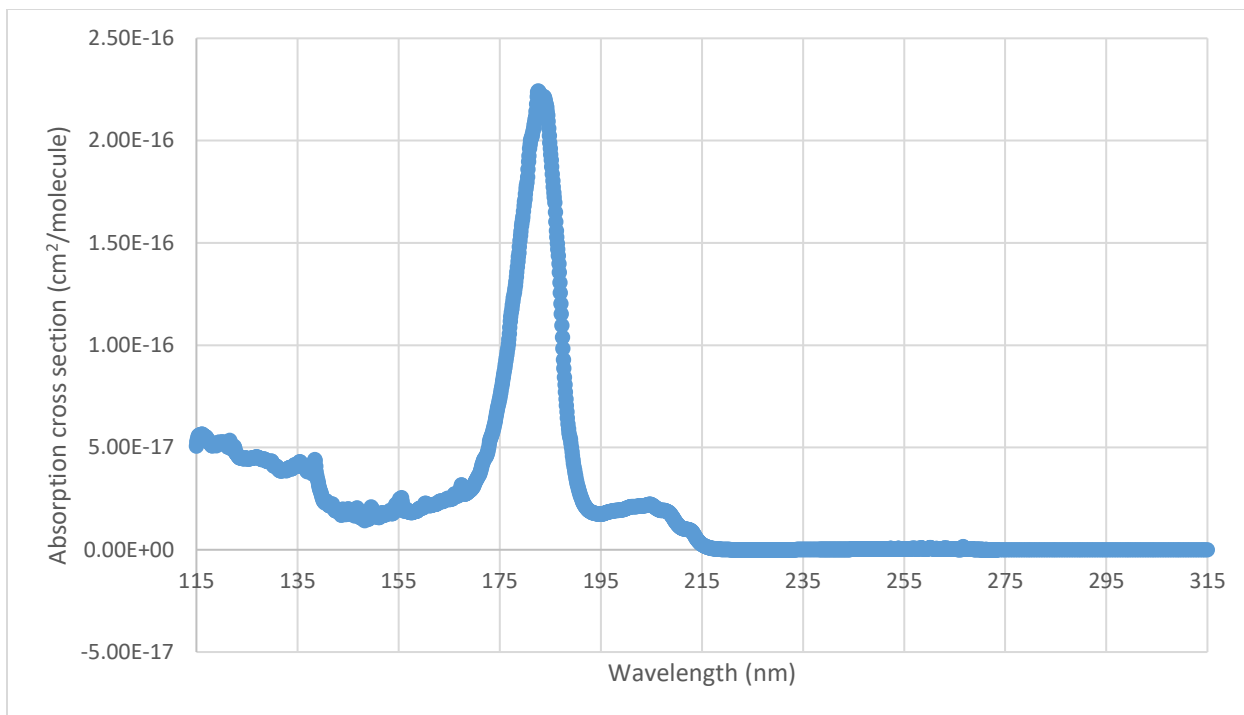


Figure 1: Absorption spectrum for toluene; the second graph shown is a selected portion of the first graph, focusing on the area around 254 nm (Data from Serralheiro et al. (2015))

In Figure 1, it can be seen that toluene has a minor absorption peak that includes 254 nm. This peak is greater than the absorption values for wavelengths of 300+ nm. 300+ nm UV light is known to promote SOA formation via photodegradation. Since toluene is more photoactive at 254 nm

than 300+ nm, it is expected that it will absorb and react more significantly with germicidal UV light. However, the largest absorbance peak for toluene is around light with a wavelength of 185 nm, and therefore toluene will react more significantly with UV light in the range of that peak.

2.3 Secondary Organic Aerosols

Atmospheric aerosols are defined as solid or liquid particles that are suspended in air (Hallaquist et al., 2009). A significant portion of aerosol particles present in the troposphere are SOAs, which can represent anywhere from 20-90% of all the aerosols present in the troposphere, depending on the local conditions (Kroll and Seinfeld, 2008). SOAs are aerosol particles that are formed in the atmosphere as a result of gas-phase oxidation of volatile organic compounds (Huang et al., 2013). The properties of SOA particles can vary greatly, due to the wide variety of compounds that can make up the particle. Only some of the products produced by the numerous VOC degradation pathways will contribute to SOAs, and individual compounds may contribute to either the mass of the particles, the number of particles, or both (Hallaquist et al., 2009). Airborne particles are categorized by size, fine particulate matter, or particles with a diameter of 2.5 μm or smaller, is of particular concern with respect to health effects. Elevated levels of fine particulate matter have been identified in situations with higher production of SOA particles, therefore it is probable that SOA particles primarily fall into the size range for fine particulate matter (Hallaquist et al., 2009). The negative health effects of fine particulate matter are better understood than those of solely SOAs, therefore the primary concern with respect to health effects is the levels of fine particulate matter that are present (Hallaquist et al., 2009).

Since there are so many variables that affect SOA formation, it is difficult to predict the formation mechanisms or particle composition in any particular situation. In addition, only a few VOC degradation reaction mechanisms have been studied in depth, and these typically involve the VOCs with the simplest structures. Select types of more complex VOCs, such as certain terpenes and aromatic hydrocarbons, have also had aspects of their degradation chemistry studied experimentally. Using the knowledge of the degradation pathways of the simpler compounds, details about the mechanisms of degradation can be inferred for more complex compounds (Hallaquist et al., 2009). However, the existing knowledge may not be applicable to all types of VOCs, so the assumptions made may not always accurately reflect the reactions actually occurring, and the resultant composition of SOA particles formed.

Most commonly, gaseous VOCs will degrade as a result of either direct photolysis, or reaction mechanisms involving hydroxyl radicals (OH), ozone (O₃), or nitrous compounds (NO_x) (Kroll and Seinfeld, 2008). Exposure to UV light can result in increased levels of VOC oxidation in two ways; through direct photolysis, or enhancing the formation of OH radicals (Bhowmick and Semmens, 1994). Direct photolytic degradation of VOCs occurs as the compounds absorb the energy from the UV light, and then consequently break down. The resulting compounds may undergo a direct photolysis again, or react with other oxidative compounds. The extent of the effect of direct photolysis depends on the absorptivity of the VOC and of the resulting degradation products (Bhowmick and Semmens, 1994). UV light can also aid in the formation of OH radicals, as shown in the sample set of general reactions shown in Figure 2.

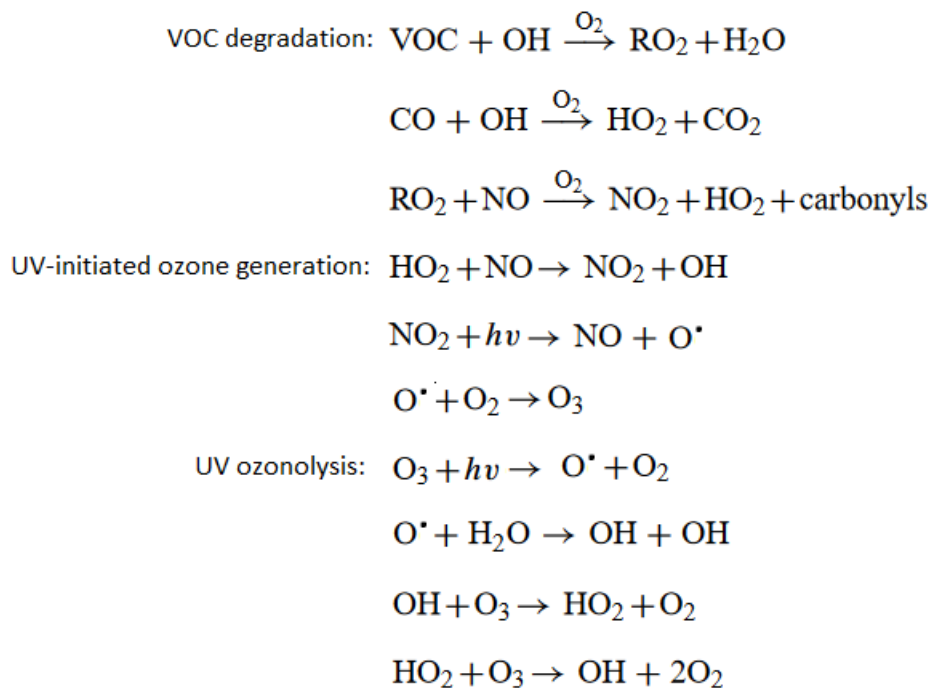


Figure 2: Mechanism of UV photooxidation of VOCs, where R is the portion of the compound structure not involved in this reaction mechanism (Xue et al., 2013)

Figure 2 shows that UV light can break down ozone, forming hydroxyl radicals that will then react with and break down VOCs. In situations with adequate NO levels, UV light is also able to promote the formation of ozone. Thus, it is possible for UV light to aid in the continuous formation and degradation of ozone, which leads to the formation of hydroxyl radicals, which in turn react with VOCs to degrade them. Increasing the dose of UV results in increased levels of

VOC degradation, which leads to increased levels of SOA particle formation (Shen and Yu, 1999) (Hildebrant et al., 2009). Therefore, it is expected that longer periods of UV exposure will result in greater amounts of SOA formation. However, this particular type of reaction pathway is unlikely to occur with germicidal UV systems, as significant levels of NO and ozone are undesirable, and often eliminated from indoor environments. Direct photolysis is more likely to occur in indoor environments, and the exact mechanism will depend more strongly on the structure of the VOC in question. An example of such a mechanism for toluene degradation is shown later in Figure 3, in Section 2.3.1 SOA Formation from Toluene.

In addition to the sample VOC degradation reaction shown, other possible reaction pathways may occur, depending on the structure and properties of the VOCs present. Upon oxidation, VOCs can gain functional groups, which decreases volatility and increases the chance of SOA formation. Alternatively, VOC oxidation can also result in the cleavage of carbon-carbon bonds, producing smaller, more volatile compounds that are less likely to contribute to SOAs (Hallaquist et al., 2009). Thus, the rate at which both of these types of pathways occur will determine the rate of formation of different types of products, and therefore also the degree of SOA formation and growth.

Much of the existing work done on UV photolytic oxidation investigates UV light with wavelengths of 300 nm or greater, which corresponds to the range of UV wavelengths emitted from the sun reaching the Earth's atmosphere, as well as from blacklights. These wavelengths of UV light are known to promote SOA formation via photolysis (Huang et al., 2006). Oxidation reactions and SOA formation can also occur in the absence of UV light, as VOCs can also react with other components in the air, such as OH radicals generated through non-UV mechanisms (Rösch et al., 2015). The ambient conditions and types of VOCs present will have a significant effect on the extent to which the different types of reactions will occur, the products formed, and thus the degree of SOA formation (Hallaquist et al., 2009). The initial step in the oxidative decomposition results in the VOC reacting and breaking down to form products. The products that are related to SOA formation are those with lower volatility and higher water solubility. Often, the products of the initial reaction will undergo a number of additional oxidation reactions,

each producing products of subsequently lower volatility and higher solubility. Theoretically, these additional oxidation reactions could continue to occur until all the carbon atoms in the initial VOC have been converted into CO₂, however practical conditions do not typically allow this to occur (Hallaquist et al., 2009). SOA particles are formed when the semivolatile products of VOC oxidation partition from the gas to the particle phase. This gas to particle phase transfer of semivolatile compounds competes with further oxidation in the gas phase (Hallaquist et al., 2009).

SOA particles can be formed in one of two ways. In the first, the VOC oxidation products are able to condense on existing particle matter in the environment. Alternatively, the semivolatile compounds may also self-nucleate to form particles (Huang et al., 2006). As long as there is some absorbing mass present in the air, a portion of any semivolatile compound capable of particle formation will partition into the particle phase. This happens regardless of whether or not the gas phase concentration is above or below the saturation point (Hallaquist et al., 2009). Thus, this suggests that as long as a mechanism of reaction exists for the degradation of VOCs, there is likely some mechanism by which aerosol particles are able to form.

Pre-existing absorbing mass that promote aerosol particle growth is referred to as seed particles. The most effective seed particles are typically inorganic, often in the form of salts (Huang et al., 2013). The presence of these pre-existing seed particles are found to promote the growth of SOA particles (Ng et al., 2007) (Huang et al., 2013). Since the air in typical indoor environments is not well-filtered to remove fine particulate matter, it is likely that there will often be seed particles present, resulting in the promotion of SOA formation during germicidal UV usage.

There is significant variation in the composition of aerosols found in the environment, and thus it is extremely difficult to determine their independent effects on human health. Furthermore, it is also difficult to isolate the effects of SOAs from that of all the other types of atmospheric aerosols that may be present. However, it is reasonable to conclude that SOAs contribute significantly to the overall effect of all the aerosols present, since SOAs are known to make up anywhere from 20-90% of all the atmospheric aerosols (Kroll and Seinfeld, 2008). The specific effects will primarily depend on factors such as concentration, size, structure, and chemical composition of the aerosols or aerosol mixture involved (Poschl, 2005). In addition, since much

of SOAs can also be categorized as fine particulate matter, the health effects associated with fine particulate matter are also applicable.

Fine particulate matter and aerosol particles are known to be associated with causing damaging respiratory and cardiovascular effects, as well as enhance other health issues, such as infectious diseases and allergic effects (Mauderly and Chow, 2008) (Hallaquist et al., 2009) (Poschl, 2005). Specifically, they have been associated with conditions such as lung inflammation, reduced lung function, allergic responses, asthma exacerbations, heart arrhythmias, and myocardial infarctions. In particular, aerosol particles have pronounced negative health effects on those with already compromised health, such as the elderly, and asthmatics (Mauderly and Chow, 2008). In addition, SOAs in particular may cause noticeable sensory irritation in the eyes and upper airways, with a particularly enhanced effect on asthmatics (Wolkoff, 2012).

UV germicidal air treatment is often used in environments with individuals at a higher risk of infection. Thus, it is important to determine the degree of SOA formation associated with the use of UV lights, in order to determine whether the use of germicidal UV treatment puts these types of individuals at risk for aerosol particle induced health effects.

2.3.1 SOA Formation from Toluene

In this work, toluene was chosen as the representative VOC. Toluene is the most abundant aromatic compound in urban air, and is also commonly found at levels of 1.60 – 776.5 $\mu\text{g}/\text{m}^3$ in indoor environments (Hurley et al., 2001) (Salonen et al., 2009). SOA formed from toluene oxidation products typically exists in the form of fine particulate matter, or particles with diameters of 2.5 μm or smaller, which is the particle size fraction of concern (Huang et al., 2006). Investigation of toluene-based SOAs suggests that a number of oxidation steps are required in order for toluene to produce the compounds found in the SOA particles (Hildebrant et al., 2009). Figure 3 shows a proposed simplified mechanism for the formation of toluene-based SOA (Ng et al., 2007).

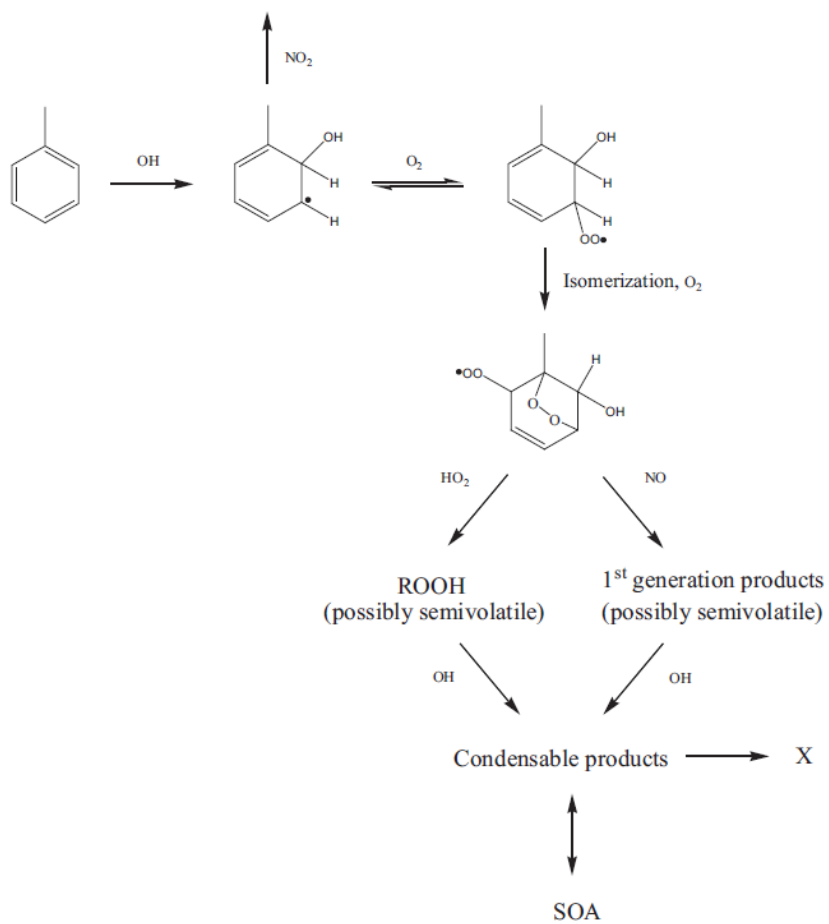


Figure 3: Proposed SOA formation mechanism from toluene, where X represents non-particle products from all gas phase loss processes. (Ng et al., 2007)

2.4 Photocatalytic Oxidation

Similar to germicidal UV systems, UV photocatalytic systems are often used for treatment of indoor air. These systems are typically marketed for the purpose of improving indoor air quality by eliminating VOCs from indoor air (Quici et al., 2010) (Huang et al., 2016). Photocatalytic oxidation is capable of and highly effective at removing almost all organic and inorganic gas phase pollutants, notably those produced by many industries (Huang et al., 2016) (Zou et al., 2006). In addition, photocatalysis is an attractive method for indoor air treatment, as the systems operate at room temperature, and are highly chemically stable, non-toxic, and inexpensive (Huang et al., 2016) (Zou et al., 2006).

UV photocatalytic systems operate by breaking down pollutants on a catalyst surface activated by irradiation with UV light (Huang et al., 2016). These photocatalytic systems can use various UV wavelengths, up to 400 nm. Most commonly, titanium dioxide (TiO_2) will be used as the catalyst. TiO_2 is ideal for this application, as it has superior photocatalytic ability, and high photocorrosion resistance, as well as being non-toxic, biologically and chemically inert, inexpensive and able to be effectively immobilized on various different surfaces (Huang et al., 2016) (Zou et al., 2006). Essentially, UV photocatalysis involves the absorption of photons from the UV light by the TiO_2 surface, which produces active reaction sites. The organic pollutants then undergo redox reactions on the catalyst surface, possibly forming intermediates, before being completely oxidized to H_2O , CO_2 , and inorganic compounds (Huang et al., 2016).

The mechanism of photocatalysis differs from that of photolytic oxidation primarily due to the fact that photocatalysis occurs at the catalyst surface. In photocatalysis, photons from the UV light are absorbed by the catalyst surface, creating active sites for the VOCs to absorb and react. Thus, photocatalytic systems tend to be limited by the amount of catalyst surface available for absorption and reaction. Contrarily, in photolytic oxidation, UV light reacts directly with the compounds in the air to either break down VOCs, or form other compounds that will then react to decompose VOCs.

2.5 Related Existing Work

There are a number of existing studies, a few of which are represented in Table 6, that have been done regarding the UV photolytic formation of SOA. However, there is limited work investigating the effects of germicidal UV in this regard. The majority of the work focuses on longer wavelength UV light, similar to sunlight, with wavelengths of 300-400 nm. In addition, most of the experiments are done in specifically formulated gas mixtures, in order to investigate certain effects. Therefore, although there is a lot of existing work that is similar and relevant, it cannot be directly related to the effects of germicidal UV on SOA formation in indoor environments. Table 6 provides the key related aspects for some similar existing work found in literature.

Table 6: Comparison of SOA formation experiments in literature

	Gas mixture and VOC(s) added	UV wavelength and exposure	Particle formation and toluene consumption
Huang et al., 2006	<ul style="list-style-type: none"> • Air, CH₃ONO, NO • Toluene 	<ul style="list-style-type: none"> • 300-400 nm lamps 	<ul style="list-style-type: none"> • Particle diameter: 0.5-3.5 μm (majority <2.5 μm) • Peak at 0.75 μm diameter
Hurley et al., 2001 Experiment 1	<ul style="list-style-type: none"> • Air, 13 ppm CH₃ONO, 13 ppm NO • 2.6 – 13 ppm toluene 	<ul style="list-style-type: none"> • 315+ nm blacklight lamps • 3-7 periods of 1-15 minutes irradiation 	<ul style="list-style-type: none"> • Particle diameter: 0.04-0.35 μm <ul style="list-style-type: none"> • After 4 mins UV, peak at 0.1 μm; after 40 mins UV, peak at 0.2 μm • Particle concentration: 170-225 $\mu\text{m}/\text{cm}^3$ • 18-34% toluene consumption, equal to 411-2482 $\mu\text{m}/\text{m}^3$
Hurley et al., 2001 Experiment 2	<ul style="list-style-type: none"> • Air, 0.191-0.461 ppm NO_x, propene • 2.1-5.02 ppm toluene 	<ul style="list-style-type: none"> • 315+ nm blacklight lamps • 3.5 hours irradiation 	<ul style="list-style-type: none"> • Particle concentration: 200-210 $\mu\text{m}/\text{cm}^3$ • At 1890 $\mu\text{g}/\text{m}^3$ toluene consumed, 180 $\mu\text{g}/\text{m}^3$ particles formed
Hurley et al., 2001 Experiment 3	<ul style="list-style-type: none"> • Air, 0.045-0.25 ppm NO_x • 0.8-2.02 ppm toluene 	<ul style="list-style-type: none"> • Sunlight • 3 hours exposure 	<ul style="list-style-type: none"> • Particle diameter: 0.1-0.4 μm <ul style="list-style-type: none"> • Initial particles peak at 0.01 μm • Particle concentration: 75-175 $\mu\text{m}/\text{cm}^3$ • 15-25% toluene loss
Vivanco et al., 2011 Experiment 1	<ul style="list-style-type: none"> • Air, HONO • Mixture of toluene, 1,3,5-trimethylbenzene, o-xylene, octane 	<ul style="list-style-type: none"> • Sunlight 	<ul style="list-style-type: none"> • Particle diameter: 0.0175-0.122 μm • Particle concentration: 25-65 $\mu\text{g}/\text{m}^3$
Vivanco et al., 2011 Experiment 2	<ul style="list-style-type: none"> • Air, HONO • Mixture of α-pinene, isoprene, limonene 	<ul style="list-style-type: none"> • Sunlight 	<ul style="list-style-type: none"> • Particle diameter: 0.0414-0.289 μm • Particle concentration: 375 $\mu\text{g}/\text{m}^3$
Zhao et al., 2008 Experiment 1	<ul style="list-style-type: none"> • Air • α-pinene 	<ul style="list-style-type: none"> • 365 nm lamps • 5 hours irradiation 	<ul style="list-style-type: none"> • Particle diameter: 0.02-0.3 μm • Particle concentration: 120 $\mu\text{g}/\text{m}^3$

Through the studies investigated in Table 6, it is evident that UV light with wavelengths between 300-400 nm will cause certain VOCs to form SOA particles. Most of the particles formed are small enough to be considered fine particulate matter. In fact, most of the studies observed particles in the nanometer size range, far from the upper size limit of fine particulate matter. As well, the work by Hurley et al. (2001) concluded that the amount of aerosol particles formed correlates positively with the amount of toluene initially present in the system, as well as the amount of toluene consumed by the reactions.

The existing studies provide a good starting point for establishing a hypothesis for the effect of germicidal UV on SOA formation in indoor environments. It is evident that UV photolysis does promote SOA particle formation. However, the majority of the work done on SOA formation from UV photooxidation involves wavelengths of light similar to atmospheric sunlight, or 300+ nm. In addition, the results for these types of studies are typically reported in mass concentrations, which does not give a representation of the number of particles formed, or the growth in size of particles. The existing studies also do not necessarily use or observe the same parameters that are of interest for indoor environments. For instance, of primary interest is the amount of SOA particles, or more specifically FINE PARTICULATE MATTER, formed from an initial concentration of VOC after a certain duration of exposure to germicidal UV light. With the studies reported in literature, it is difficult to draw a relationship between the initial amount of VOC, the duration of UV exposure, and the resulting particle size distribution.

Chapter 3 - Equipment

3.1 Experimental Setup

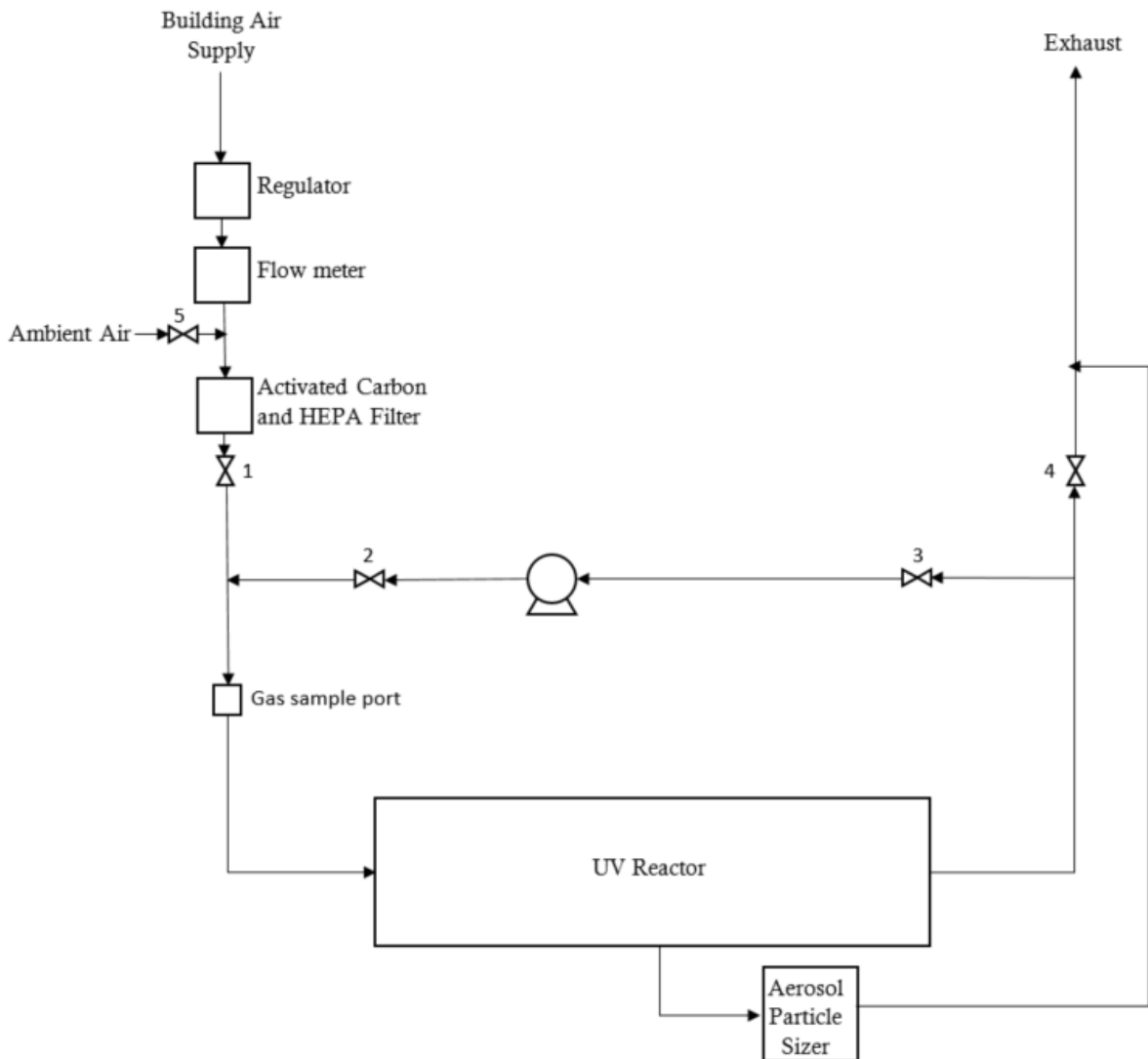


Figure 4: Diagram of experimental setup

A diagram of the experimental setup used for this project is shown above in Figure 4, and photos of the setup are also shown in below Figure 5 and Figure 6. The system setup consists of a custom built UV reactor vessel, containing a UV lamp that runs the length of the reactor. The gas in the system is recirculated using a Cole Parmer Masterflex peristaltic pump. This pump uses 60 cm of Masterflex size 17 Norprene tubing, which has an inner diameter of 6.4 mm. The rest of the tubing

used for recirculating the system is 370 cm of 0.935 cm (3/8 inch) ID polytetrafluoroethylene (PTFE) tubing. The recirculation rate of the system gas was 415 mL/min, which is equivalent to one vessel air exchange every 63.5 minutes. The flow rate was consistent across all the experiments done. All of the fittings and valves used in the setup are stainless steel or brass. Just upstream from the inlet port of the UV reactor vessel is a gas sample port, which consists of a stainless steel fitting with a silicone septum, through which a gas syringe can be used to draw a sample of the system gas.



Figure 5: Front view photo of experimental setup



Figure 6: Side view photos of experimental setup

A more detailed diagram of the UV reactor is shown below in Figure 7, and photos of the side views of the reactor are shown in Figure 6. The UV reactor vessel is a cylindrical stainless steel vessel with a diameter of 20.3 cm, and a length of 81.3 cm. The effective volume of the UV reactor is 26 359 mL. The UV lamp is a Sterilight model S8RL/4P, a 40 W lamp which produces monochromatic UV light with a wavelength of 254 nm, and it is situated so that it runs horizontally down the center of the full length of the reactor. The lamp controller used is a Viqua BA-ICE-SO electronic controller, which is connected to the same switch as a cooling fan situated underneath the reactor vessel. This ensures that the UV lamp and cooling fan are turned on simultaneously. Since the UV lamp creates heat, the fan ensures the regulation of the temperature in the vessel. The temperature profile of the system during operation is discussed in Section 4.1.2.1 Vessel Temperature.

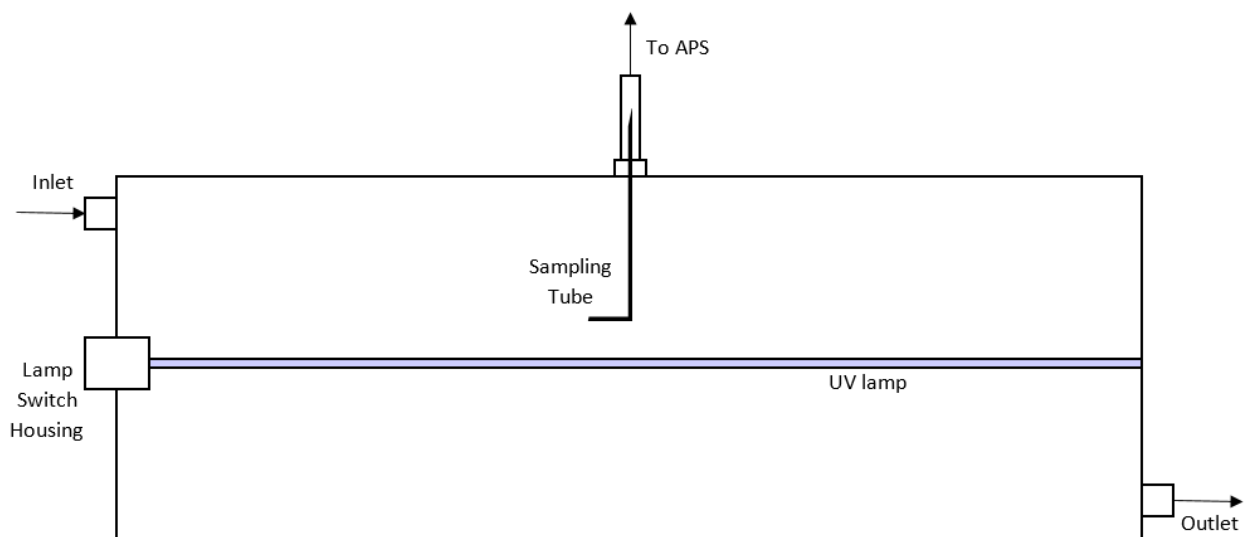


Figure 7: Diagram of reactor vessel

The aerosol particle sizer (APS) used for analysis of particle size distributions is attached via a sample port on the center of the reactor. The sample port includes an L-shaped stainless steel sampling tube with an inner diameter of 2 mm, which extends 5 cm into the reactor, and has a 4.5 cm long bent arm that allows the sampling to be done in the same direction as the gas flow through the vessel (see Figure 7). The sampling tube feeds the sample gas into copper tubing with a larger inner diameter of 3.1 mm (1/8 inch), to which the sample valve is attached. When the valve is open, the APS is able to sample the system gas from the reactor. The copper tube is then attached to conductive silicon tubing, which fits the inlet port of the APS. Figure 8 shows how the vessel is attached to the APS for sampling the reactor gas. The use of copper and conductive silicon tubing for sampling ensures that particle loss while sampling is minimized. The specifications of the APS and conductive silicon tubing will be further discussed in Section 3.3 Aerosol Particle Sizer.

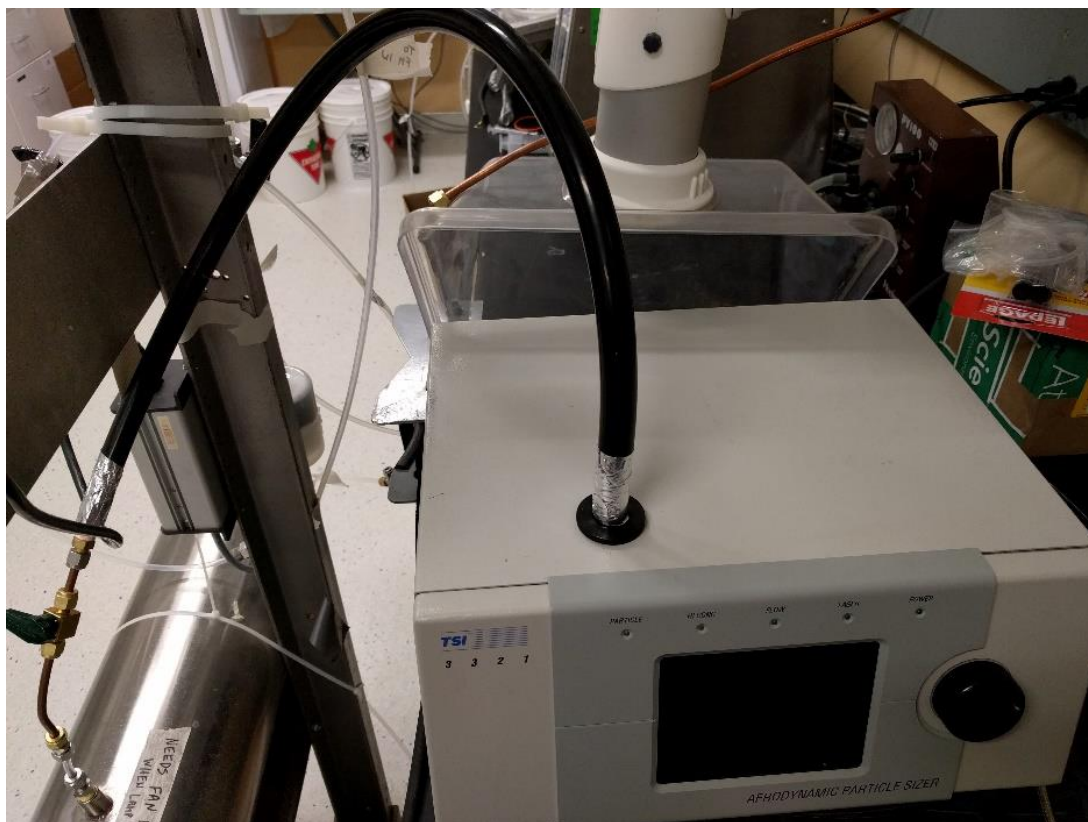


Figure 8: Photo of APS attached to reactor vessel

For the majority of the experiments, the source of the system air is compressed air supplied from the building's system, and is passed through a filter before reaching the UV reactor vessel. This filtered compressed air is essentially dry, with a relative humidity measurement of around 11%. The filter used is a ZenPure PureFlo Capsule containing both an activated carbon portion and a HEPA filter. The activated carbon removes VOCs from the gas, while the HEPA filter ensures 99.97% removal of particulate material larger than 0.3 μm in diameter. There are also experiments that require the use of room air, rather than the building supplied compressed gas. These experiments use a Gast vacuum pump, model DOA-P104-AA, to draw air from the room to be circulated as the system gas. For the introduction of both the building's compressed gas and room air via the vacuum pump, the air flowrate is regulated by a flowmeter, and kept consistent at 8 L/min for the duration of the system purge. Afterwards, the purge gas flow was stopped, and the recirculation was controlled by the peristaltic pump. In addition, there are some experiments that use unfiltered air, which utilizes the same system with the filter removed. For the experiments

that required it, the relative humidity of the room air was measured using a General handheld psychrometer, model EP8710.

Toluene was the primary VOC used in the experiments performed. The toluene was supplied by VWR International, and had a minimum purity of 99.5%. In addition, a supplemental experiment was also done using limonene. The d-limonene was also supplied by VWR, and had a minimum purity of 94%.

3.2 Gas Chromatography

Gas chromatography (GC) is used to monitor the VOC concentrations throughout the duration of the experiment. The model of gas chromatographer used is a HP 5890 Series II, with a Restek fused silica column, model Rtx-5 10240, which has an inner diameter of 0.53 mm and a length of 30 m. Toluene level detection is done using the flame ionization detector (FID).

The GC program used for toluene detection has the following specifications:

Table 7: GC Specifications

Parameter	
Injector Temperature	250°C
Detector (FID) Temperature	300°C
Oven Temperature	40°C
Air Flow Rate	350 L/min
Hydrogen Flow Rate	35 L/min
Column Head Pressure	5 psi
Program Run Time	2.500 mins
Toluene Retention Time (expected)	1.887 mins

The toluene area counts were calibrated at least once every week that experiments were being performed. The calibration samples were created by evaporating 1 μL of liquid toluene in a 250 mL gas bulb, yielding a known toluene concentration of 3440 ng toluene/mL gas sample. Gas samples for both calibration of and measurement using the GC are taken using a 500 μL Hamilton gas-tight syringe, model 1750 TLL. The full procedure for calibration of the gas chromatographer is found in Section 4.2.1 Gas Chromatography Calibration.

3.3 Aerosol Particle Sizer

In the experiment performed, a TSI Aerosol Particle Sizer (APS) model 3321 (Figure 9) was used to monitor the amount of aerosol particles present in the system. It was attached in line to the UV vessel, as shown in Figure 4 and Figure 8. This type of APS is a time-of-flight spectrometer, which determines the size of the particles by measuring their velocities. The sample gas is contained within a stream of sheath air, and the flowrate is accelerated by passing through a nozzle. The particles will then scatter light as they pass through laser beams, and the scattered light is measured as electrical pulses using a photodetector. The velocity of each of the particles can then be determined using the time between the peaks of the pulses. These velocities are then sorted into their time-of-flights, which can then be converted into the aerodynamic particle diameter of the particle, determined by a non-volatile calibration in the device. Using this method, this model of APS is able to detect particles from 0.5-20 μm in diameter using the determined aerodynamic particle sizes, as well as the unconverted light scattering data. These particles are sorted into 52 size fractions. In addition, particles between the diameters of 0.3-0.5 μm using light scattering data, and these particles are sorted together as a size fraction of $<0.523 \mu\text{m}$.



Figure 9: TSI 3321 aerosol particle sizer

The APS obtains samples from the UV reactor vessel through 21 cm of L-shaped stainless steel sampling tube with an inner diameter of 2 mm. The L-shaped tubing has a 16.5 cm section extending out of the reactor, which bends at 90° to a 4.5 cm section parallel to the direction of gas flow in the reactor. The stainless steel tubing then attaches to 11 cm of 3.1 mm (1/8 inch) inner diameter copper tubing, and 86 cm of conductive silicon tubing. The conductive silicone tubing is manufactured by TSI for use with the APS, and has an inner diameter of 11.2 mm (0.44 inches). This size of tubing is designed to fit the gas inlet nozzle at the top of the APS, which has a diameter of 18.9 mm (0.746 inches). The different types of tubing are used such that the sample gas will flow through conductive tubes of increasing diameter, which is done in order to avoid particle loss during sampling. The APS draws gas from the reactor at a rate of 5 L/min. 4 L/min of the gas is filtered within the APS and used as sheath air, while the remaining 1 L/min is used as the actual sample and analyzed for particle size distribution.

3.4 Data Analysis Software

The primary statistical software used for data analysis in this project is Statistica 11. This software was used to perform statistical analysis for the factorial experiment performed. The design of experiment ANOVA and factorial ANOVA analysis methods were used.

Chapter 4 - Methods and Experiments

4.1 Experimental Conditions

4.1.1 Parameters Tested

There were four primary variables being tested in the experiments performed. They were the type of initial air source, the amount of toluene initially present in the system, the length of time that the system is exposed to UV light, and the length of post-UV gas recirculation time.

4.1.1.1 Initial Air Source

The initial air source for the majority of the experiments was filtered compressed air from the building system. This ensured that the air was essentially dry with a relative humidity of around 11%, with the filtration removing any particles larger than 0.3 μm in diameter. Thus, all particles measured were expected to have been formed during the duration of the experiment.

In addition, there was also a number of experiments done with unfiltered compressed air, as well as filtered and unfiltered room air. The use of room air allowed for the observation of any effects resulting from relative humidity levels above 0%. The experiments using unfiltered air allowed for the determination of any effect on the overall particle distribution if there pre-existing particles in the system prior to the start of the experiment.

4.1.1.2 Toluene Concentration

A few initial experiments were done in order to determine the effective amount of gas phase toluene that would result from additions of various volumes of liquid toluene. The results are shown below in Table 8 and Figure 10.

Table 8: Gas phase concentrations of toluene at varying liquid additions

Liquid toluene addition (μL)	Theoretical gas phase toluene concentration (ng/mL)	Actual gas phase toluene	
		Concentration (ng/mL)	Percent of theoretical concentration
9	280.30	65.65	23.4%
10	311.45	87.76	28.2%
15	467.17	120.14	25.7%
18	560.60	175.66	31.3%
20	622.90	194.12	31.2%

The values shown in Table 8 show that the actual gas phase concentrations observed are far lower than the theoretical gas phase concentrations that would be observed if all the liquid toluene were to be distributed ideally in the gas phase. Therefore, this indicates that there may be other factors that are unaccounted for, such as potential wall effects, or incomplete volatilization, that play a role in how these VOCs transition from the liquid to the gas phase in this reactor.

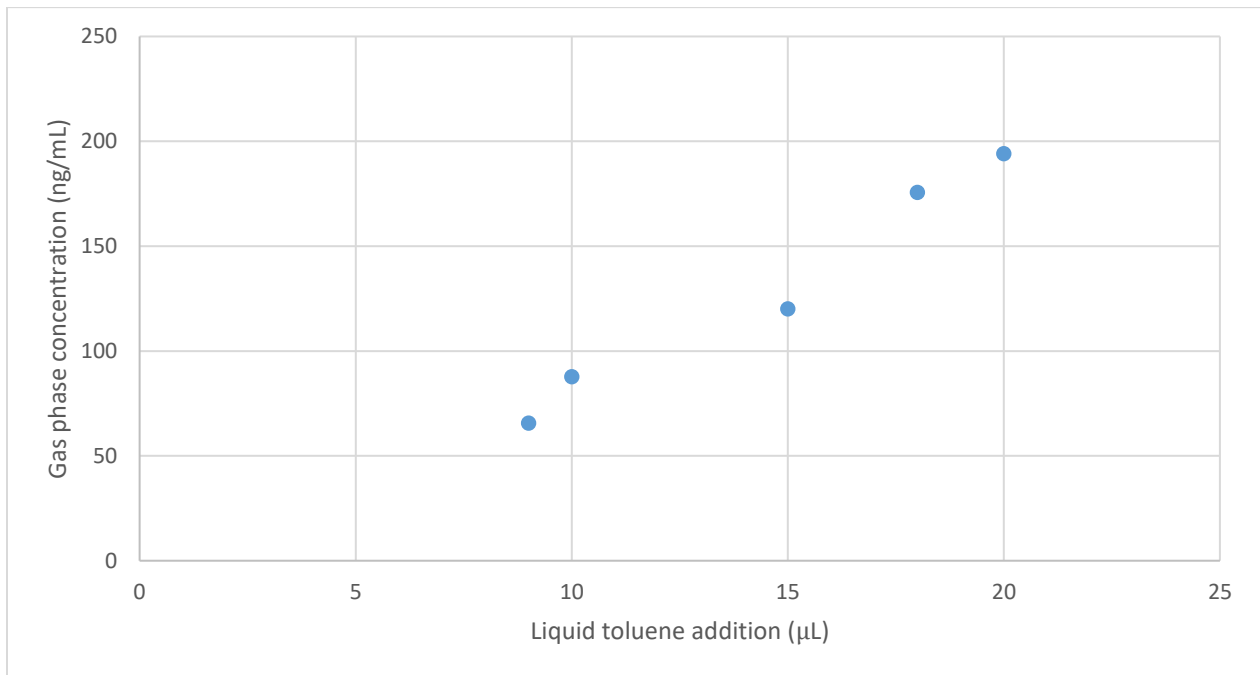


Figure 10: Graph of gas phase concentrations of toluene at varying liquid additions

As is evident from Figure 10, the relationship between the amount of liquid toluene added and the resulting gas phase toluene concentration is a relatively linear positive correlation. This suggests that any toluene additions within the range tested can be used and results can be easily related to each other. Toluene addition levels of 9 μL and 15 μL were selected for the experiments

performed, which corresponded to gas phase toluene concentration ranges of 55-85 ng/mL and 100-125 ng/mL. Varying the concentration of gas phase toluene will subsequently vary the UV absorbance, therefore it is expected that the initial toluene level will affect the degree of toluene photodegradation, and the resulting particle formation.

4.1.1.3 Length of UV Exposure

The length of time that the system is exposed to UV light affects the effectiveness of the treatment system. It is known that UV exposure for as little as 5 minutes can result in a significant germicidal effect (Hunt and Anderson, 2016). Thus, since relatively short exposure times can be used for indoor germicidal UV treatments, this will be the starting point for testing for observable particle formation.

The length of UV exposure time can be related to the level of UV dosage that the gas mixture is subjected to. This can be determined by calculating the average irradiance rate in the UV reactor. Bolton (2000), provides an equation for estimating the average irradiance rate in a cylindrical reactor with a single UV lamp that runs down the centre. Using this equation, the average irradiance rate in the reactor used in these experiments is 19.52 mW/cm². The use of a 40 W bulb in a relatively small reactor results in a significantly higher amount of UV irradiance than those found in existing work, as outlined in Table 1.

A set of minimal exposure experiments was designed in order to determine the minimum amount of time required to generate observable particle formation. In addition, a complete degradation experiment was done to determine the amount of time required to completely degrade the amount of gas phase toluene added to the vessel. The results from these experiments are shown in Section 5.1 Complete Degradation Experiment and Section 5.3 Minimal Exposure Experiment.

These results were used as the basis for selecting the UV exposure times used in further experiments. For the majority of the experiments, UV irradiation times from 1 to 15 minutes were tested.

4.1.1.4 Length of Post-UV Recirculation

The formation of SOA particles is a result of the condensation of semivolatile compounds formed via oxidation reactions. Since these reactions can occur in the absence of UV light, it is hypothesized that particle growth can continue to occur after UV exposure has ended (Rösch et al., 2015). In addition, the transition of compounds from the gas to the particle phase may not occur instantaneously, and thus it is possible for compounds in the gas phase to continue to condense after the termination of the UV treatment. Therefore, particle formation or growth may continue to occur, despite the fact that UV photoreactions are no longer occurring. Post-UV recirculation times from 1 to 15 minutes were tested in the experiments performed.

4.1.2 Other System Variables

4.1.2.1 Vessel Temperature

One condition of interest in the experiments performed was the temperature of the system. In particular, it is known that the 254 nm UV lamp used gives off an observable amount of heat. As a result, the gas in the system could be expected to increase in temperature to some degree over the duration of an experiment. The fan was always running when the UV lamp was on, in order to control the increase in temperature.

In order to quantify the temperature increase of the system, a digital temperature probe was placed in various orientations in the system in order to create temperature profiles. The probe used was a VWR Traceable Ultra Thermometer, which is accurate to $\pm 0.2^\circ\text{C}$ between $-50 - 150^\circ\text{C}$. Figure 11 shows the temperature profile when the probe was placed at different depths in the sample port located halfway along the length of the vessel. Since the vessel is approximately 20 cm in diameter, the furthest the probe could be placed into the vessel without contacting the lamp was 9.5 cm. At each of the different depths of the probe, the temperature was monitored over 15 minutes with the UV lamp turned on. The exposure time was selected to be 15 minutes, since this was also the longest planned exposure for an experiment.

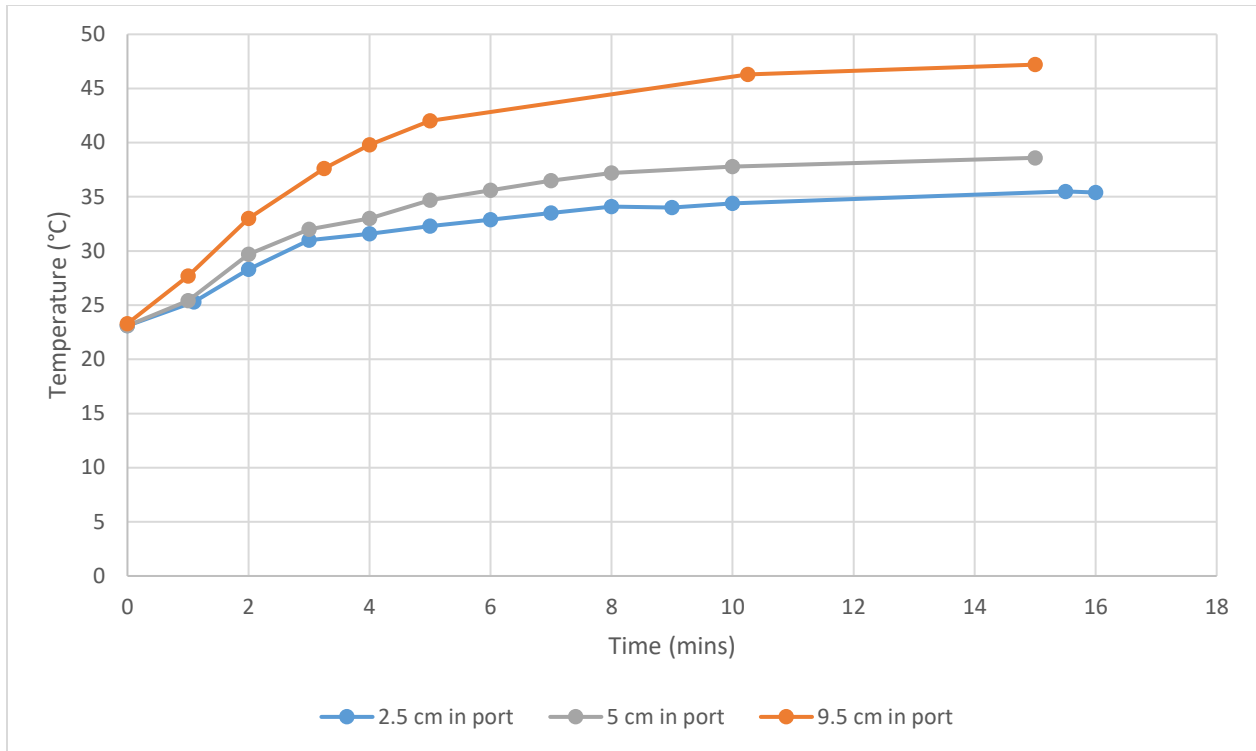


Figure 11: Vessel temperature profile taken from vessel sample port

The resultant temperature profiles from three different probe depths are shown in Figure 11. It can be observed that the closer the probe was to the lamp, the higher the measured temperature. In addition, the rate of temperature increase was the most significant over the first 5 minutes at all three depths. The maximum measured temperature was 47.2°C, at the probe depth closest to the UV lamp, resulting in a temperature difference of 23.9°C over the duration of the experiment. However, since the temperature probe is made of metal, it is possible that it will absorb energy from the light produced by the UV lamp, and thus artificially record a temperature higher than that of the actual system gas.

In order to confirm the temperature profiles taken from the sample port, as well as to remove the effect of exposing the metal temperature probe to UV light, another temperature profile was taken of the gas exiting the vessel via the outlet port. For this, the temperature probe was placed immediately after the exit of vessel, before valve 3 (see Figure 4). This temperature profile is a better representation of the overall gas temperature exiting the system. It is also a better representation of indoor germicidal UV systems, where circulation aids in moderating the air temperature.

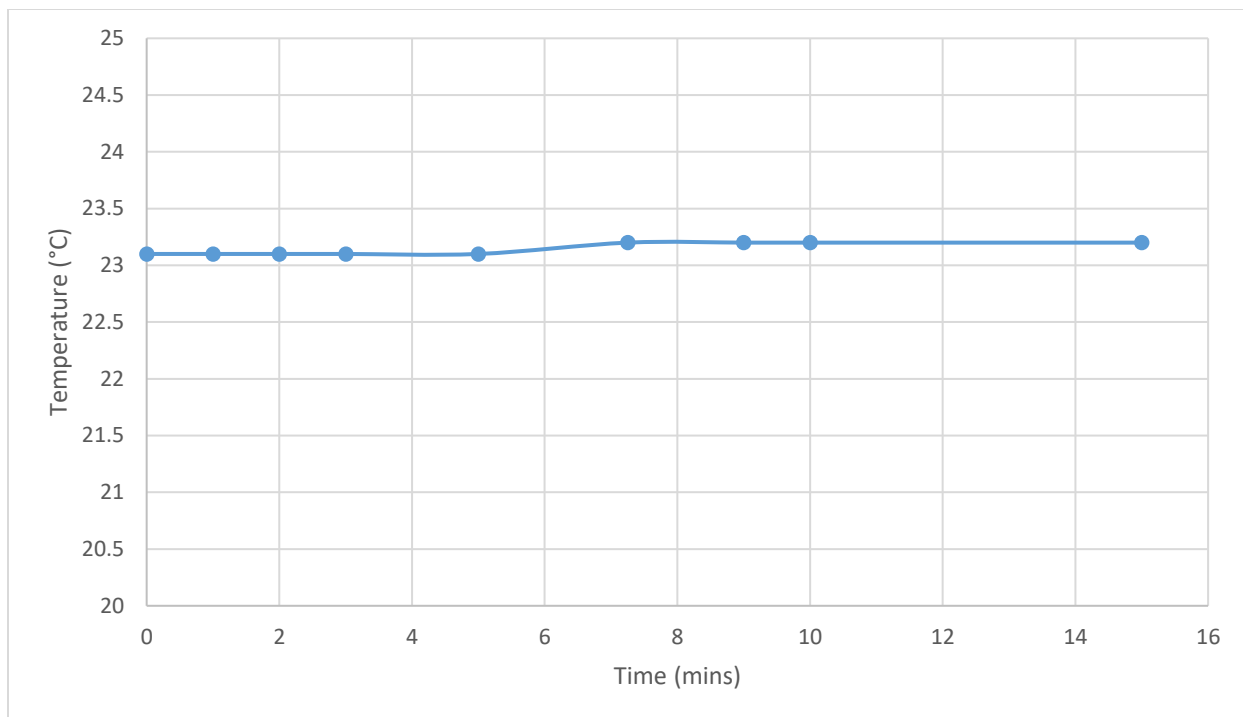


Figure 12: Temperature profile at vessel exit port

As shown in Figure 12, the temperature of gas exiting the vessel remains at essentially a constant temperature over the course of the 15 minutes with the UV lamp on. This suggests that the increased temperature observed from the sample port measurements are only local to specific areas within the reactor. Overall, since the temperature of the outlet gas remains relatively constant, it is suggested that the overall system maintains a relatively constant temperature. The small changes in temperature are not expected to have any effect on aerosol particle formation (Ng et al., 2007).

4.2 Experimental Procedure

4.2.1 Gas Chromatography Calibration

The toluene area counts for the gas chromatography were calibrated every week that experiments were performed. The calibration gas mixture was prepared by evaporating 1 μL of liquid toluene in a 250 mL bulb. This yields a gas mixture with a known toluene concentration of 3440 ng toluene/mL.

The procedure for the calibration is as follows:

1. In a sealed 250 mL gas bulb, 1 μL of liquid toluene was added. The bulb was heated briefly in a 40°C oven just until all the liquid has evaporated.
2. With a 500 μL Hamilton model 1750 TLL gas-tight syringe, the samples in the sequence listed in Table 9 were injected into the GC. The area counts measured for each of the samples was recorded.

Table 9: Gas chromatography calibration sequence

Sample	Equivalent toluene mass (ng)
500 μL room air	0
50 μL bulb gas	78.4
100 μL bulb gas	156.8
200 μL bulb gas	313.6
300 μL bulb gas	470.4
400 μL bulb gas	627.2
500 μL bulb gas	784

3. Under the toluene method, the previous area count values were replaced with the newly calibrated values.

4.2.2 UV Irradiation Experiments

The same general procedure was followed for all of the experiments involving UV irradiation. The general procedure is outlined below, and the factors that vary between the different types of experiments done are outlined in Table 10, which follows.

1. Prior to the start of each experimental run, the vessel was purged with filtered compressed air. To do this, valves 1 and 4 were opened, and valves 2 and 3 were closed, which allowed the air to pass through the vessel to the exhaust. The flowmeter was checked to ensure gas flow was regulated at 8 L/min for this purge step. The vessel was purged for at least 13 minutes, or the equivalent of at least 4 reactor volumes, in order to ensure the removal of any pre-existing material.
2. After purging, the vessel was switched to recirculation mode by closing valves 1 and 4, opening valves 2 and 3, and turning the peristaltic pump on.
3. Once recirculation was started, blank samples were taken for both the GC and APS. This was done to establish baseline measurements for VOC and particle concentrations. For the baseline VOC concentration, a 500 μ L gas sample was taken from the sample port with a gas-tight syringe, and injected into the GC for analysis. For the baseline particle distribution, an initial sample was collected using the APS via the sample port on the vessel. The experimental run was only started if the initial amount of VOC is below 5 ng/mL.
4. To start the experimental run, the desired amount of liquid toluene was injected into the system via that sample port. The system was allowed to recirculate until the level of gas-phase toluene had stabilized. The toluene level in the gas phase was monitored using 500 μ L gas samples injected into the GC for analysis. When the concentration was observed to have less than 10% difference over three samples taken over a period of at least 10 minutes, the level of gas-phase toluene was deemed to be stable. The first sample for the GC was taken around 10 minutes after the injection of the liquid toluene, as the toluene levels tended to stabilize around 15 minutes after injection.
5. When the level of gas-phase toluene was deemed to be stable, another baseline sample was taken for particles using the APS. This sample was used as a baseline for the particle size distribution present prior to UV irradiation. In addition, this allowed for the isolation of any effects on the particle size distribution from the possibility of toluene condensation.
6. The UV lamp was then switched on, and the system was allowed to irradiate and recirculate for the desired amount of time.

7. Once the designated amount of time has elapsed, the UV lamp was switched off. A GC gas sample was taken as a record of how much toluene was left in the system after the UV irradiation. The system was then allowed to continue to recirculate for the designated amount of post-UV recirculation time.
8. At the end of post-UV recirculation time, a final APS sample was taken, which gave the final particle size distribution. The particle size distributions before and after UV irradiation were compared to determine the amount of particle formation that occurred.

Table 10: Variations of the experimental procedure

Experiment	Purpose	Toluene concentration (ng/mL)	UV exposure length	Post-UV recirculation time
Complete degradation	To determine the amount of time required to reduce the amount of toluene present in the system to a negligible level, and the associated particle formation.	10 μ L	As long as required for gas phase toluene levels to decrease to a negligible level.	None.
Blank (control)	To confirm that the particle formation observed is a result of toluene degradation.	No toluene	15 minutes.	1 minute.
Minimal exposure with constant recirculation time	To find the lowest UV dose required for particle formation.	55-85 ng/mL	Starting at 1 minute, increasing in increments of 1 minute until a significant amount of particle formation is observed.	5 minutes.
Minimal exposure with constant total time	To determine if varying total time and post-UV recirculation time have different effects on particle formation. The total time was selected to be 6 minutes from the results of the previous minimal exposure test.	55-85 ng/mL	1-5 minutes, such that the sum of the UV exposure time and post-UV recirculation time equals 6 minutes.	1-5 minutes, such that the sum of the UV exposure time and post-UV recirculation time equals 6 minutes.
Factorial	To determine the effects of initial toluene level, UV exposure length, and post-UV recirculation time, relative to each other.	55-85 ng/mL and 100-125 ng/mL	5, 10, and 15 minutes.	1, 5, and 15 minutes.

Room air	To determine the effect of room air on particle formation, as compared to previous experiments using filtered compressed air.	55-85 ng/mL	5 minutes.	1 minute.
----------	---	-------------	------------	-----------

4.2.3 Unfiltered Air Experiments

Unfiltered experiments were done using both the compressed air supply from the building, as well as the room air. These experiments can be compared with the filtered experiments using the same air source in order to determine the amount of pre-existing particles in the air supply, as well as their effect on the size distribution of the particles formed from UV photolysis.

For these experiments, the procedure remains the same as for all the other experiments. The only difference is the removal of the HEPA and activated carbon filter that is located prior to the inlet port of the vessel.

4.2.4 Room Air Experiments

There were also experiments that were done using room air as the system gas instead of compressed air. These experiments allow for the observation of any changes in particle formation caused by the initial presence of any components in the air that are typical of indoor environments, such as pre-existing particles and gas-phase compounds. In addition, the room air also allows for investigation of the effects of varying relative humidity on particle formation. These experiments were performed with the room air in a university research laboratory, and took place during February 2017. The relative humidity of the system gas was determined by measuring a static sample of the air using the General handheld psychrometer.

For these experiments, the initial purge is done using a vacuum pump attached to the system at the same location the compressed air would normally be. The vacuum pump draws air from the room into reactor vessel, and the flow rate is controlled by the flowmeter to be the same 8 L/min as it was for the experiments that used compressed air.

4.2.5 Above-door Germicidal UV System Experiment

In order to determine the particle formation effects with respect to a UV system that is used for germicidal purposes, a test was done with an above-door UV system. The system involved is a Sanuvox Aseptix 1 automatic UV-C room disinfection system set up in a bathroom with a floor space of approximately 7.5 m², located in a commercial office building. This device is installed above the door of a room, and has sensors to determine if the door is closed, and motion sensors to determine if the room is occupied. Every time the room is vacated, the system will run a five minute disinfection cycle.

An experiment was done in order to determine if, under normal conditions, running a disinfection cycle will cause any increase in the size of number of particles present. The particle counts were recorded using the APS, placed in the centre of the room. The method used was as follows:

1. With the UV system disabled, an initial gas sample was taken. Since the UV disinfection is five minutes long, each sample was designated to be taken continuously over five minutes. Two initial samples of the room air were taken prior to UV treatment.
2. The APS was then set up to take three consecutive samples, and the UV system was turned on. The first sample corresponded with the five minutes that the UV system is on, and the second and third samples corresponded with the ten minutes following UV treatment.

Chapter 5 - Results and Discussion

5.1 Complete Degradation Experiment

The complete degradation experiment allowed for the determination of whether exposure of toluene to 254 nm UV light results in particle formation. This set of experiments involves exposure of the system to UV light until the amount of toluene present in the system has been reduced to a negligible amount. The subsequent measurement of the particle size distribution was then used for comparison to the initial particle size distribution in order to determine if particle formation had occurred as a result of exposure to UV light. The amount of fine particulate matter formed was determined as the difference between the amount of fine particulate matter before and after UV irradiation.

In addition, these experiments allowed for the comparison of the amount of time required to completely eliminate toluene from the air to the amount of exposure time typically employed by germicidal UV systems. They will also allow for the observation of the amount of particulate matter formed, and the effects of longer exposure times on both the amount and size distribution of the resultant particles.

The specifications and results for this experiment are shown below in Table 11, and the resultant particle size distribution is shown in Figure 13. The amount of fine particulate matter produced was determined by the difference between the amount of fine particulate matter present prior to and after UV irradiation.

Table 11: Complete degradation experiment data

Toluene added	10 uL
Toluene concentration before UV (ng/mL)	141.36
Initial fine particulate matter concentration (# of particles/cm ³)	1.748
Length of UV irradiation (h:mm:ss)	1:56:15
Toluene concentration after UV (ng/mL)	0
Fine particulate matter formation (# of particles/cm ³)	1925.632

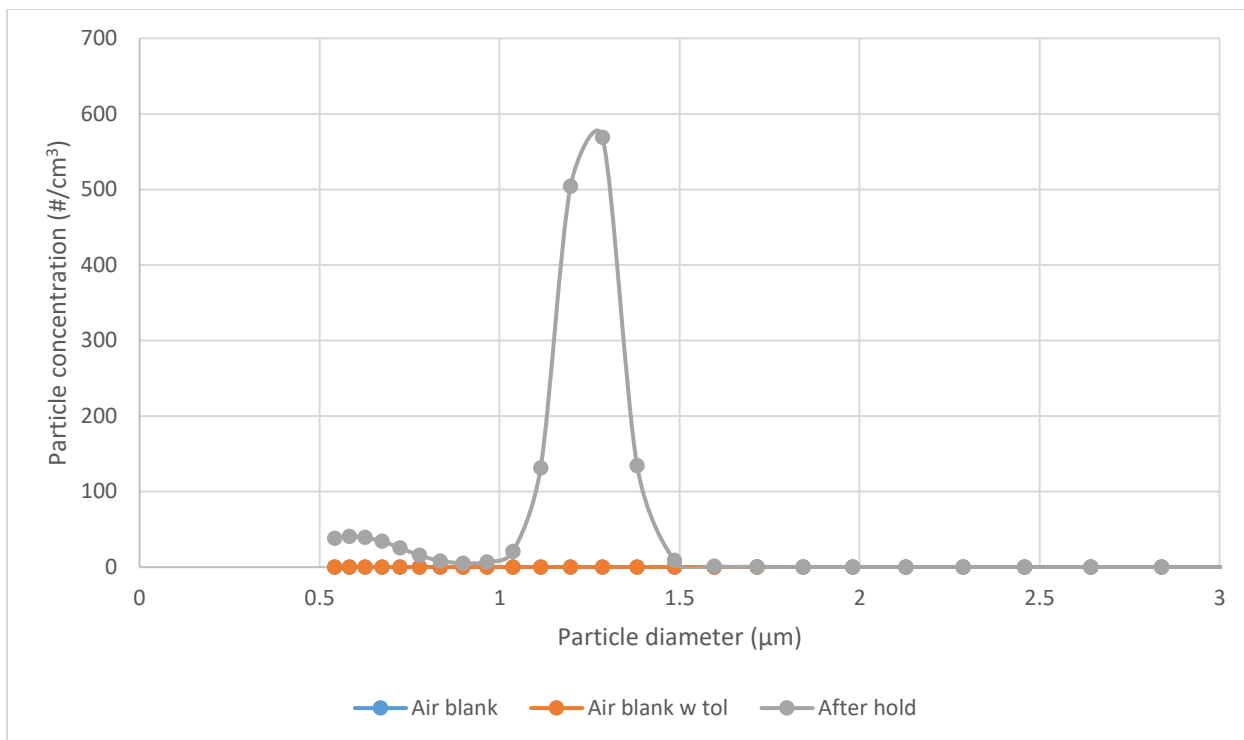


Figure 13: Particle size distribution for complete degradation experiment of toluene

In this experiment, complete degradation of 10 μL , or 141.36 ng/mL , of toluene from UV exposure took approximately 2 hours. The particle size distribution shows a distinct peak of particles with diameters between 1.114-1.382 μm , as well as a smaller peak for particles below 0.777 μm . All of the significant particle formation in this experiment falls under the classification of fine particulate matter. Overall, 1925.632 particles/ cm^3 were formed over the course of the UV exposure, effectively showing that exposure of toluene to UV light resulted in the formation of aerosol particles.

5.2 Controls

In order to confirm that the particle formation is a result of the photodegradation of the added toluene, it needs to be determined that both toluene and UV exposure are required for particle formation to occur. Thus, the cases in which each of these factors is present without the other need to be investigated.

5.2.1 UV Light

In the blank experiment, filtered compressed air without the addition of toluene was exposed to 15 minutes of UV irradiation. The particle size distribution for this experiment is shown below in Figure 14.

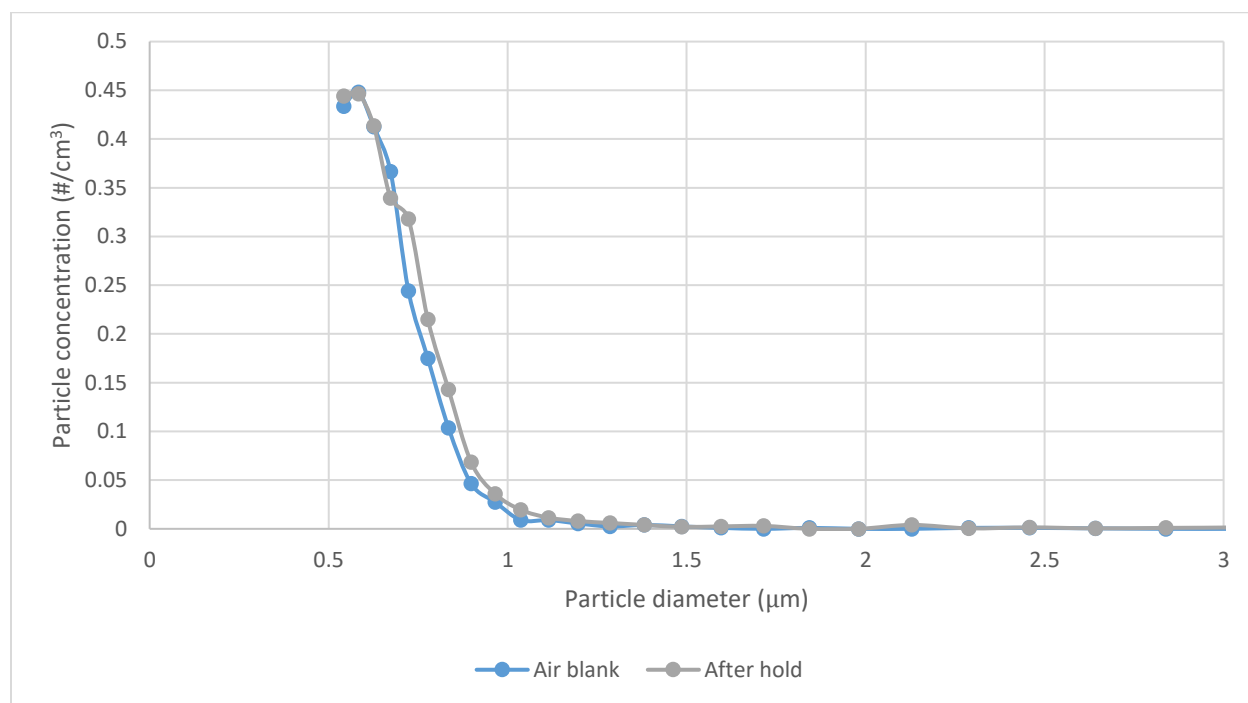


Figure 14: Particle size distribution for blank experiment with no toluene

The particle size distributions before and after the UV irradiation are very similar, therefore it is reasonable to conclude that no particle formation occurred. In addition, the overall particle concentrations are very low. Since the period of UV irradiation did not result in an observable increase in the particle concentration, or a change in the shape of the particle size distribution, it can be concluded that the presence of toluene is necessary for particle formation under UV irradiation in this experimental setup.

5.2.2 Toluene

In order to determine whether gas phase toluene produces particles in the absence of UV light, the difference between the fine particulate matter levels before and after toluene addition was analyzed. The system was allowed to recirculate for a minimum of 10 minutes between the measurements. The addition of liquid toluene is hypothesized to not affect the amount of particles initially present in the reactor. In order to confirm this, a paired t-test was done to compare the fine particulate matter levels. The results of this test are presented below in Table 12. The data for this analysis can be found in Appendix A-1.3 Determine of Significant Particle Formation Level.

Table 12: Results of t-test for air blank and air blank with toluene samples

	Air blank	Air blank with toluene
Mean	6.920521	6.580472
Variance	22.69409	18.015
Observations	29	29
Pearson Correlation	0.925553	
Hypothesized Mean Difference	0	
df	28	
t Stat	1.01106	
P(T<=t) one-tail	0.160323	
t Critical one-tail	1.701131	
P(T<=t) two-tail	0.320645	
t Critical two-tail	2.048407	

Since the p value is greater than 0.05, the difference between the means of the two sample sets are not significant at a 95% confidence interval. Thus, this confirms that gas phase toluene in the reactor in the absence of UV light does not significantly affect the amount of fine particulate matter present.

5.3 Minimal Exposure Experiment

5.3.1 Constant Recirculation Time

The set of minimal exposure experiments was performed to determine the minimal amount of UV light exposure required for observable particle formation to occur. To do this, the first experiment included 1 minute of UV exposure, and each following experiment increased the duration of UV exposure by 1 minute, until significant particle formation was observed. The toluene concentration in each experiment was fixed at 55-85 ng/mL, and the post-UV recirculation time was fixed at 5 minutes. The particle formation results from this set of experiments is shown below in Figure 15.

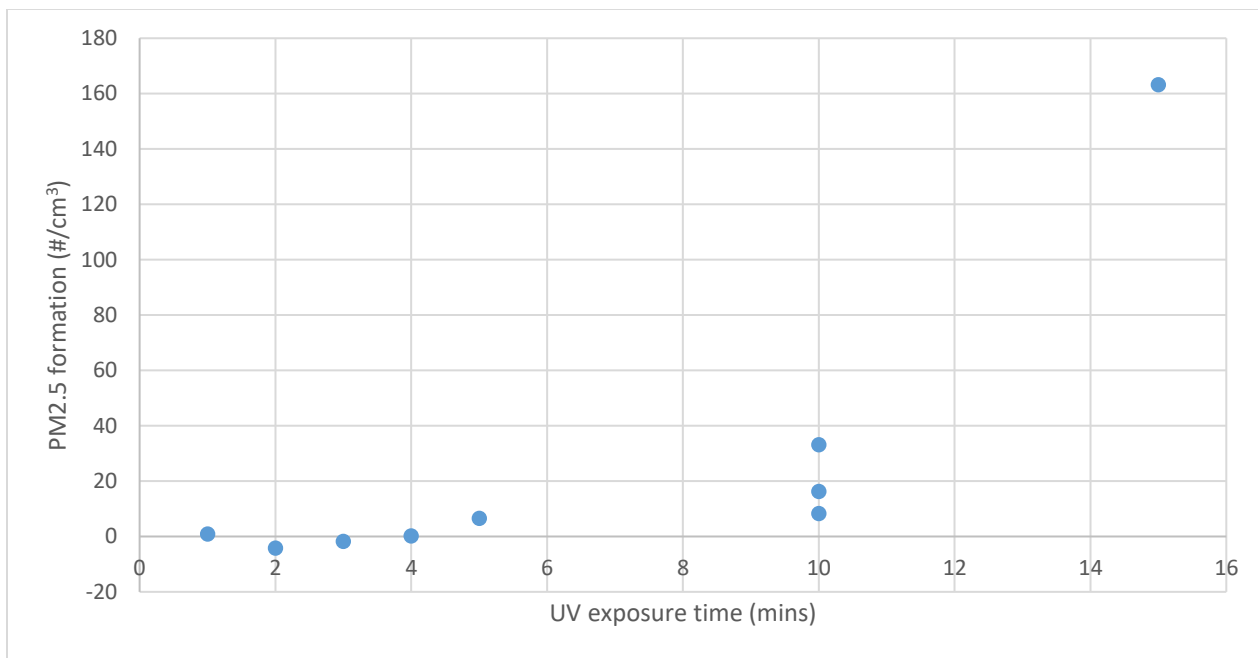


Figure 15: Fine particulate matter formation vs. UV exposure time in minimal exposure experiments with constant recirculation time

The criteria for determining whether significant particle formation has occurred was selected to be relative to the difference in fine particulate matter before and after toluene addition to the reactor, as presented in Table 12 of Section 5.2.2 Toluene. The mean of the difference between the two sample sets was -0.340 particles/cm³, and the standard deviation was 1.780 particles/cm³. The data and analysis can be found in Appendix A-1.3 Determine of Significant Particle Formation Level. The minimum level of fine particulate matter formation determined to be significant is the

amount that would exceed the level of the difference considered to be normal. This is equal to the sum of the mean and one standard deviation of the particle difference before and after toluene addition, meaning the minimum amount of particle formation considered to be significant would be 1.440 particles/cm³. Therefore, for the minimal exposure experiments with constant recirculation time, the minimum amount of UV exposure required for significant particle formation is 5 minutes.

Figure 16 below shows the particle size distribution for the experiment with 5 minutes of UV exposure followed by 5 minutes of post-UV recirculation.

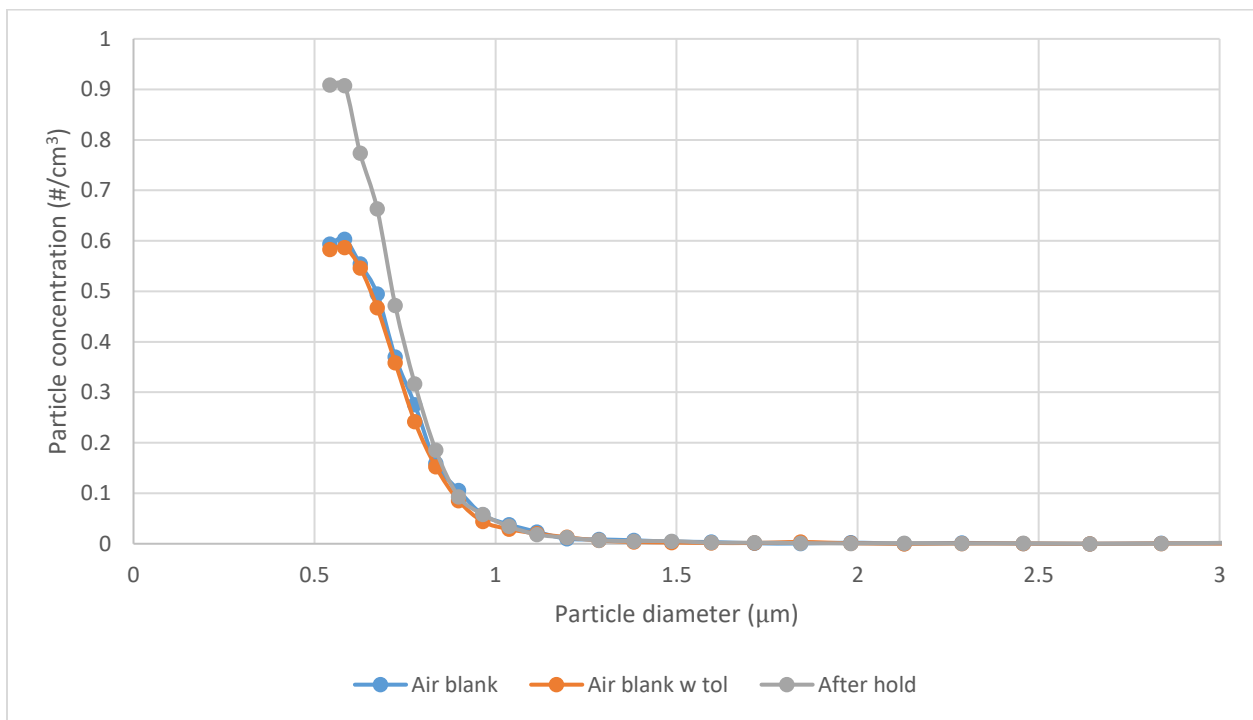


Figure 16: Particle size distribution for minimal exposure experiment with constant post-UV recirculation, with 5 minutes of UV exposure and 5 minutes of post-UV recirculation

As is evident in Figure 16, most of the particles formed during the UV exposure are close to the lower detection limit of the APS. The peak particle size formed occurs at particle diameters of 0.542-0.583 µm, with 0.909 particles/cm³. This can be compared to the air blank sample before the UV exposure, which showed a peak of 0.587 particles/cm³ at a particle diameter of 0.583 µm. With the short duration of UV exposure and post-UV recirculation, there is an observable increase in particle number, but not in particle diameter.

5.3.2 Constant Total Time

Since the duration of each of the minimal exposure experiments with constant recirculation time was short in comparison to the duration of the post-UV recirculation, a second set of minimal exposure experiments was carried out. This set of experiments fixed the total experiment time, including both the UV exposure time and the post-UV recirculation time. Fixing the total experiment time allows the determination of whether the recirculation of existing particles will noticeably cause further increased particle formation. The total time was designated to be 6 minutes, in order to be able to relate the results to those from the minimal exposure experiment with constant recirculation time. The particle production results for the experiment are presented below in Figure 17.

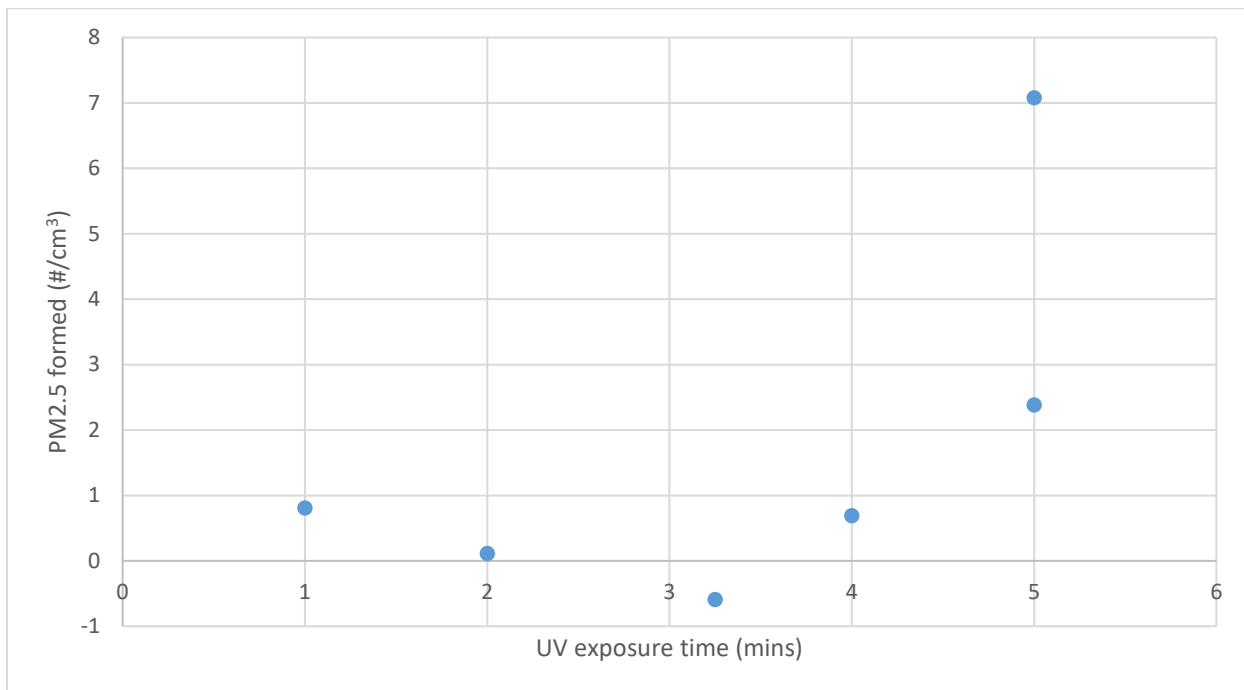


Figure 17: Fine particulate matter formation vs. UV exposure time in minimal exposure experiments with constant total time

The significance of particle formation was done using the same values as those in the minimal exposure with constant recirculation experiment. Similar to the minimal exposure experiment with constant recirculation time, the minimum UV exposure duration for which significant particle formation was observed was 5 minutes. Figure 18 below shows the particle size distribution from one of the minimal exposure experiments with 5 minutes of UV exposure and 1 minute of post-UV recirculation.

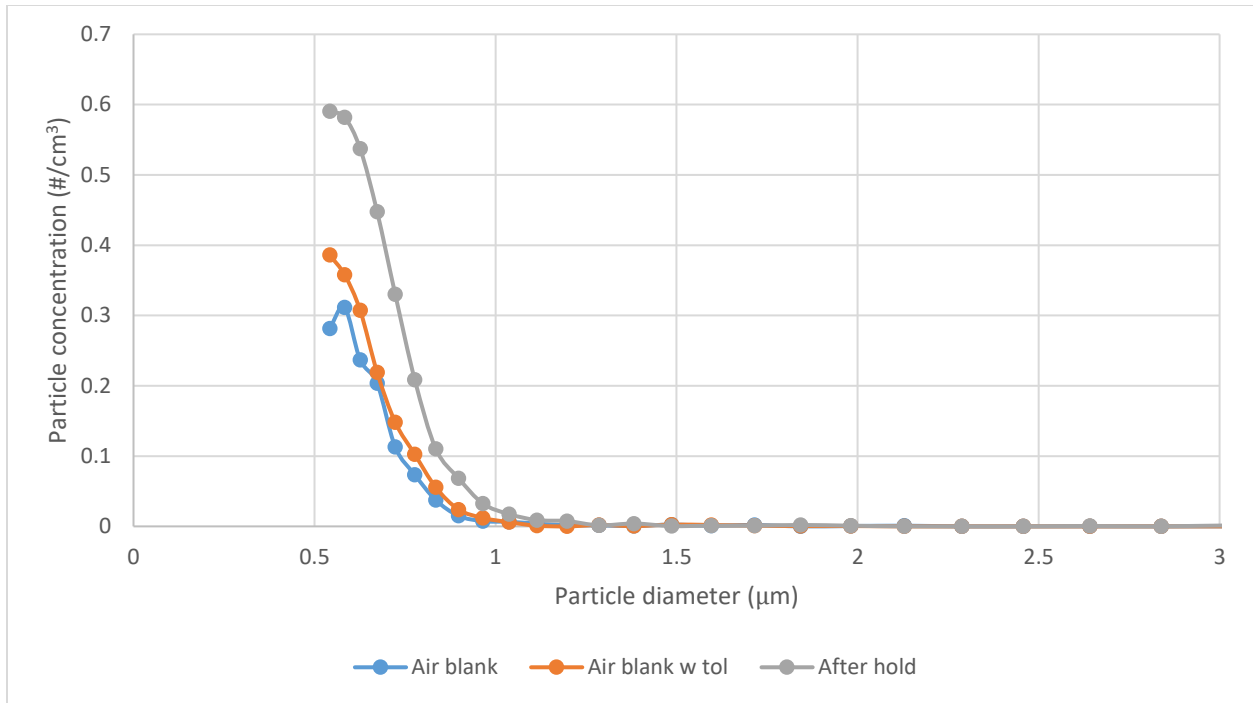


Figure 18: Particle size distribution for minimal exposure experiment with constant post-UV recirculation, with 5 minutes of UV exposure and 1 minute of post-UV recirculation

The particle size distribution for the minimal exposure experiment in Figure 18 is similar to the previous one shown in Figure 16. The particle diameter peaks in both the experiments are found at 0.542 μm, and the fine particulate matter formation levels are similar at 7.079 particles/cm³ (Figure 18) and 6.523 particles/cm³ (Figure 16). This is expected, as the only variable that differed between the two experiments is the duration of the post-UV recirculation. The experiment represented by Figure 18 had 1 minute of post-UV recirculation, while the experiment shown by Figure 16 had 5 minutes of recirculation time. This suggests that the amount of post-UV recirculation time has a relatively small, if any, effect on the amount of particle formation.

5.4 Factorial Experiment

The factorial experiment was designed to investigate the effects of three factors that were considered to be likely to have an effect on UV-induced particle formation. These factors are the initial amount of toluene present in the system, the duration of the UV irradiation, and the duration of the post-UV recirculation time. Two levels were selected for the initial toluene levels and three levels were selected for both the UV irradiation time and the post-UV recirculation time. A summary of the levels of the factors tested is shown below in Table 13.

Table 13: Summary of levels of factors in factorial experiment

Factor	Levels
Toluene concentration	55-85 ng/mL 100-125 ng/mL
UV irradiation time	5 minutes 10 minutes 15 minutes
Post-UV recirculation time	1 minute 5 minutes 15 minutes

Due to factors external to the experimental conditions, the amount of toluene injected into the system did not correspond directly to the amount of gas-phase toluene present measured by the GC. Thus, the two levels for initial toluene level were designated to be additions of 9 μL and 15 μL of liquid toluene. Injection of 9 μL of liquid toluene into the system resulted in between 55-85 ng/mL of gas-phase toluene, and injection of 15 μL of liquid toluene resulted in 100-125 ng/mL of gas-phase toluene.

The three levels of UV irradiation time were 5 minutes, 10 minutes, and 15 minutes. The shortest irradiation time of 5 minutes was selected from the results of the minimal exposure experiment, being the minimum amount of UV irradiation time required to see significant particle formation. In addition, 5 minutes of UV exposure is known to have a noticeable germicidal effect, and thus is a realistic duration of time that could be used for germicidal UV treatment (Hunt and Anderson, 2016). The higher two levels were selected to be double and triple the minimum required time.

For post-UV recirculation time, the three levels selected were 1 minute, 5 minutes, and 15 minutes. 1 minute of recirculation was selected as the shortest time in order to see the effect of minimal recirculation. It was not possible to incorporate experiments with no post-UV recirculation time, since some time was required to switch over the equipment from recirculation to sampling. 5 minutes and 15 minutes were selected to mimic the durations of the shortest and longest UV irradiation levels.

The fine particulate matter production values for the factorial experiments are shown below in Table 14. Particle size distribution graphs for all of factorial experiments can be found in Appendix A-2.2 Particle Size Distributions.

Table 14: Fine particulate matter production in factorial experiments

Initial toluene level	Length of UV exposure (mins)	Length of post-UV recirculation (mins)	Fine particulate matter production (# of particles/cm ³)
9 μ L (55-85 ng/mL)	5	1	7.0789
		5	6.5228
		15	1.2095
	10	1	213.9533
		5	8.2193
		15	33.0308
	15	1	16.2047
		5	6.8654
		15	27.2079
15 μ L (100-125 ng/mL)	5	1	27.2079
		5	163.1487
		15	42.8421
	10	1	8.3504
		5	82.5780
		15	4.4056
	15	1	18.2016
		5	261.3203
		15	59.6718
15	1	1449.7600	
	5	698.9044	
	15	868.4290	

For comparison, the specifications of the experiments yielding the highest and lowest fine particulate matter formation in Table 14 are compared below in Table 15. The graphs of the corresponding particle size distributions are also shown below in Figure 19 and Figure 20.

Table 15: Comparison of specifications of select factorial experiments

	Lowest fine particulate matter formation	Highest fine particulate matter formation
Toluene added (μL)	9	15
Toluene consumption (ng/mL)	1.22	7.66
UV irradiation time (hh:mm:ss)	00:05:00	00:15:00
Post-UV recirculation time (hh:mm:ss)	00:15:00	00:01:00
Initial fine particulate matter ($\#/ \text{cm}^3$)	6.126	5.370
Fine particulate matter formed ($\#/ \text{cm}^3$)	1.210	1449.760
Particle diameter peak(s) (μm)	0.542	0.542
Particle concentration at peak ($\#/ \text{cm}^3$)	0.176	14.583

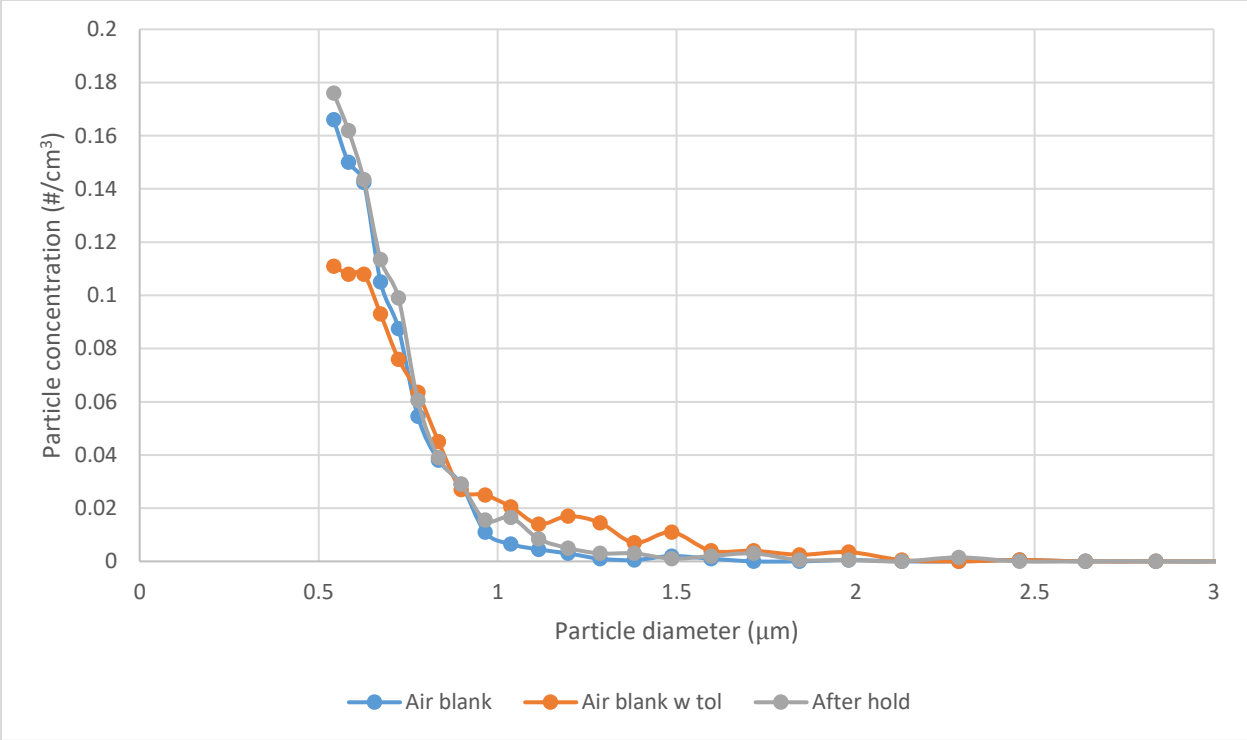


Figure 19: Particle size distribution for the factorial experiment with the lowest fine particulate matter formation (55-85 ng/mL toluene, 5 minutes UV, 15 minutes recirculation)

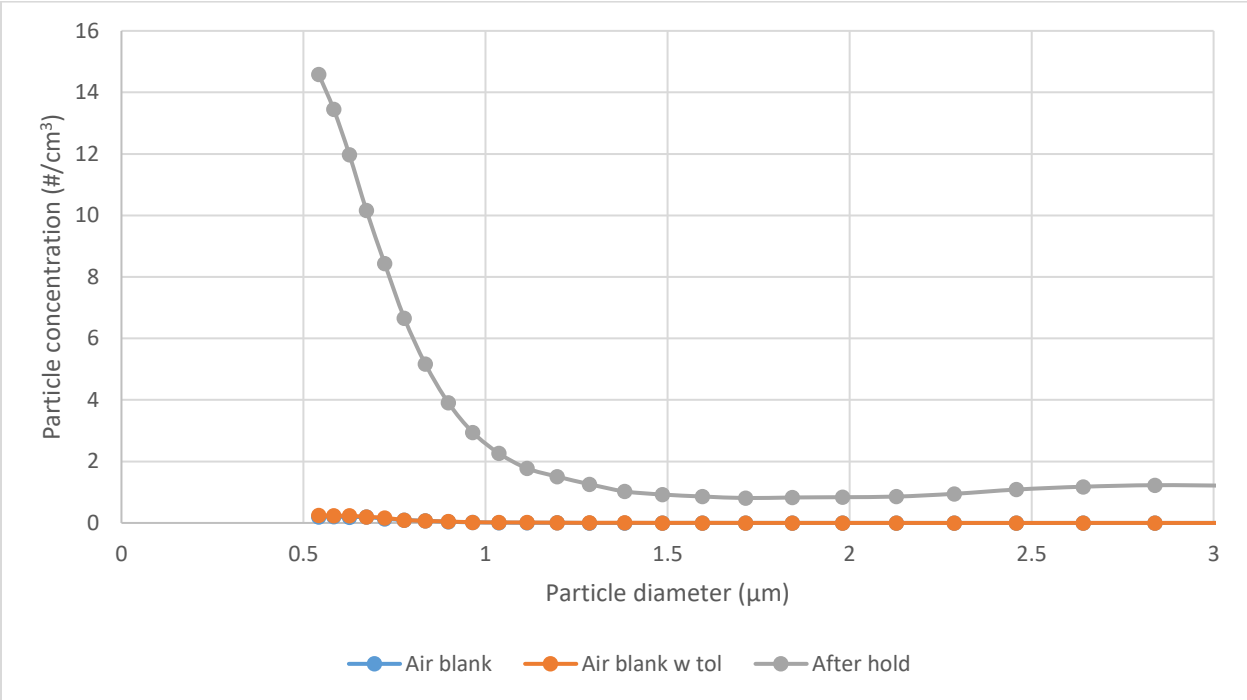


Figure 20: Particle size distribution for the factorial experiment with the lowest fine particulate matter formation (100-125 ng/mL toluene, 15 minutes UV, 1 minute recirculation)

From the specifications and particle size distributions of the two selected experiments, there are a number of aspects to compare. Initially, both experiments had a similar amount of pre-existing particles, thus seeding of SOA particles should not have a significant effect on the difference overall particle formation between the experiments. The experiment with the lowest fine particulate matter formation level had a toluene concentration of 55-85 ng/mL, a UV exposure time of 5 minutes, and a post-UV recirculation time of 15 minutes. Meanwhile, the experiment with the highest fine particulate matter formation level had a toluene concentration of 100-125 ng/mL, a UV exposure time of 15 minutes, and a post-UV recirculation time of 1 minute. From these results, it appears that higher levels of toluene and longer periods of UV irradiation result in higher levels of particle formation. In addition, the experiment with the highest fine particulate matter formation had toluene consumption that was about 6 times greater than that of the lowest fine particulate matter formation experiment. This indicates that the higher levels of initial toluene and longer UV irradiation period allowed for a greater amount of the initial gas phase toluene to be converted into particulate matter. Most notably, the experiment with the highest amount of fine particulate matter formation shows observable amounts of particles larger than fine particulate matter as well. However, both experiments show the same large peak at a particle diameter of 0.542 μm . Although one experiment shows a much higher amount of particle formation than the other, the general shape of the particle size formations are relatively similar.

For all of the sets of conditions tested in the factorial experiment, the observations are similar. The particle size distributions are all very similar in shape, with the same initial peak at a particle diameter of 0.542 μm , with no other major peaks. The magnitude of the peak and amount of particles formed varies between the experiments, but the shape of the particle size distributions are consistent between all of them.

5.4.1 Statistical Analysis

For the purpose of using Statistica 11 for data analysis, the initial toluene levels are represented by the number of microliters of liquid toluene injected into the system. This divides the initial gas phase toluene concentrations into two categories, and allows for the comparison of the effects of

higher and lower levels of initial toluene present. Table A-5 in Appendix A-2.3 Data for Statistica 11 Analysis outlines the exact data values used for this analysis.

Using Statistica's design of experiment (DOE) analysis of variance (ANOVA) for a 3³ design, the results in Table 16 were obtained. This analysis considered both linear (L), quadratic (Q), and combined (L+Q) trends for the factors being considered.

Table 16: Design of experiment ANOVA analysis in Statistica 11

	Sum of squares	Degrees of freedom	Mean square	F	p
(1)Toluene (L)	480975	1	480975.0	5.817481	0.030170
(2)UV (L)	821710	1	821710.3	9.938737	0.007055
UV (Q)	123132	1	123131.8	1.489302	0.242482
(3)Recirculation (L)	45773	1	45772.6	0.553628	0.469144
Recirculation (Q)	3071	1	3070.7	0.037140	0.849947
Error	1157486	14	82677.5		
Total SS	2708874	19			

	Sum of squares	Degrees of freedom	Mean square	F	p
(1)Toluene L	480975	1	480975.0	5.817481	0.030170
(2)UV L+Q	944842	2	472421.1	5.714020	0.015336
(3)Recirculation L+Q	45773	2	22886.4	0.276815	0.762249
Error	1157486	14	82677.5		
Total SS	2708874	19			

A confidence interval of 95%, or $p < 0.05$, was selected to be used in the factorial experiment. From the DOE ANOVA analysis, the initial toluene level, and the duration of UV exposure were considered to be significant, while the length of the post-UV recirculation time was not significant. The lowest p level corresponds to the length of UV irradiation, therefore it is suggested that this would be the most significant factor with respect to particle formation.

Another analysis that was done was the factorial ANOVA in Statistica 11, as shown in Table 17.

Table 17: Factorial ANOVA analysis in Statistica 11

	Sum of squares	Degrees of freedom	Mean square	F	p
Intercept	895411.1	1	895411.1	5581.808	0.000179
Toluene	506721.2	1	506721.2	3158.795	0.000316
UV	967188.9	2	483594.4	3014.628	0.000332
Recirculation	47569.3	2	23784.7	148.269	0.006699
Toluene*UV	822240.2	2	411120.1	2562.838	0.000390
Toluene*Recirculation	14845.1	2	7422.6	46.271	0.021155
UV*Recirculation	86563.8	4	21641.0	134.905	0.007372
Toluene*UV*Recirculation	252625.0	4	63156.2	393.703	0.002535
Error	320.8	2	160.4		

With the factorial ANOVA analysis, the software deemed all factors and combinations of factors to be significant by the significance criteria of $p < 0.05$ from the data provided. Further investigation of the p-values determined that the individual factors of initial toluene level and duration of UV exposure were considered to be more significant than the length of the post-UV recirculation time, which agrees with the DOE ANOVA analysis. As for the combinations of factors, the interaction of toluene and UV duration is to be the only interaction to have a p-value close to those of the individual factors considered to be significant. The p-values for post-UV recirculation time, the combination of UV exposure time and post-UV recirculation, and the combination of all three factors were around 10 times larger, indicating that they are less significant. Finally, the p-value for the combination of initial toluene level and post-UV recirculation time was around 100 times greater than the p-values of the most significant factors, showing that it has the least significance on the amount of fine particulate matter formed.

From these results, it can be concluded that the amount of post-UV recirculation time does not have a significant effect on the amount of particle formation. This means that in indoor air environments that utilize germicidal UV treatment, the amount of time that has elapsed after the completion of the UV treatment will not have a significant effect on the amount of fine particulate matter present.

5.5 Unfiltered Air Experiment

For the purpose of comparison, an experiment was done with unfiltered compressed air, while all other experimental conditions remained unchanged. The capsule filter removes VOCs and particulate material larger than $0.3\ \mu\text{m}$ in diameter from the gas stream. The removal of this filter means that all components present in the air will be part of the gas being tested. Figure 21 shows a comparison of the initial toluene levels from the minimal exposure experiments, which includes all the filtered and unfiltered experiments using the compressed air from the building supply.

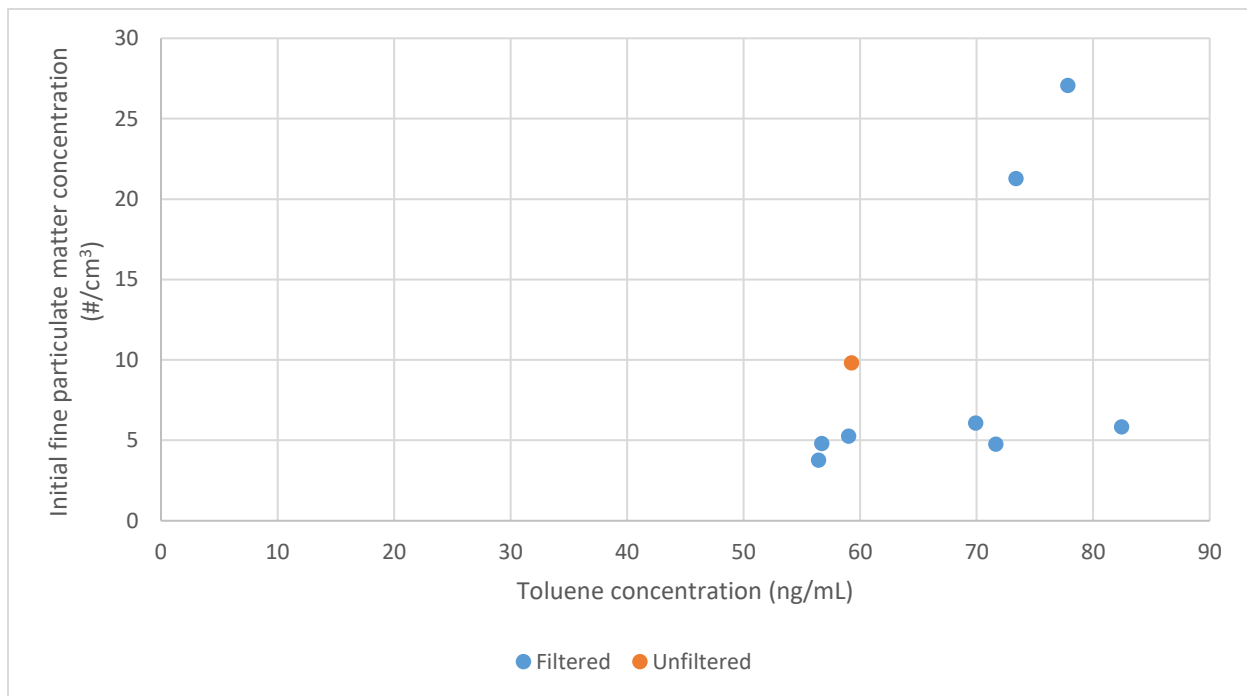


Figure 21: Initial toluene concentration vs. initial fine particulate matter concentration for compressed air experiments

From Figure 21, it is can be observed that the initial fine particulate matter level in the unfiltered experiment is slightly higher than those of filtered experiments with similar initial toluene levels, however it is not significantly higher than some of the maximum levels observed.

Figure 22 below is the same graph as Figure 17: Fine particulate matter formation vs. UV exposure time in minimal exposure experiments with constant total time, with the addition of the fine particulate matter production from the unfiltered compressed air experiment.

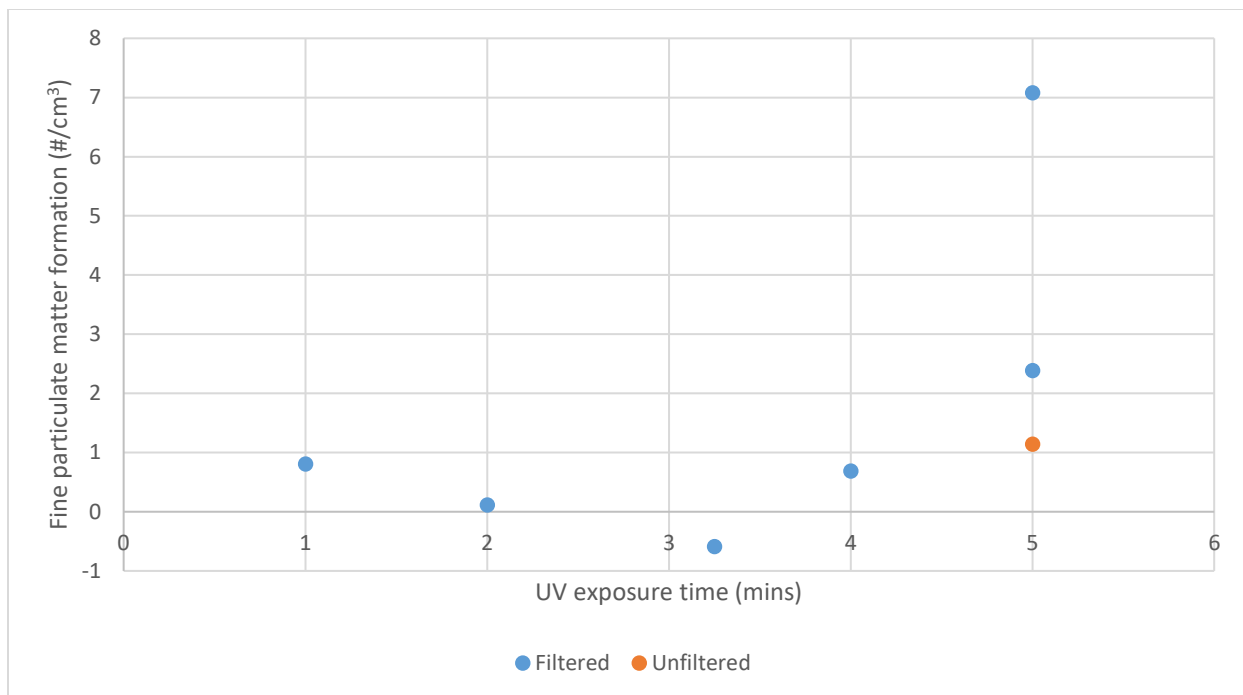


Figure 22: UV exposure time vs. fine particulate matter formation for compressed air experiments

From Figure 22, it can be observed that the fine particulate matter formation in the unfiltered experiment is similar to those in the filtered experiments. Despite having a comparatively higher amount of particles initially present, the unfiltered experiment did not yield a significantly higher amount of fine particulate matter production, contrary to expectation. Therefore, there are not a significant number of particles present in the compressed air from the building system, and the particles present do not significantly increase the amount of fine particulate matter formation. This could be due to the fact that since there were so few particles initially present, any resultant effects may not be observable in this experiment. The effects of pre-existing particles are likely to be better observed in the unfiltered room air experiments, as it is likely that there will be more particles initially present in room air than in the compressed air from the building. These results will be discussed in the following Section 4.2.4 Room Air Experiments.

Another point of comparison between the filtered and unfiltered compressed air experiments is the amount of particle growth observed over the period of UV irradiation. Figure 23 shows a comparison of the particle increase for each size fraction between the filtered and unfiltered compressed air experiments with the same conditions. The experiments both had toluene concentrations of 55-85 ng/mL, 5 minutes of UV irradiation, and 1 minute of post-UV

recirculation. The particle increase for each particle size fraction is calculated by subtracting the number of particles present at the particular size fraction before UV irradiation from the number of particles present at the same fraction after UV irradiation.

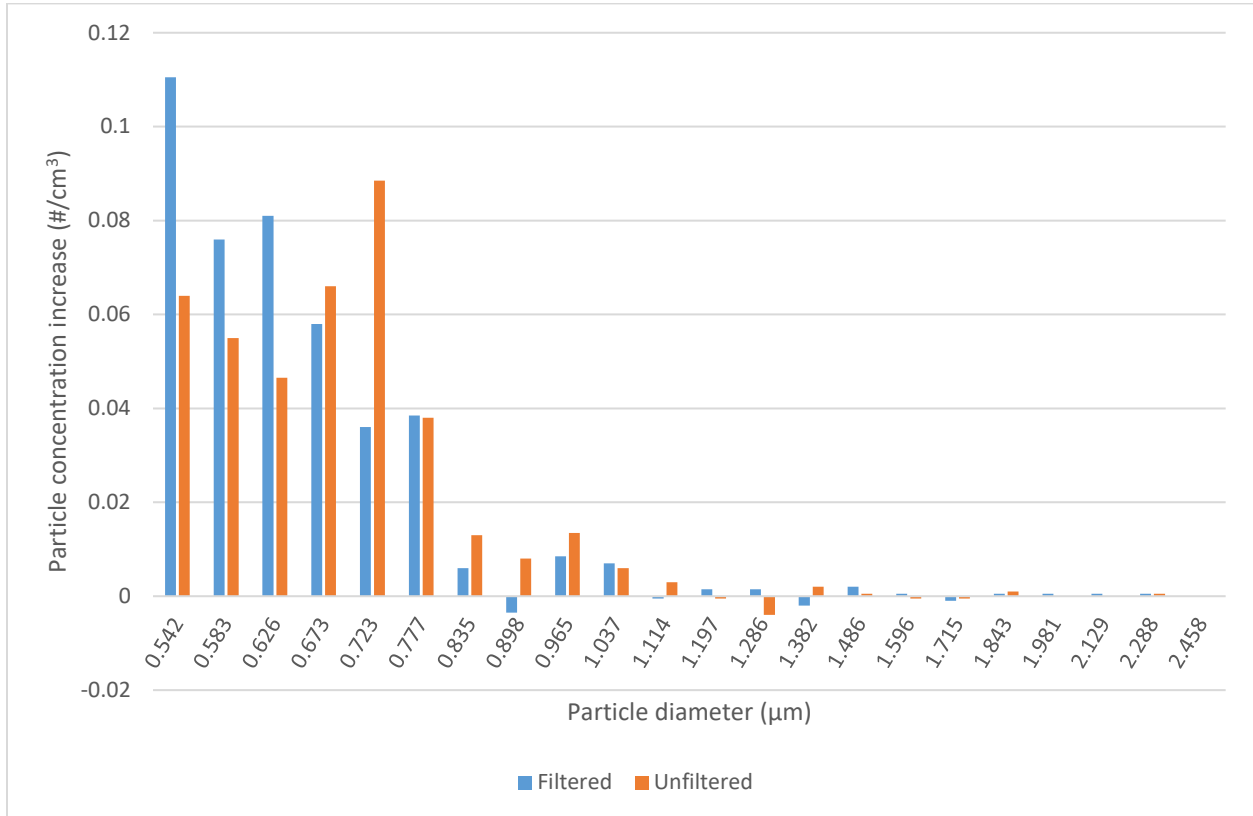


Figure 23: Particle increase for filtered and unfiltered compressed air experiments with 55-85 ng/mL toluene, 5 minutes UV exposure, 1 minute post-UV recirculation

Since the unfiltered experiment did not have significantly higher particle formation as compared to the filtered experiment, despite having more initial particles, it can be hypothesized that instead, there may be an increased rate of particle growth. In Figure 23, it can be observed that the larger particles with diameters from 0.673-1.114 µm had either greater or similar levels of increase in the unfiltered experiment. However, for particles with diameters from 0.542-0.626 µm, there was a greater increase observed in the filtered experiment. Higher levels of increase are only observed for larger size fractions in the unfiltered experiment. Therefore, it is plausible that the lower level of particle formation in the unfiltered experiment is correlated with a higher levels of particle growth.

5.6 Room Air Experiments

The room air experiments were designed to give a better representation of the effects of germicidal UV treatment on particle formation by using air from an actual room. The compressed air from the building supply used in the most of the experiments is essentially clean, filtered air. Using room air means that any pre-existing particles or compounds found in the room will also be found in the initial air supplied to the reactor. In addition, the use of room air allows for the consideration of the effects of higher levels of humidity in the air. The relative humidity of indoor air can vary greatly, depending on a number of factors. Some of these factors include what the room is used for, the effectiveness of the room ventilation, the climate, and the time of year. For comparison, the ideal indoor relative humidity in terms of human comfort is between 30-40% (Wolkoff and Kjærgaard, 2007).

All the room air experiments were performed under the same conditions, with the only two variations being whether or not the air was initially passed through the filter, and the relative humidity of the air. For comparison, the relative humidity of the building's compressed air was 0.01%. The compressed air was collected in a sealed bag containing the General handheld psychrometer, in order to measure the relative humidity of a static sample of the gas. All the experiments were performed with a toluene concentration of 55-85 ng/mL, 5 minutes of UV irradiation, and 1 minute of post-UV recirculation.

The amount of fine particulate matter present before UV irradiation in all of the room air experiments is shown in Figure 24. The trend across all of the experiments appears to be that higher relative humidity levels yield higher initial fine particulate matter levels. In addition, it is evident that the use of the filter results in lower levels of fine particulate matter, as expected. Even for a filtered experiment with a high relative humidity of 43.2%, the amount of fine particulate matter initially present is lower than that of any of the unfiltered experiments. For comparison, the initial amounts of fine particulate matter present in filtered room air experiments under 25% relative humidity are similar to initial fine particulate matter levels in the experiments using compressed air from the building supply.

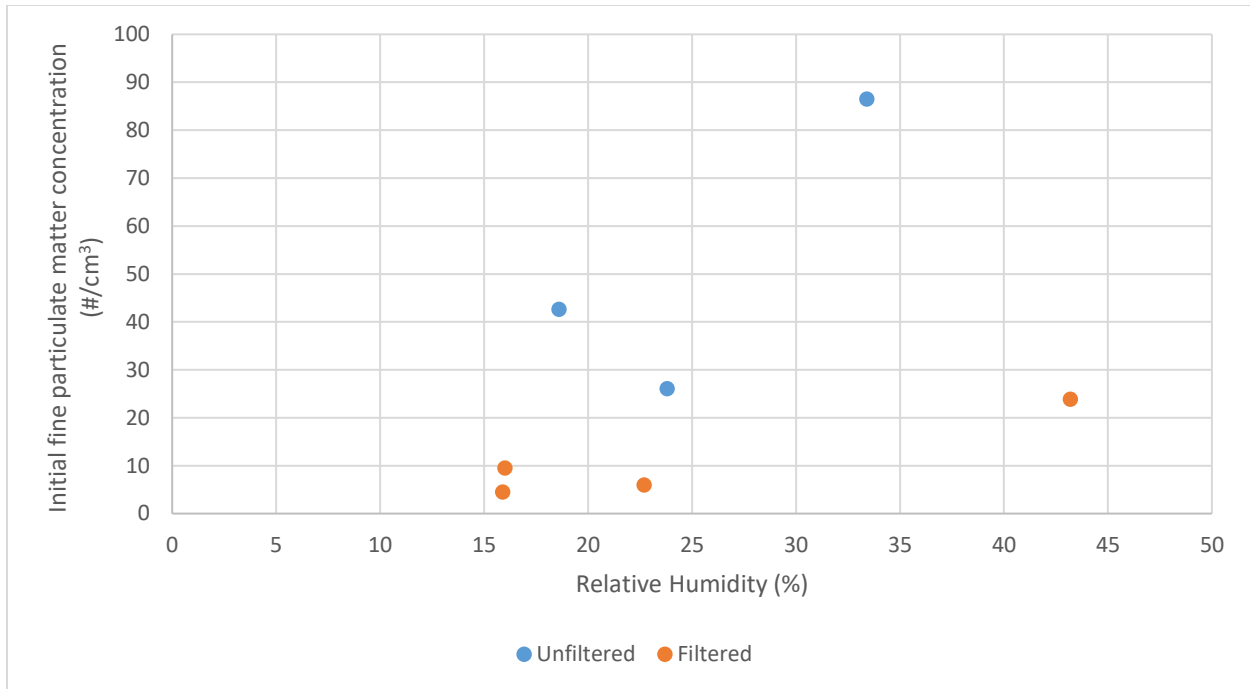


Figure 24: Initial fine particulate matter levels for unfiltered and filtered room air experiments

Figure 25 shows the fine particulate matter formation results of both the unfiltered and filtered experiments. The filtered experiments involved passing the room air through the HEPA and activated carbon filter. As with previous experiments, the amount of fine particulate matter formed was calculated as the amount of fine particulate matter present before UV irradiation subtracted from the amount present before the irradiation. It is evident in both of these sets of experiments that higher levels of relative humidity yield greater levels of particle formation.

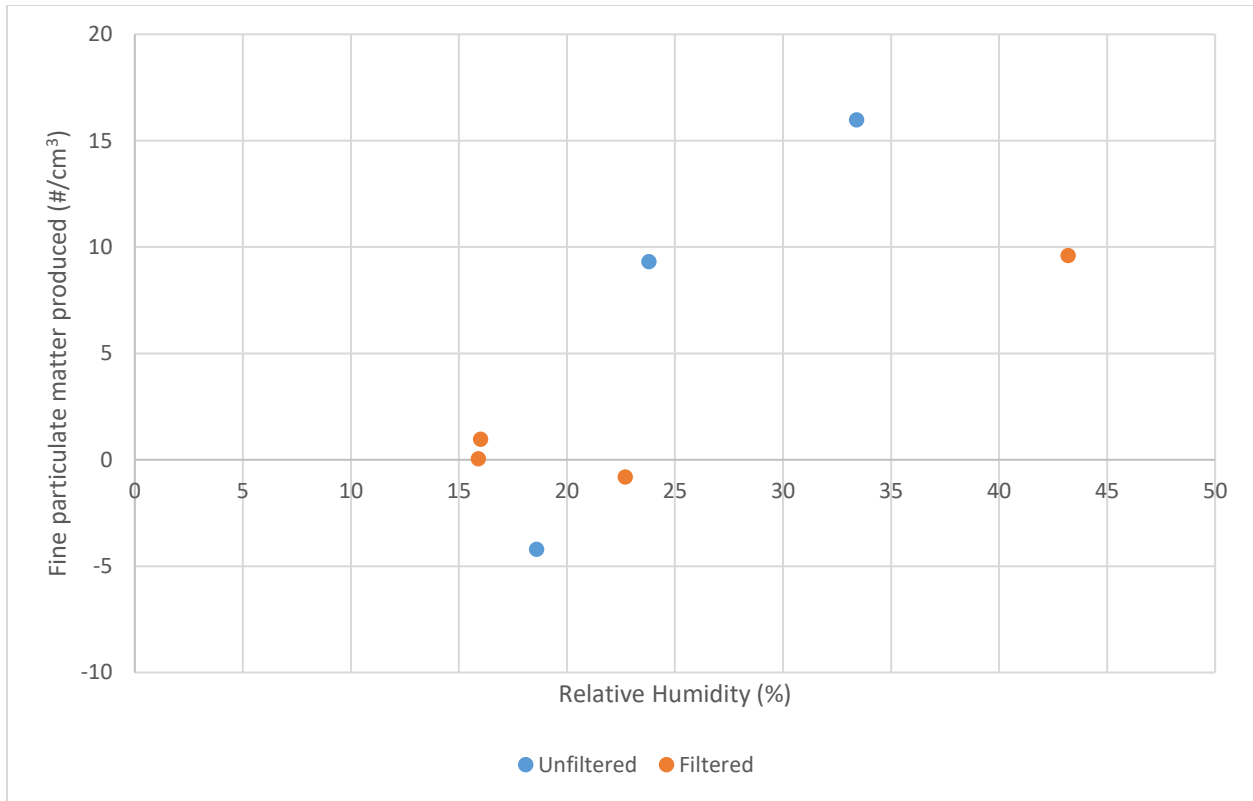


Figure 25: Fine particulate matter production for unfiltered and filtered room air experiments

Thus, it can be observed from the room air experiments that higher humidity levels result in higher amounts of fine particulate matter formed through UV photooxidation. This is true for both the filtered and unfiltered room air, despite the fact that the unfiltered air has a larger amount of particles present initially. In addition, the level of fine particulate matter formation for the filtered experiments at a relative humidity under 25%, and the unfiltered experiment with a relative humidity under 20%, was similar to that from the experiments using the compressed air supply from the building.

Similar to the analysis for the unfiltered air experiment, the particle increase values for the unfiltered and filtered room air experiments were graphed. Figure 26 and Figure 27 show the particle increase values for all of the unfiltered and filtered room air experiments respectively. Figure 28 provides a comparison between the highest and lowest relative humidity experiments for both the unfiltered and filtered room air experiments.

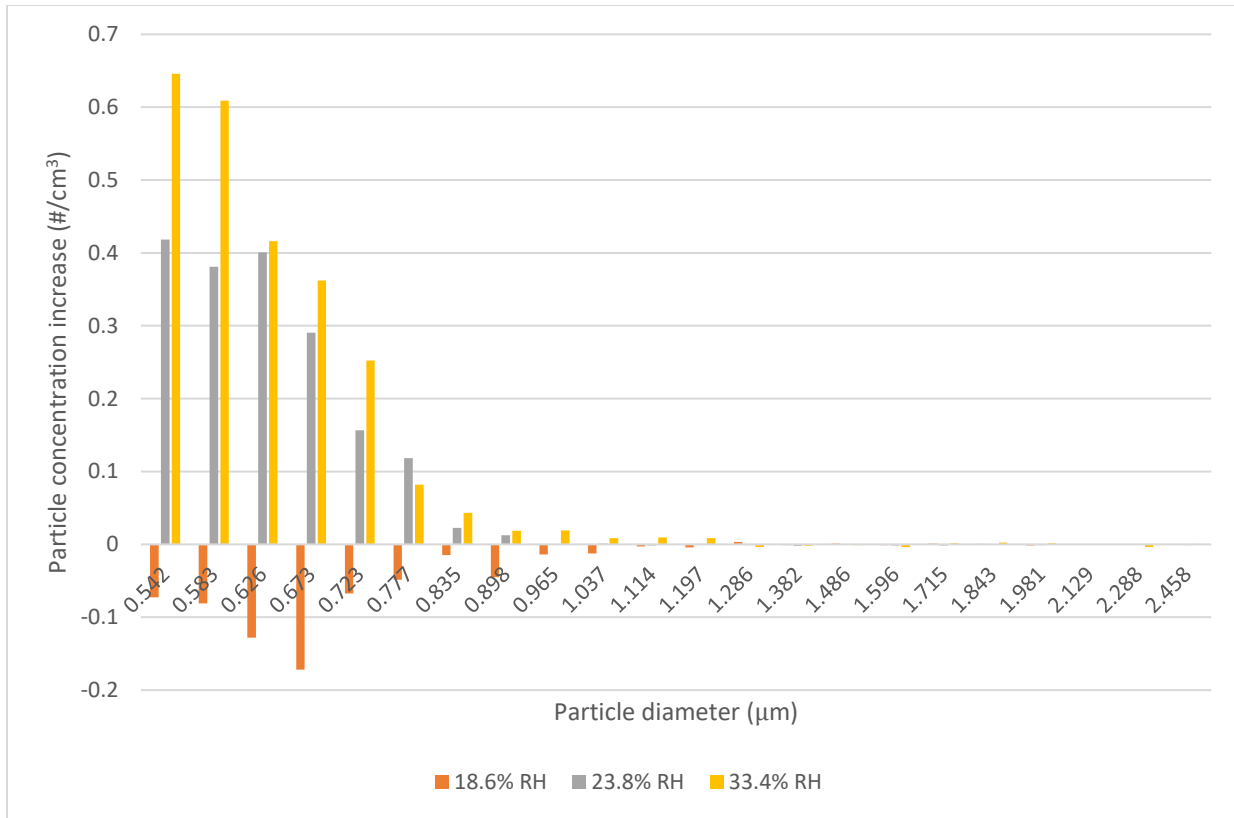


Figure 26: Particle increase values for unfiltered room air experiments

In comparing the particle increase values for the unfiltered room air experiments, it is evident that the lowest humidity experiment shows a different trend from the higher humidity experiments. At 18.6% RH, there does not appear to be any increase in concentration for particles with diameters of 0.542 µm and larger. Instead, the number of particles with diameters of 0.542-1.037 µm decreased between the samples taken before and after UV irradiation. For the higher two levels of relative humidity, particle concentration increases were generally observed to be higher at 33.4% RH than 23.8% RH for all particles larger than 0.542 µm in diameter. The increase in concentration for a multiple consecutive increasing particle sizes suggests that particle growth is occurring. This agrees with the earlier conclusion that higher levels of relative humidity result in greater fine particulate matter formation; it appears that with increasing levels of relative humidity in unfiltered room air, there are increased levels of both particle formation and particle growth.

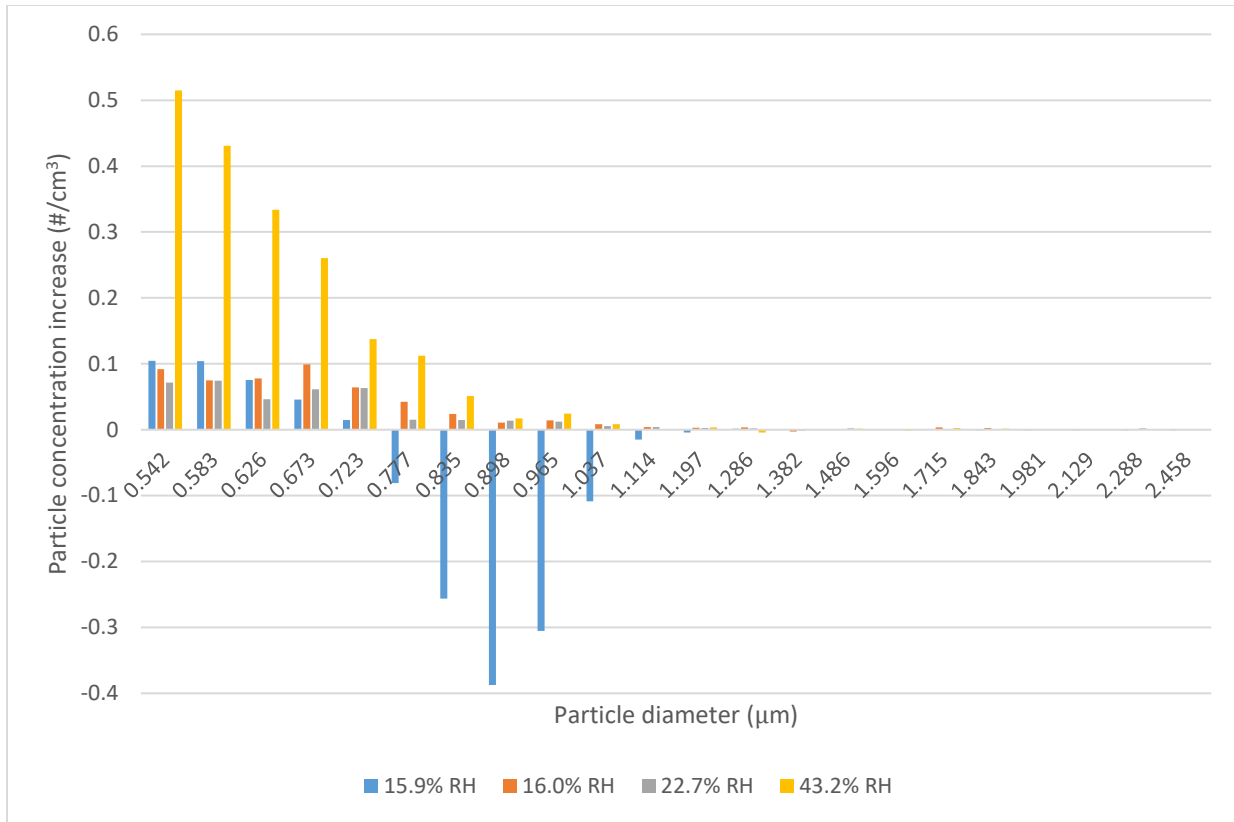


Figure 27: Particle increase values for filtered room air experiments

For filtered room air experiments, the experiments had lower levels of fine particulate matter initially present in the reactor, and generally show a different trend from the unfiltered experiments. For relative humidity levels from 15.9-22.7%, the increase in concentration of particles was relatively similar between the experiments, all showing small increases of around 0.1 particles/cm³ or less. At 15.9% RH, particle increase values for particles with diameters of 0.777-1.114 µm differ from the trend, showing decreases of up to 0.4 particles/cm³. Another experiment had a very similar relative humidity level at 16.0%, but did not show the same trend as the experiment with 15.9% RH. The most significant difference was observed for the experiment with 43.2% RH, as it showed significantly higher levels of particle increase. The highest increase was observed for particles with diameters of 0.542 µm, with the levels of increase becoming smaller with increasing particle size. Similar to the results for the unfiltered room air experiments, this increase in particle concentration for a number of consecutive particle size fractions suggest that significant particle growth is occurring. This suggests that for higher levels

of relative humidity in filtered room air experiments, there is also a higher level of particle growth, along with the increased level of particle formation concluded from earlier results.

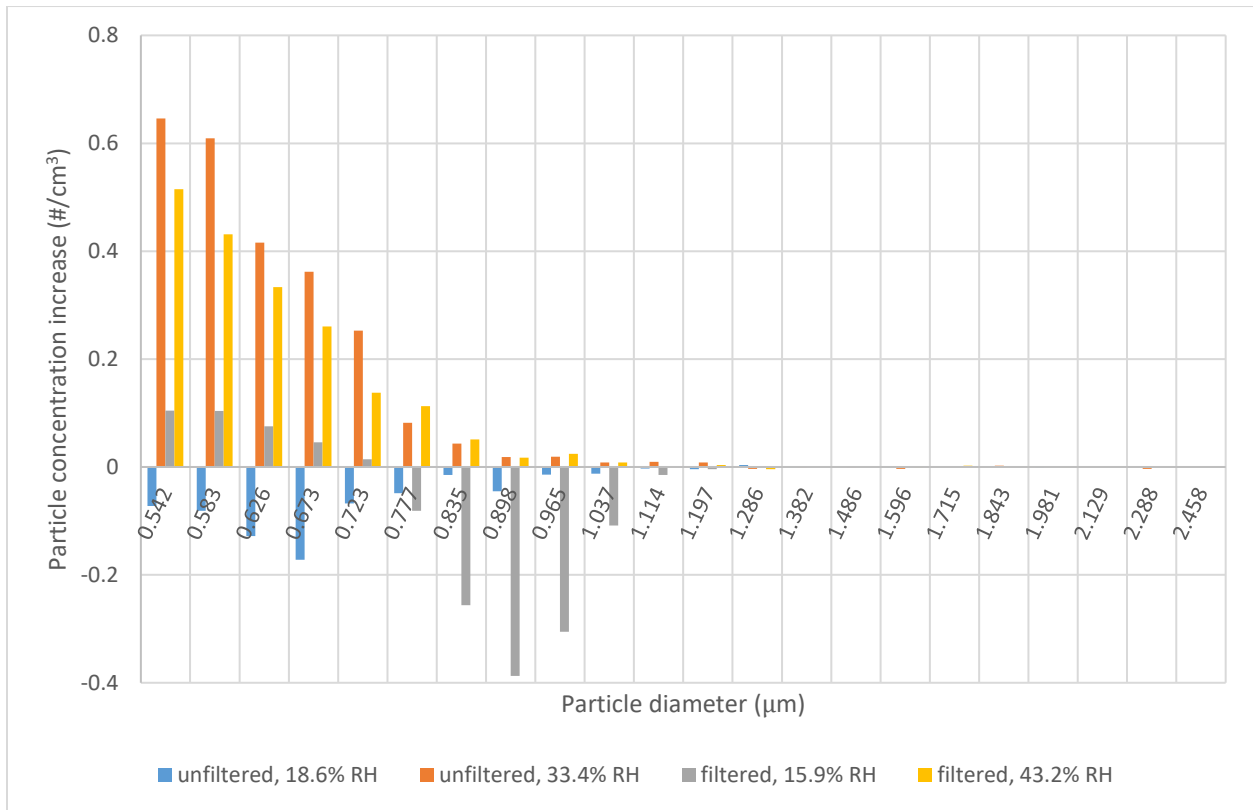


Figure 28: Comparison of particle increase values between unfiltered and filtered room air experiments

Figure 28 provides a comparison of the results for the experiments with the highest and lowest levels of relative humidity for both the unfiltered and filtered room air experiments. It is evident that the level of particle growth was greatest for the unfiltered room air experiment at 33.4% RH, despite the fact that the filtered room air experiment had a higher relative humidity of 43.2%. However, the trend for particle growth with both of these higher RH experiments is similar. This suggests that the higher level of particles initially present has a greater effect on the degree of particle growth than just the relative humidity alone.

5.7 Replicate Experiments

In order to investigate the reproducibility of the results, analysis was done on two sets of replicated experiments. Each set of these experiments used the same experimental conditions, and only varied in the amount of particles initially present, as well as the initial gas phase concentration of toluene, as these variables could not be directly controlled. Since the experiments were done using the same conditions, the resulting particle formation values can be compared to observe effects independent of the experimental conditions. The data for these replicated experiments is shown in Table 18.

Table 18: Analysis of replicate experiments

	Initial toluene concentration (ng/mL)	Initial fine particulate matter concentration (#/cm³)	Fine particulate matter formation (#/cm³)
Experiment set 1 55-85 ng/mL toluene 10 mins UV 5 mins post-UV recirculation	70.34	1.956	8.2193
	75.97	4.1084	33.0308
	56.77	7.7988	16.2047
	Mean		19.1516
	Standard deviation		10.3414
Experiment set 2 10 μ L toluene 8 mins UV 1 min post-UV recirculation	87.76	5.0164	8.8461
	72.49	2.2234	5.0087
	76.48	2.5184	7.9503
	Mean		7.2684
	Standard deviation		1.6392

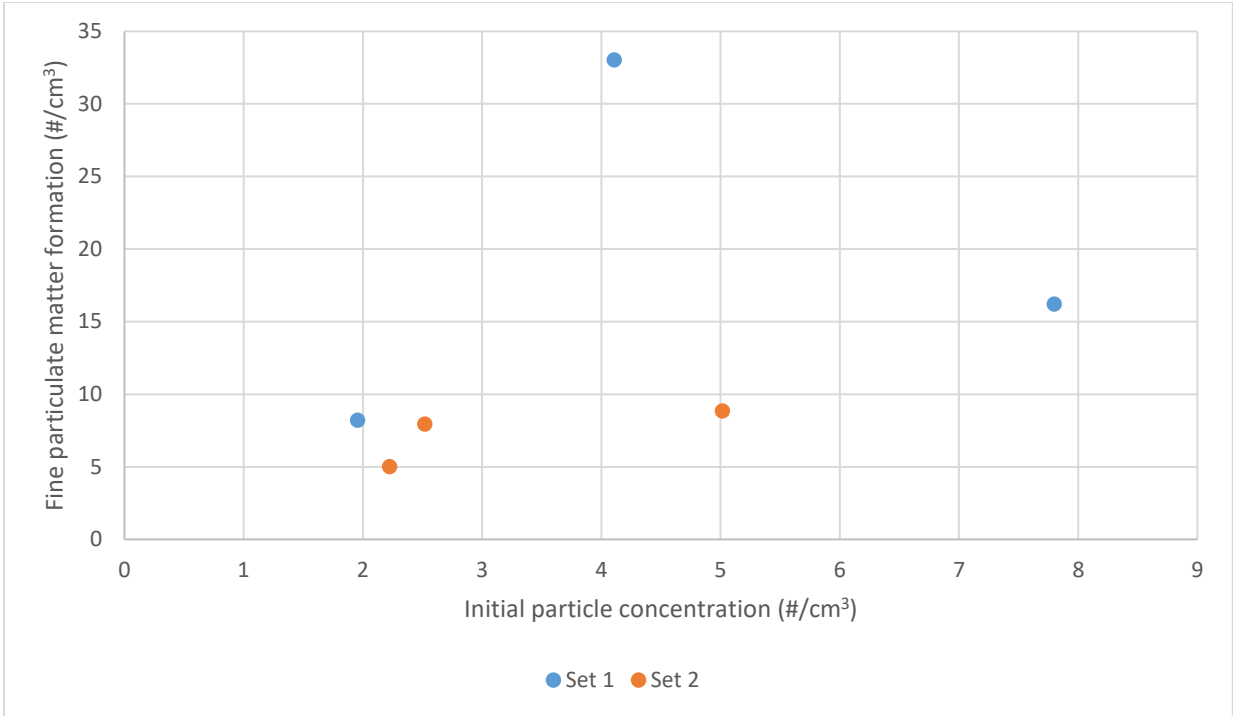


Figure 29: Initial fine particulate matter concentration vs fine particulate matter formation for replicate experiments

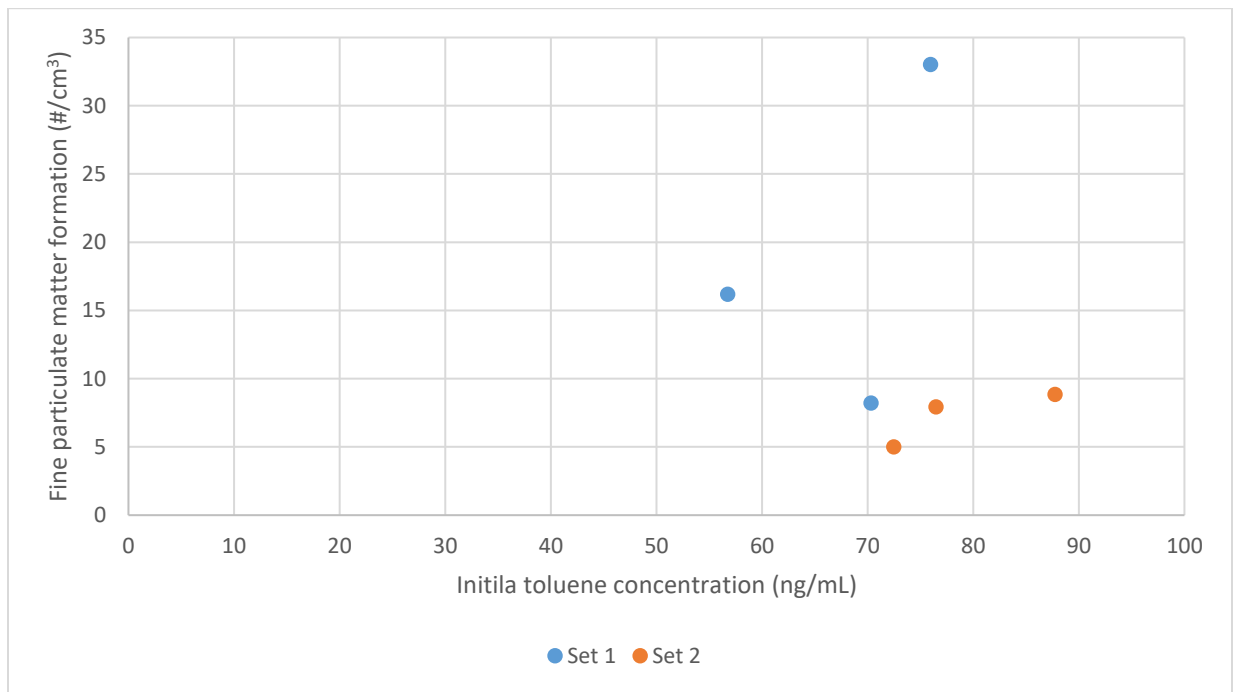


Figure 30: Initial toluene concentration vs fine particulate matter formation for replicate experiments

Figure 29 and Figure 30 can be analyzed for the relationship between the initial conditions and the amount of fine particulate matter formed during the experiments. The graphs suggest that there is no apparent correlation between either of the variables and the resulting fine particulate

matter formation. Any relationship between these either of the initial conditions and the amount of fine particulate matter formed is most likely to be minor compared to the effects of the other experimental factors.

The standard deviation of the amount of fine particulate matter formed is quite large for set 1, but much smaller for set 2. The large standard deviation in set 1 suggests that there are likely other external factors that may be influencing the amount of particle formation observed in these experiments. This may possibly include variations in the building-supplied compressed gas, or the conditions of the room, such as temperature.

5.8 Toluene Mass Balance

To determine the efficiency of the conversion of toluene to SOA particles, a mass balance can be done between the beginning and end of the experiment. In order to get an estimate of the mass balance, the difference between the sum of the masses of the toluene and particles present before and after UV exposure was calculated. For the purpose of simplification, all particles were assumed to have a density of 1.23 g/cm³, as done by Huang et al. (2013). Table 19 provides the details for two mass balances, which were done using the data from the factorial experiments with the highest and lowest levels are particle formation as examples again.

Table 19: Toluene mass balances

Experiment specifications	55-85 ng/mL toluene 5 mins UV 15 mins post-UV recirculation	100-125 ng/mL toluene 15 mins UV 1 min post-UV recirculation
Initial toluene mass (µg)	1921.308	3116.425
Initial particle mass (µg)	78.910	112.963
Final toluene mass (µg)	1889.150	2914.515
Final particle mass (µg)	74.070	126972.785
Toluene mass consumed (µg)	32.158	201.910
Particle mass formed (µg)	-4.840	126859.822
Mass balance (µg) (Initial total mass – final total mass)	36.998	-126657.912

As is evident from the non-zero mass balances in both experiments, the mass of toluene consumed in the reactions does not directly relate to the amount of particle mass formed. In fact, both of these experiments show atypical characteristics. The first experiment, the lowest particle formation experiment, shows a negative mass of particles formed. The second experiment shows a significantly higher amount of particle mass formed than toluene mass consumed. This suggests that there are significant factors affecting the mass balance that are not considered in these simplified calculations. It would be very unlikely for all the toluene mass consumed to be converted to particle mass, and it is also unlikely that all of the oxidation products formed will partition into the particle phase. One major assumption made is that the particle density is constant for all particles at 1.23 g/cm³. This is likely to be inaccurate, as the density may vary

depending on the composition of the particles, particle size, duration of UV exposure, or some other variables.

5.9 Comparison of Results

Table 20: Comparison of particle formation in experiments using compressed air from the building supply

	Experiment name				
	Complete degradation	Minimal exposure		Factorial	
		Constant recirculation time	Constant total time	Lowest fine particulate matter formation	Highest fine particulate matter formation
Toluene added (μL)	10	9	9	9	15
UV irradiation time (hh:mm:ss)	01:56:15	00:05:00	00:05:00	00:05:00	00:15:00
Post-UV recirculation time (hh:mm:ss)	0	00:05:00	00:01:00	00:15:00	00:01:00
Toluene consumption (ng/mL)	141.36	8.76	16.04	1.22	7.66
Initial fine particulate matter ($\#/cm^3$)	1.748	13.951	6.513	6.126	5.370
Fine particulate matter formed ($\#/cm^3$)	1925.632	6.523	7.079	1.210	1449.760
Particle diameter peak(s) (μm)	1.286	0.542	0.542	0.542	0.542
Peak particle concentration ($\#/cm^3$)	568.822	0.909	0.590	0.176	14.583

There are a number for points of comparison for the various experiments done using compressed air from the building supply shown in Table 20. First, it is evident that the particle formation from the complete degradation experiment is significantly different from all the other experiments with shorter UV exposure times. The particle diameter with the highest concentration is much larger for the complete degradation experiment than all the other experiments. In addition, the concentration of the particles at that peak, as well as the overall fine particulate matter formation is the largest for the complete degradation experiment. This is likely related to the significantly longer UV exposure time used in that experiment, which resulted in a significantly larger amount of toluene consumption.

The factorial experiment with the highest fine particulate matter formation also differed from the other experiments in a couple aspects. This experiment had a toluene addition of 15 μL , and 15 minutes of UV exposure, both of those being more than found in the other factorial experiment and the minimal exposure experiments. This experiment yielded a larger amount of fine particulate matter formation, as well as a greater peak concentration. This comparison supports the conclusion from the analysis of the factorial experiment that the initial toluene concentration and duration of UV irradiation both correlate positively with the amount of fine particulate matter formation.

Through all the experiments performed, the UV absorbance of toluene varied only with the variation of the concentration of toluene in the system. Since the reactor setup was the same across all the experiments, the path length did not change, and since all the experiments used 254 nm UV light and toluene, the molar absorptivity also did not change. Thus, the relationship between the toluene concentration and the amount of particle formation can likely be attributed to a variation in absorbance. At higher concentrations of toluene, the UV absorbance levels are also higher, likely resulting in increased toluene degradation, and the observed increase in particle formation levels.

A comparison can also be done with the results from the room air experiments. The effects of air filtration and relative humidity can be determined by comparing a set of experiments with all other variables consistent. This set of experiments all used 55-85 ng/mL of toluene, 5 minutes of UV irradiation, and 1 minute of post-UV recirculation. The results of these experiments are compared below in Table 21.

Table 21: Comparison of particle formation in for filtered and unfiltered experiments using compressed and room air

	Filtered compressed air	Unfiltered compressed air	Filtered room air		Unfiltered room air	
Relative humidity (%)	0.01	0.01	15.9	43.2	18.6	33.4
Initial fine particulate matter (#/cm ³)	5.273	9.831	4.502	23.852	42.636	86.485
Fine particulate matter formed (#/cm ³)	2.383	1.143	0.048	9.603	-4.202	15.979
Particle diameter peak(s) (µm)	0.542	0.542	0.542	0.542	0.542	0.542
Peak particle concentration (#/cm ³)	0.292	0.546	0.211	1.602	2.132	5.276

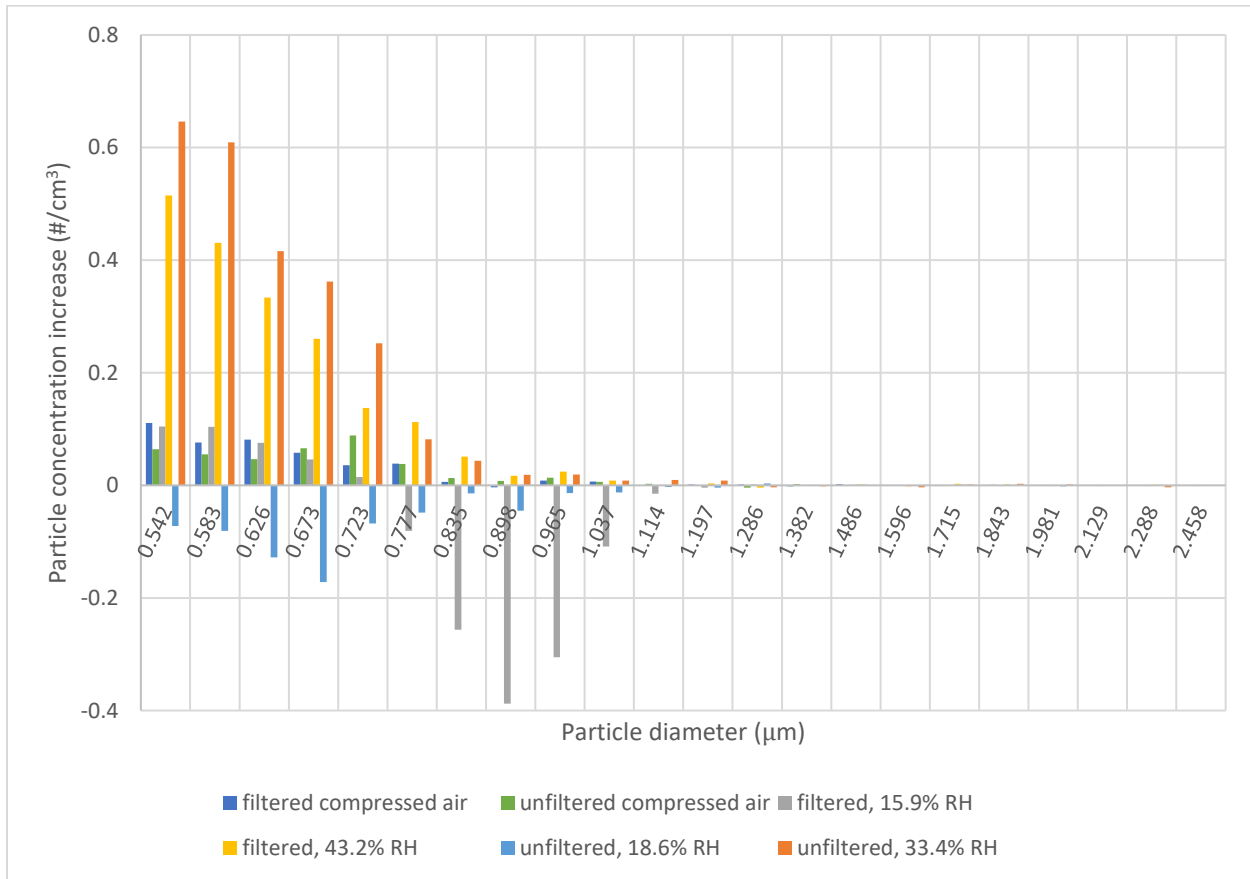


Figure 31: Comparison of particle increase in for filtered and unfiltered experiments using compressed and room air

From the comparisons in Table 21, the effects of the different air sources and varying relative humidity can be observed. As discussed in Section 4.2.3 Unfiltered Air Experiments, although the unfiltered compressed air experiment had a higher amount of fine particulate matter initially

present, there was not an increased level of fine particulate matter formation as compared to the filtered compressed air experiment. However, it is plausible that in the place of particle formation, there is increased particle growth in the unfiltered experiment. In addition, in Section 4.2.4 Room Air Experiments, it was determined that higher levels of relative humidity resulted in higher amounts of initial fine particulate matter, as well as increased levels of fine particulate matter formation over the duration of the experiment. However, comparing the lower levels of relative humidity in the room air experiments to the compressed air experiments shows a different trend. The lower humidity level in the filtered room air experiment was 15.9% and yielded fine particulate matter formation of 0.048 particles/cm³, while the lower humidity unfiltered room air experiment was at a relative humidity of 18.6% and showed fine particulate matter formation of 4.202 particles/cm³. These particle formation levels in the room air experiments are lower than those of the compressed air experiments, where the filtered and unfiltered experiments yielded fine particulate matter formation levels of 2.383 and 1.143 respectively.

Particle growth, as shown by the particle increase for each size fraction in Figure 31, was found to be similar between the two types of compressed air experiments, and the two types of lower humidity room air experiments. However, both the lower humidity experiments showed decreases in particle concentration in different particle size fractions, while no significant particle concentration decreases were observed for the compressed air experiments. Thus, the reduced levels of fine particulate matter formation in the room air experiments are not explained by increased levels of particle growth during UV irradiation. These results suggest that there may be different factors that influence fine particulate matter formation at different levels of relative humidity.

The results obtained in this work can be compared with existing work done presented in literature, as previously summarized in Table 6. The existing work investigated UV light with wavelengths of 300-400 nm, whereas this work uses germicidal UV light with a wavelength of 254 nm. As can be observed in the toluene absorption spectrum in Figure 1, UV light with a wavelength of 254 nm falls within a band of higher absorption, while wavelengths of 300-400 nm

do not. Thus, if toluene degradation and particle formation can be observed with UV wavelengths that have lower absorption, it can be hypothesized that germicidal UV will produce more significant amounts of particles. In addition, as mentioned previously, much of the existing work presents the amount of particle formation in mass concentration, rather than the number concentrations with which this work is concerned. Thus, it is difficult to compare the results, and determine the degree of particle formation and growth. In general, the particles observed are around the same size, with the majority being smaller than 0.5 μm in diameter. Since the particle formation mass calculated in this experiment had a wide variability, as discussed in Section 5.8 Toluene Mass Balance, comparisons cannot reasonably be made to the literature results.

Chapter 6 - Extended Experiments

6.1 Above-door Germicidal UV System Experiment

The initial amount of fine particulate matter found in the commercial office bathroom was 33.304 particles/cm³. This is similar to the initial fine particulate matter concentrations in the unfiltered room air experiments in the lab, which had initial particle concentrations ranging from 26.076 - 86.485 particles/cm³. These initial fine particulate matter levels for bathroom room air are all higher than the initial particles present in the filtered compressed gas used in the majority of the lab experiments. In the lab, the initial particle concentration from the filtered compressed air ranged from 1.280 – 15.291 particles/cm³.

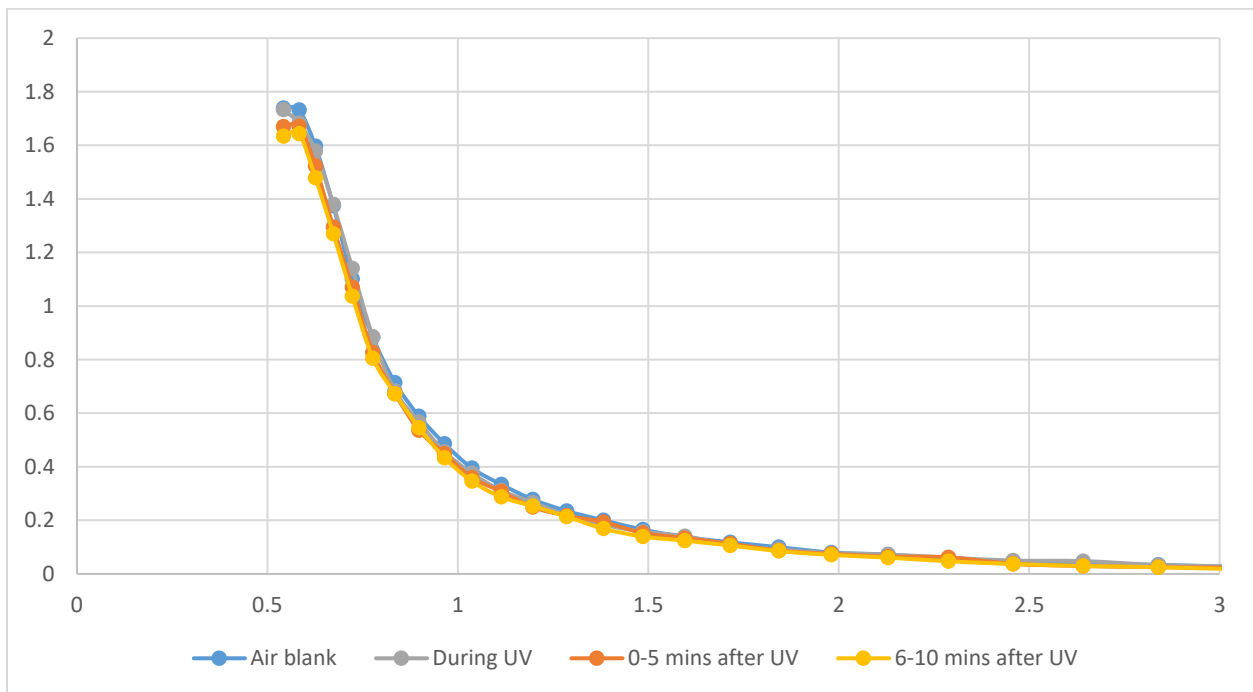


Figure 32: Particle size distribution for above-door UV system experiment

The particle size distributions for the experiment with the above-door UV disinfection system as described in Section 4.2.5 Above-door Germicidal UV System Experiment are shown above in Figure 32. It is evident that the particle size distributions before, during, and after UV exposure are all very similar in both magnitude and shape. Of particular importance is the fact that the only slight variation is that there is slightly higher concentration of the particles in the smallest size fraction in the blank sample taken before running the UV system. Thus, it can be concluded

that under these normal room conditions, UV irradiation does not result in measurable particle formation or growth.

In comparison to the other experiments performed in this work, this experiment took place in a typical office environment, and did not use any added VOCs. Thus, the results from this experiment indicate that particle formation is not likely to occur in indoor environments with this type of VOC profile.

6.2 185 nm UV with Ozone

Since UV light with a wavelength of 254 nm has proven to promote SOA formation similar to the way 300+ nm UV light does, another experiment was done to investigate if even shorter wavelengths of UV would also promote particle formation. UV wavelengths shorter than 240 nm are not typically used in indoor applications, since these shorter wavelengths tend to promote the formation of ozone via the photolysis of O₂ (Eliasson and Kogelschatz, 1990) (Kowalski, 2009). Ozone is known to cause health problems and reduced air quality, and thus ozone-producing UV lamps would not be suitable for indoor air treatment (United States Environmental Protection Agency, 2017). However, the presence of ozone is also known to promote the photooxidation of VOCs, and thus SOA formation is also promoted (Shen and Ku, 1999). As mentioned earlier, the presence of ozone is a very important factor in promoting photooxidation reactions under UV light.

The experiments used a 185 nm ozone-producing UV lamp. The other conditions of the experiment were similar to those in the complete degradation experiments using the 254 nm lamp. The specifications of the experiment are shown below in Table 22, and the particle size distribution is shown in Figure 33.

Table 22: Specification for toluene degradation experiment with 185 nm ozone-producing lamp

Liquid toluene addition	10 μ L
Initial gas toluene concentration	86.48 ng/mL
Length of UV exposure	30.33 minutes
Fine particulate matter formation	2982.90 particles/cm ³

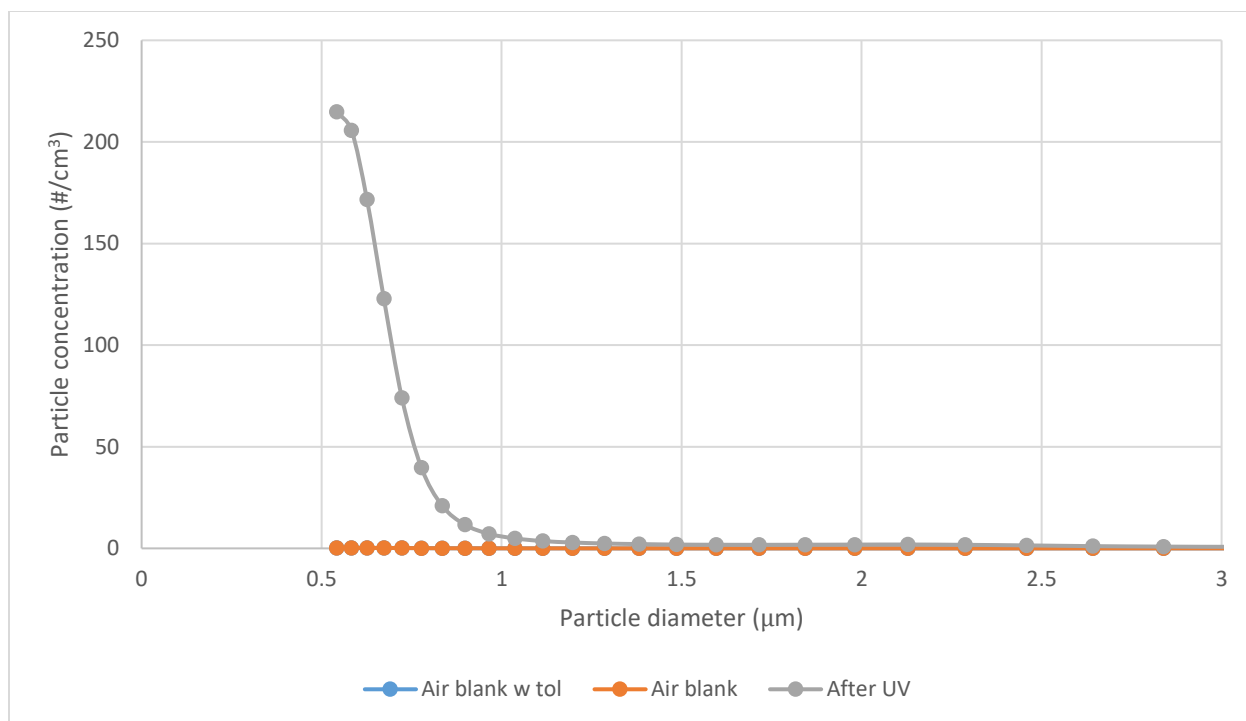


Figure 33: Particle size distribution for toluene degradation under 185 nm ozone-producing UV

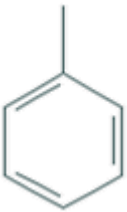
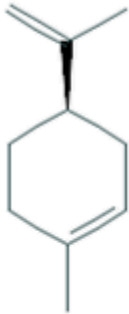
It is evident that the presence of ozone with the 185 nm UV lamp resulted in a much faster reaction of toluene. The amount of time required for the 254 nm UV lamp to degrade the same amount of toluene was approximately 4 times greater than the 185 nm lamp. As seen in the toluene absorption spectrum in Figure 1, the absorbance peak is far greater at 185 nm than 254 nm, which would cause an increase in the rate of photooxidation. The presence of ozone in this experiment may also contribute to the difference in particle formation observed, but likely to a lesser extent than that difference in absorbance. Another point of note is the difference in the particle size distributions from the different UV lamps. With the 254 nm lamp, the most prominent peak was around 575 particles/cm³ at a particle diameter of around 1.25 µm, with the 185 nm lamp, the primary peak exists at around 215 particles/cm³ with a particle diameter of 0.5 µm. Thus, the use of the shorter wavelength ozone-producing UV light results in the formation of particles that are much smaller than those formed under 254 nm UV. This formation of smaller particles could also be attributed to the shorter duration of UV exposure.

6.3 Other VOCs

There is a large variety of different types of VOCs that can be found in the atmosphere, as well as in indoor environments. They can vary vastly in structure and physical properties. Thus, it is important to investigate whether or not the particle formation for different types of VOCs are related to any of their properties or characteristics.

As part of this work, a complete degradation experiment was done using limonene instead of toluene, in order to compare the particle formation. A comparison of some of the properties of toluene and limonene is shown below in Table 23, and the absorption spectra are shown in Figure 34 and Figure 35 respectively.

Table 23: Comparison of properties of toluene and limonene

Compound	Toluene C ₇ H ₈	Limonene C ₁₀ H ₁₆
Structure		
Molecular Mass	92.14 g/mol	136.23 g/mol
Vapour Pressure 298 K	28.4 mmHg	1.98 mmHg
Boiling Point 1 atm	110.8°C	177°C
Liquid Density	0.86 g/mL	0.84 g/mL
Absorption Cross Section 254 nm UV at 298 K	5.525033×10^{-19} cm ² /molecule	1.158295×10^{-19} cm ² /molecule

Note: Structure images from National Center for Biotechnology Information; Molecular masses and boiling points obtained from Perry and Green (2008); toluene vapour pressure obtained from Daubert and Danner (1989); limonene vapour pressure obtained from Yaws (1994); liquid densities obtained from Haynes (2014); toluene absorption cross section obtained from Serralheiro et al. (2015); limonene absorption cross section obtained from Smialek et al. (2012)

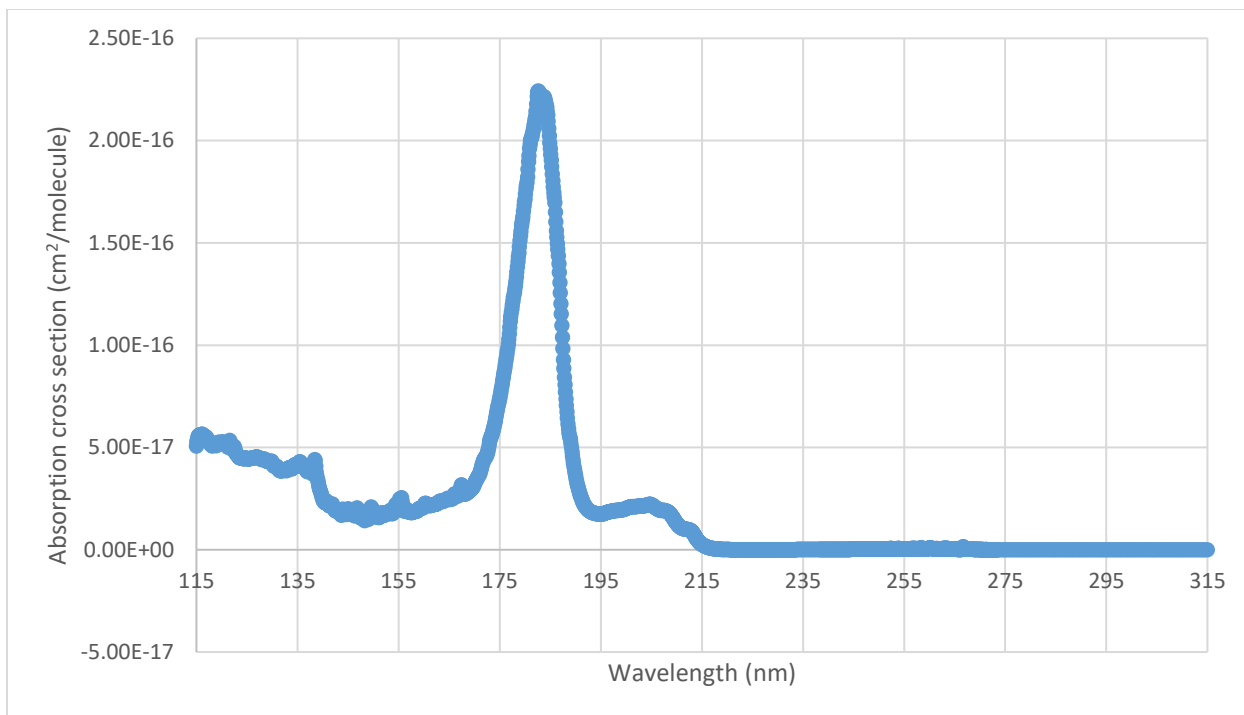


Figure 34: Absorption spectrum for toluene (Data from Serralheiro et al. (2015))

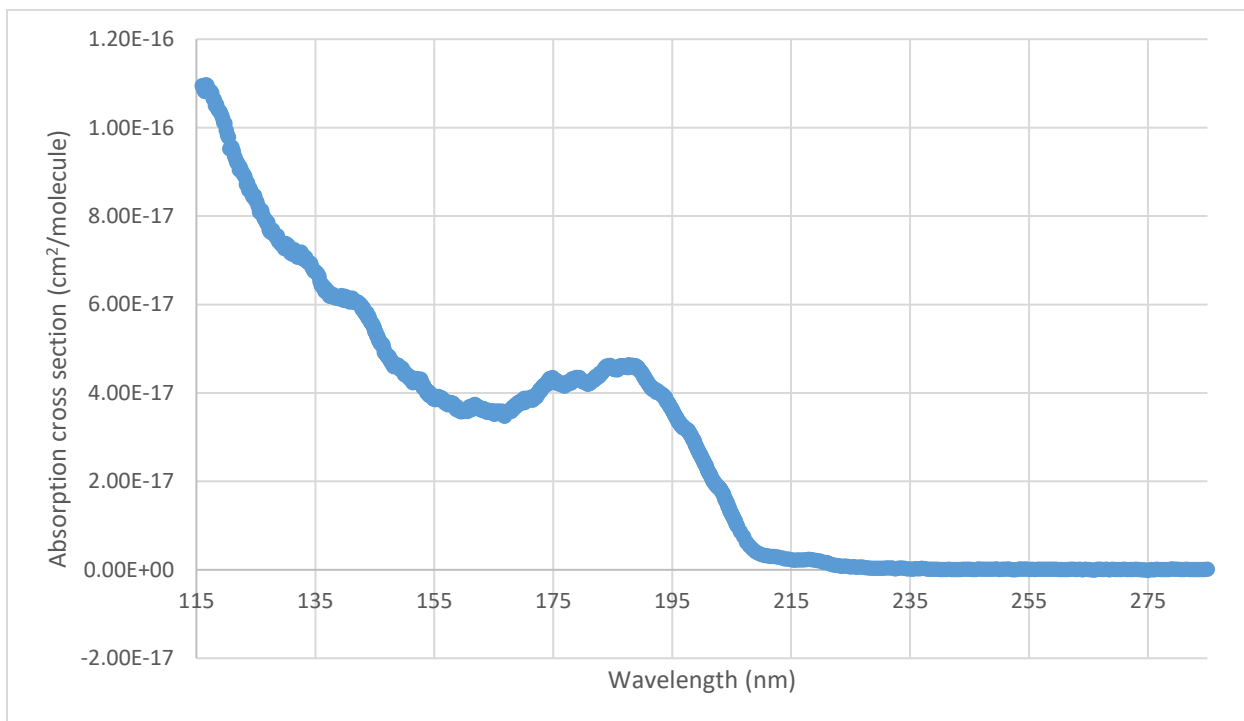


Figure 35: Absorption spectrum for limonene (Data from Smialek et al. (2012))

Toluene and limonene are similar in structure, both being cyclic compounds, as well as liquid density. Equal liquid additions of each of these compounds into the reactor will result in similar amounts in the gas phase. However, toluene has a lower boiling point, as well as a significantly

higher vapour pressure at room temperature than limonene. Thus, toluene is expected to be much more volatile than limonene. In addition, the 254 nm UV light absorption cross section of toluene is approximately four times greater than that of limonene. The absorption cross section is a measure of the ability for a molecule to absorb a photon of a particular wavelength, thus having a higher UV cross section means that toluene can be expected to have a higher reaction rate with germicidal UV light.

A set of complete exposure experiments were done testing limonene as the photooxidized VOC. As expected, limonene behaved differently from toluene in a number of different aspects. The comparisons of the experiments are shown below in Table 24.

Table 24: Comparison of long exposure experiment results for toluene and limonene

		Toluene	Limonene
Amount of liquid VOC (μL)		10	10
Theoretical concentration (ng/mL)		311.45	304.57
Experiment 1	Initial gas phase concentration (ng/mL)	135.9	16.88
	Time for complete degradation (h:mm:ss)	1:54:00	2:13:00
Experiment 2	Initial gas phase concentration (ng/mL)	141.36	14.29
	Time for complete degradation (h:mm:ss)	1:56:15	2:40:00

Initially, despite adding the same volume of each of the liquid VOCs to the reactor, the initial concentration of gas phase limonene measured was significantly lower than that of toluene. From the physical properties in Table 23, this is expected, since toluene has a lower molecular mass, a lower boiling point, and a higher vapour pressure. As seen in Table 24, the gas phase concentrations achieved in the reactor by the two compounds differ by a degree of magnitude. In addition, the experimental yields for both compounds are far lower than the expected gas phase concentration if all the liquid VOC added were to be distributed ideally in the gas phase. Therefore, this indicates that there may be other factors that are unaccounted for, that play a role in how these VOCs transition from the liquid to the gas phase in this reactor.

Another significant difference between the two compounds was the amount of UV exposure time required to reduce the gas phase VOC concentrations to a negligible amount. Despite the fact that the initial amount of limonene present in the gas phase is nearly 10 times lower than toluene, it took up to 1.4 times longer to achieve complete limonene degradation. This can be accounted for by the difference in absorbance of 254 nm UV light between toluene and limonene. Since the level of absorbance depends on the concentration of the VOC, it is likely that the difference in the VOC concentration, as well as the absorption cross section for 254 nm UV light contribute to the difference in the time required to achieve complete degradation.

In addition, the particle size distributions from complete degradation of each of the two compounds are significantly different. The particle size distributions for the complete degradation of toluene and limonene are shown below in Figure 36 and Figure 37 respectively. The complete toluene degradation experiment shown in Figure 36 is the same experiment as discussed earlier in Figure 13.

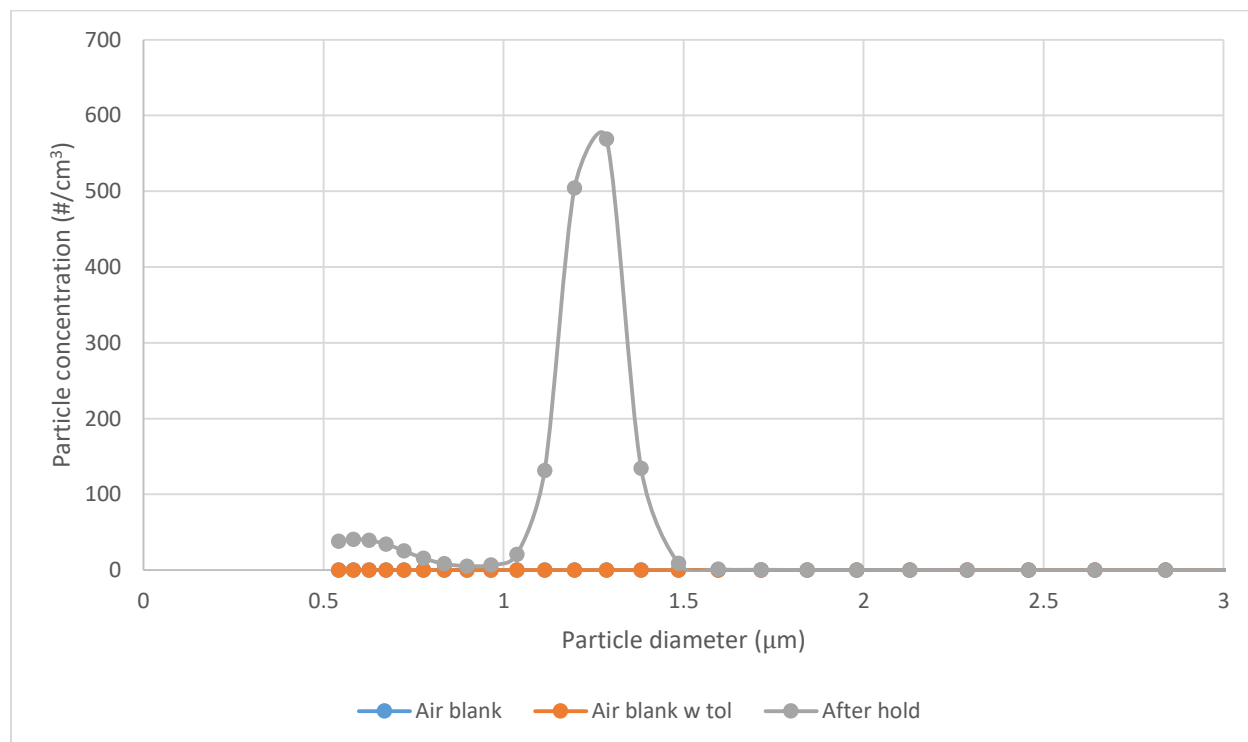


Figure 36: Toluene particle size distribution (Experiment 2)

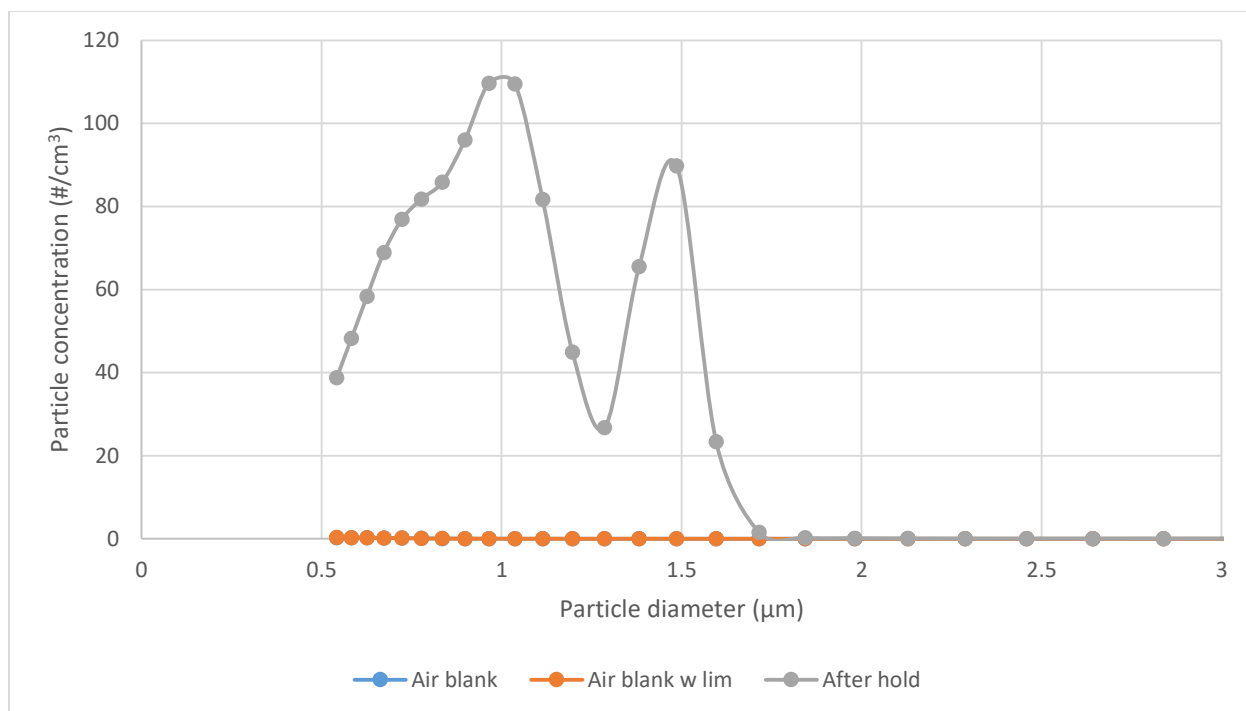


Figure 37: Limonene particle size distribution (Experiment 2)

As is evident from the particle size distributions resulting from the complete photolysis of each of the two compounds, toluene and limonene yielded different particle size distributions. Most evidently, the two compounds have concentration peaks at different particle sizes. In addition, toluene produces a significantly higher number of particles than limonene. Toluene has a primary peak of around 575 particles/cm³ at a particle diameter of around 1.5 µm, while limonene has two major peaks of around 110 particles/cm³ at a particle diameter of around 1 µm and 90 particles/cm³ at a particle diameter of around 1.5 µm. One aspect that is common between the two experiments is that the vast majority of all the particles measured are smaller than 2.5 µm in diameter, therefore they can be classified as fine particulate matter. Overall, these two compounds were found to be quite different with respect to particle formation from UV photooxidation.

Chapter 7 – Conclusions and Recommendations

7.1 Conclusions

The goal of this project was to determine the effects of germicidal UV light on SOA formation in indoor environments. Using toluene as a representative VOC, a number of experiments were performed, exposing an air mixture to 254 nm UV light for specific durations of time. The particle size distributions in a filtered compressed air mixture were compared before and after the UV exposure to determine whether particle formation had occurred during that time. The minimal exposure experiments concluded that significant fine particulate matter formation occurs in as little as 5 minutes of UV exposure. In addition, it was found that the amount of fine particulate matter formed correlated positively with both the toluene initially present in the system, as well as the duration of the UV irradiation. As well, higher initial particle concentrations were observed in experiments with higher levels of relative humidity, and these experiments also yielded higher levels of fine particulate matter formation. It was also determined that the amount of fine particulate matter formed is not significantly affected by the duration of the post-UV recirculation, nor by the amount of ambient particulate matter present initially. Overall, it can be concluded that SOA formation is promoted by exposure of toluene to germicidal UV light.

7.2 Recommendations

The variables investigated in this work are only a limited selection, and further work needs to be done in order to get a more complete understanding of the effects of 254 nm UV light on SOA formation.

7.1.1 Smaller Size Fraction

One area that could benefit from further investigation is the particle size distribution within the smallest size fraction measured by the APS. The APS collect all particles with diameters of less than 0.523 microns, and greater than the lower detection limit of 0.3 microns, into one size fraction. However, many similar experiments in literature observe the highest concentrations of particles in the nanometer size range, suggesting that there is significant portion of the particle size distribution that the APS is unable to detect. In addition, looking at the particle size distribution graphs, particularly those of the experiments using shorter durations of UV exposure, it is evident that a major particle peak occurs close to the lower particle size detection limit of the APS. This also suggests that there could be significant concentrations of particles that are just smaller than the lower detection limit. Therefore, in order to get a better understanding of the mechanisms of particle formation and growth, using an instrument more sensitive to the smaller particles would be beneficial.

7.1.2 Expanding on Variables

The results of these experiments are limited to the conditions and variables that were tested. In order to accurately determine the SOA formation behaviour under a wider variety of environments, more work needs to be done on expanding the variables tested.

One way that this can be done is by expanding the experiments testing the particle formation in a room-sized setting. The experiment described in Section 6.1 Above-door Germicidal UV System Experiment showed no particle formation. However, it would be useful to see if there is a relationship between the initial VOC concentration and particle formation in this type of room sized environment. Although similar work has been done with testing indoor UV treatment

systems for their germicidal efficiency, it would be beneficial to observe any correlating effects on particle size distribution.

In addition, it would be useful to determine the particle formation levels under lower gas phase concentrations of toluene. Since the toluene levels investigated were higher than the concentrations typically found in indoor environments, it would be beneficial to investigate the particle formation behaviour at typical indoor toluene concentrations.

Another aspect that would be useful to expand on is the durations of the UV irradiation and the post-UV recirculation. In the experiments done, the focus was on single doses of UV light, followed by a short recirculation period. However, it may be interesting to observe the effect of extended post-UV recirculation periods, or multiple separate UV doses separating by varying amounts of recirculation time. This would be more representative of the way indoor air UV treatment systems are used.

7.1.3 Other VOCs

As mentioned with the set of limonene experiments, it would also be beneficial to investigate the SOA formation differences for different VOCs and mixtures of VOCs. There is various existing work investigating different SOA formation from various types of VOCs, however comparisons of the particle formation properties of different classes of VOCs is limited. Comparisons of different types of VOCs with varying properties and structures will allow for a better understanding of the major variables affecting SOA formation.

7.1.4 Particle Composition

Determining the compounds formed from VOCs that go on to form SOA particles would be another area of interest. Analyzing the constituents of the aerosol particles would allow for a better understanding of VOC reaction mechanisms that contribute to particle formation and growth. Knowledge of what types of compounds make up the SOA particles would also aid in developing a more in depth mass balance, as well as making it easier to model and predict SOA particle formation.

7.1.5 Modelling SOA Particle Formation and Growth

Upon further development of the variety of VOCs and experimental conditions tested, the results may be applied to a model to predict the degree of SOA formation and growth under specific sets of conditions. In order to accurately represent SOA particle formation in a model, the model needs to be able to account for the different types of products formed via VOC oxidation. Since VOC oxidation can either add functional groups to decrease the volatility of the compounds, or cleave carbon-carbon bonds to increase their volatility, it is important to consider both of these types of reaction pathways when modelling the rate of SOA particle formation (Hallaquist et al, 2009). Many existing explicit models consider the types of semivolatile products formed from VOC oxidation, and calculate the degree to which each of those will partition into the particle phase depending on the composition of the aerosol absorbing mass present (Hallaquist et al., 2009).

The simpler types of models utilize experimentally-derived equilibrium constants from the absorption of gas phase semivolatile compounds into the particle phase (Hallaquist et al., 2009) (Odum et al., 1996). However, despite the fact that these types of models have been widely employed for many years, they are not able to account for the complex reaction pathways and interactive dynamics of SOA systems (Hallaquist et al., 2009). The most complex and rigorous explicit models, such as the Master Chemical Mechanism and the NCAR Self-Generating Mechanism, are able to account for the products formed by many possible pathways of VOC oxidation, as well as the reaction of multiple generations of the products formed, using a library of thousands of possible reactions (Hallaquist et al., 2009). However, even the most complex existing models are not able to account for all of the continuing reactions that occur in the particle phase.

Many existing models are much more highly specified in terms of variables, and more rigorous than the specifications of the work done in this study. In order to employ many models, an understanding of the reaction pathways and VOC oxidation products is required. Since this study did not investigate the constituents of the SOA particles formed, it would be difficult to apply the results to existing models in a meaningful way. Analysis of the constituents of the SOA particles after UV exposure would likely provide a framework for using models to particle formation.

References

- Bhowmick, M., and Semmens, M.J. (1994). Ultraviolet photooxidation for the destruction of VOCs in air. *Water Research*, 28(11), 2407-2415.
- Bolton, J.R. (2000). Calculation of ultraviolet fluence rate distributions in an annular reactor: significance of refraction and reflection. *Water Research*, 34(13), 3313-3324.
- Cometto-Muñiz, J. E., and Abraham, M. H. (2015). Compilation and analysis of types and concentrations of airborne chemicals measured in various indoor and outdoor human environments. *Chemosphere*, 127, 70-86.
- Darynay, M. K. A., Hosseini, S. M., Raie, M., Fakharie, J., and Zareh, A. Study on continuous (254 nm) and pulsed UV (266 and 355 nm) lights on BVD virus inactivation and its effects on biological properties of fetal bovine serum. *Journal of Photochemistry and Photobiology B: Biology*, 94(2), 120-124.
- Daubert, T.E., and Danner, R.P. (1989). *Physical and Thermodynamic Properties of Pure Chemicals Data Compilation*. Washington, D.C.: Taylor and Francis.
- De Blas, M., Navazo, M., Alonso, L., Durana, N., Gomez, M. C., and Iza, J. (2012). Simultaneous indoor and outdoor on-line hourly monitoring of atmospheric volatile organic compounds in an urban building. The role of inside and outside sources. *Science of the Total Environment*, 426, 327-335.
- Eliasson, B., and Kogelschatz, U. (1990). Ozone Generation with Narrow-Band UV Radiation. *Ozone: Science & Engineering*, 13(3), 365-373.
- Hallaquist, M., Wenger, J.C., Baltensperger, U., Rudich, Y., Simpson, D., Claeys, M. ... Wildt, J. (2009). The formation, properties and impact of secondary organic aerosol: current and emerging issues. *Atmospheric Chemistry and Physics*, 9, 5155-5236.
- Haynes, W.M. (2014). *CRC Handbook of Chemistry and Physics, 95th Edition*. Boca Raton: FL: CRC Press LLC.
- Hildebrant, L., Donahue, N.M., and Pandis, S.N. (2009). High formation of secondary organic aerosol from the photo-oxidation of toluene. *Atmospheric Chemistry and Physics*, 9, 2973-2986.

- Huang, M., Hao, L., Gu, X., Hu, C., Zhao, W., Wang, Z. ... Zhang, W. (2013). Effects of inorganic seed aerosols on the growth and chemical composition of secondary organic aerosol formed from OH-initiated oxidation of toluene. *Journal of Atmospheric Chemistry*, 70, 151-164.
- Huang, M.Q., Zhang, W.J., Hao, L.Q., Wang, Z.Y., Zhou, L.Z. ... Fang L. (2006). Chemical Composition and Reaction Mechanisms for Secondary Organic Aerosols from Photooxidation of Toluene. *Journal of the Chinese Chemical Society*, 53, 1149-1156.
- Huang, Y., Ho, S. S. H., Lu, Y., Niu, R., Xu, L., Cao, J., and Lee, S. (2016). Removal of Indoor Volatile Organic Compounds via Photocatalytic Oxidation: A Short Review and Prospect. *Molecules*, 21(56).
- Hunt, B., and Anderson, W.A. (2016). Reduction of Hospital Environmental Contamination Using Automatic UV Room Disinfection. *Infection Control tips*.
- Hurley, M.D., Sokolov, O., Wallington, T.J., Takekawa, H., Karasawa, M., Klotz, B., ... Becker, K.H. (2001). Organic Aerosol Formation during the Atmospheric Degradation of Toluene. *Environmental Science & Technology*, 35(7), 1358-1366.
- Katara, G., Hemvani, N., Chitnis, S., Chitnis, V., and Chitnis, D.S. (2008). Surface disinfection by exposure to germicidal UV light. *Indian Journal of Medical Microbiology*, 23(3), 241-242.
- Kowalski, W. (2009). *Ultraviolet Germicidal Irradiation Handbook: UVGI for Air and Surface Disinfection*. New York: Springer-Verlag Berlin Heidelberg.
- Kroll, J.H., Ng, N.L., Murphy, S.M., Flagan, R.C., and Seinfeld, J.H. (2005). Secondary organic aerosol formation from isoprene photooxidation under high NO_x conditions. *Geophysical Research Letters*, 32(18).
- Kroll, J.H., Ng, N.L., Murphy, S.M., Flagan, R.C., and Seinfeld, J.H. (2006). Secondary organic aerosol formation from isoprene photooxidation. *Environmental Science & Technology*, 40(6), 1869-1877.
- Kroll, J.H., and Seinfeld, J.H. (2008). Chemistry of secondary organic aerosol: Formation and evolution of low-volatility organics in the atmosphere. *Atmospheric Environment*, 42, 3593-3624.
- Kujundzic, E., Hernandez, M., and Miller, S. L. (2007). Ultraviolet germicidal irradiation inactivation of airborne fungal spores and bacteria in upper-room air and HVAC in-duct configurations. *Journal of Environmental Engineering and Science* 6, 1-9.

- Lau, J., Bahnfleth, W., and Freihaut, J. (2008). Estimating the effects of ambient conditions on the performance of UVGI air cleaners. *Building and Environment*, 44, 1362-1370.
- Lim, S., and Blatchley III, E. R. (2009). UV disinfection system of cabin air. *Advances in Space Research*, 44, 942-948.
- Lin, C-Y., and Li, C-S. (2002). Control Effectiveness of Ultraviolet Germicidal Irradiation on Bioaerosols. *Aerosol Science and Technology*, 36, 474-478.
- Mauderly, J.L., and Chow, J.C. (2008). Health Effects of Organic Aerosols. *Inhalation Toxicology*, 20(3), 257-288.
- National Center for Biotechnology Information. PubChem Compound Database; CID=440917 (D-Limonene). Retrieved from <https://pubchem.ncbi.nlm.nih.gov/compound/440917> (accessed June 11, 2017).
- National Center for Biotechnology Information. PubChem Compound Database; CID=1140 (Toluene). Retrieved from <https://pubchem.ncbi.nlm.nih.gov/compound/1140> (accessed June 11, 2017).
- Ng, N.L., Kroll, J.H., Chan, A.W.H., Chhabra, P.S., Flagan, R.C., and Seinfeld, J.H. (2007). Secondary organic aerosol formation from m-xylene, toluene, and benzene. *Atmospheric Chemistry and Physics*, 7(14), 3909-3922.
- Odum, J.R., Hoffman, T., Bowman, F., Collins, D., Flagan, R.C., and Seinfeld, J.H. (1996). Gas/Particle Partitioning and Secondary Organic Aerosol Yields. *Environmental Science and Technology*, 30(8), 2580-2585.
- Perry, R.H., and Green, D.W. (2008). *Perry's Chemical Engineers' Handbook, 8th edition*. New York: McGraw-Hill.
- Poschl, U. (2005). Atmospheric Aerosols: Composition, Transformation, Climate and Health Effects. *Atmospheric Chemistry*, 44, 7520-7540.
- Presto, A. A., Huff Hartz, K. E., and Donahue, N. M. (2005). Secondary Organic Aerosol Production from Terpene Ozonolysis. 1. Effect of UV Radiation. *Environmental Science Technology*, 39, 7036-7045.

- Quici, N., Vera, M. L., Choi, H., Puma, G. L., Dionysiou, D. D., Litter, M. I., and Destailats, H. (2010). Effect of key parameters on the photocatalytic oxidation of toluene at low concentrations in air under 254 + 185 nm UV irradiation. *Applied Catalysis B: Environmental*, 95, 312-319.
- Rösch, C., Wissenbach, D. K., von Bergen, M., Franck, U., Wendisch, M., and Schlink, U. (2015). The lasting effect of limonene-induced particle formation on air quality in a genuine indoor environment. *Environmental Science and Pollution Research*, 22(18), 14209-142019.
- Salonen, H. J., Pasanen, A-L., Lappalainen, S. K., Riuttala H. M., Tuomi, T. M., Pasanen P. O. ... Reijula, K. E. (2009). Airborne Concentrations of Volatile Organic Compounds, Formaldehyde and Ammonia in Finnish Office Buildings with Suspected Indoor Air Problems. *Journal of Occupational and Environmental Hygiene*, 6, 200-209.
- Serralheiro, C., Duflot, D., Ferreira da Silva, F., Hoffmann, S.V., Jones, N.C., Mason, N.J., ... Limão-Vieira, P. (2015). Toluene valence and Rydberg excitations as studied by ab initio calculations and vacuum ultraviolet (VUV) synchrotron radiation. *The Journal of Physical Chemistry A*, 119, 9059-9069.
- Sharp, D. G. (1938). A quantitative method of determining the lethal effect of ultraviolet light on bacteria suspended in air. *Journal of Bacteriology*, 35(6), 589-599.
- Sharp, D. G. (1938). A quantitative method for determining the lethal effect of ultraviolet light on bacteria suspended in air. *Journal of Bacteriology*, 35, 589-599.
- Sharp, D. G. (1940). The effects of ultraviolet light on bacteria suspended in air. *Journal of Bacteriology*, 39(5), 535-547.
- Shen, Y-S., and Ku, Y. (1999). Treatment of Gas-phase Volatile Organic Compounds (VOCs) by the UV/O₃ Process. *Chemosphere*, 38(8), 1855-1866.
- Smialek, M.A., Hubin-Franskin, M.J., Delwiche, J., Duflot, D., Mason, N.J., Vrønning-Hoffmann, S. ... Limão-Vieira, P. (2012). Limonene: electronic state spectroscopy by high-resolution vacuum ultraviolet photoabsorption, electron scattering, He(I) photoelectron spectroscopy and ab initio calculations. *Physical Chemistry Chemical Physics*, 14, 2056-2064.
- Tseng, C-C., and Li, C-S. (2005). Inactivation of Virus-Containing Aerosols by Ultraviolet Germicidal Irradiation. *Aerosol Science and Technology*, 39(12), 1136-1142.

- United States Environmental Protection Agency. (2017, June 8). Ozone Pollution. Retrieved June 16, 2017, from <https://www.epa.gov/ozone-pollution>
- Vivanco, M. G., Santiago, M., Martínez-Tarifa, A., Borrás, E., Ródenas, M., García-Diego, C., and Sánchez, M. (2011). SOA formation in a photoreactor from a mixture of organic gases and HONO for different experimental conditions. *Atmospheric Environment*, 45, 708-715.
- Wells, W.F., and Wells, M. W. (1936) Air-borne infection. *Journal of the American Medical Association*, 107, 1805-1809.
- Wolkoff, P. (2012). Indoor Air Pollutants in Office Environments: Assessment of Comfort, Health, and Performance. *International Journal of Hygiene and Environmental Health*, 216, 371-394.
- Wolkoff, P., and Kjærgaard, S. K. (2007). The dichotomy of relative humidity on indoor air quality. *Environment International*, 33(6), 850-857.
- Xue, L.K., Wang, T., Guo, H., Blake, D.R., Tang, J., Zhang, X.C., ... Wang., W.X. (2013). Sources and photochemistry of volatile organic compounds in the remote atmosphere of western China: results from the Mt. Waliguan Observatory. *Atmospheric Chemistry and Physics*, 13, 8551-8567.
- Yaws, C.L. (1994). *Handbook of Vapor Pressure, Vol 3: C8-C28 Compounds*. Houston, TX: Gulf Publishing Company.
- Zhao, Z., Hao, J., Li, J., and Wu, S. (2008). Second organic aerosol formation by irradiation of α -pinene-NO_x-H₂O in an indoor smog chamber for atmospheric chemistry and physics. *Chinese Science Bulletin*, 53(21), 3294-3300.
- Zou, L., Luo, Y., Hooper, M., and Hu, E. (2006). Removal of VOCs by photocatalysis process using adsorption enhanced TiO₂-SiO₂ catalyst. *Chemical Engineering and Processing*, 45, 959-964.

Appendices

Appendix A: Data Sets and Graphs

A-1 Minimal Exposure Experiments

A-1.1 Data Sets

Table A-1: Fine particulate matter formation in minimal exposure experiment with constant recirculation time

Length of UV exposure (mins)	Fine particulate matter before UV exposure ($\#/cm^3$)	Fine particulate matter after UV exposure ($\#/cm^3$)	Fine particulate matter produced ($\#/cm^3$)
1	21.29607	22.09458	0.80601437
2	27.08195	22.81206	-4.25938955
3	4.779404	2.926942	-1.84846205
4	5.846384	5.951379	0.105994953
5	13.95074	20.4735	6.522765088
10	1.955962	10.1753	8.219336513
10	4.108416	37.13925	33.03083854
10	7.662349	23.86704	16.20468831
15	10.67579	173.8245	163.148699

Table A-2: Fine particulate matter Formation in minimal exposure experiment with constant total time

Length of UV exposure (mins)	Length of post-UV recirculation (mins)	Fine particulate matter before UV exposure ($\#/cm^3$)	Fine particulate matter after UV exposure ($\#/cm^3$)	Fine particulate matter produced ($\#/cm^3$)
1	5	21.2960699	22.09458442	0.806014
2	4	3.781424073	3.895420067	0.113996
3.25	3	4.811402277	4.220415823	-0.59099
4	2	6.08387833	6.77186548	0.688487
5	1	6.513370817	13.59224065	7.07887
5	1	5.272893023	7.65634623	2.383453

A-1.2 Particle Size Distributions

Note: Some experiments results for the minimal exposure experiments were duplicated in the factorial experiments, and the particle size distribution graphs can be found under Appendix A-2 Factorial Experiment.

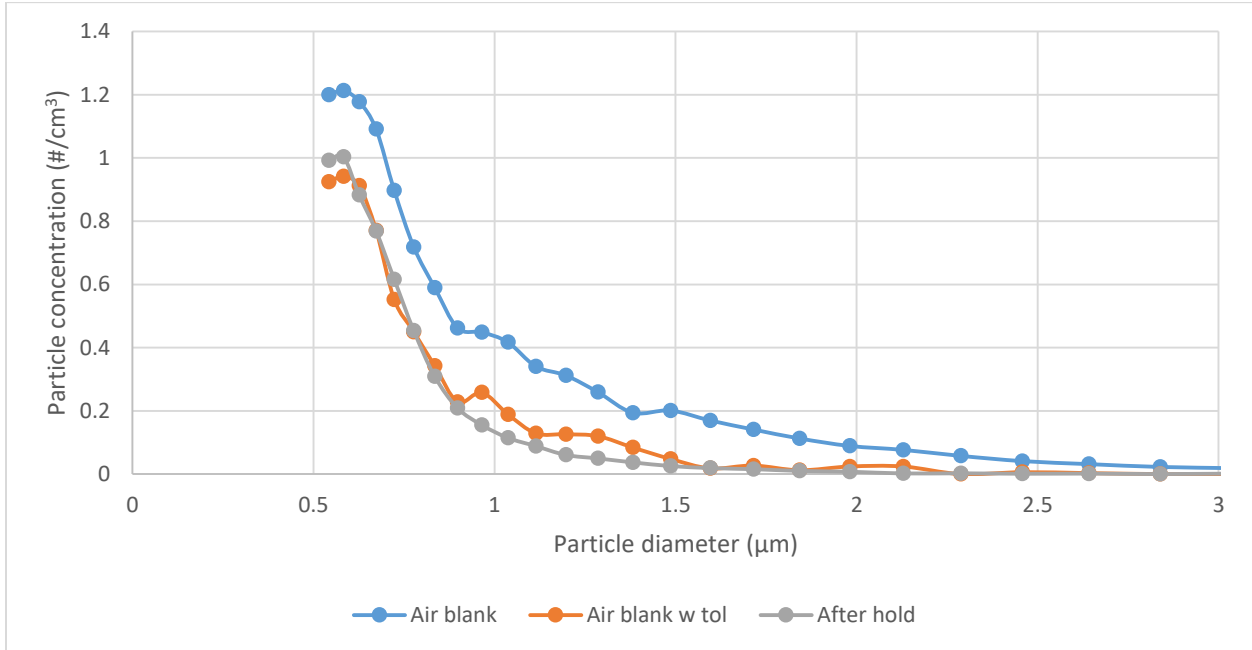


Figure A-1: 55-85 ng/mL toluene, 1 minute UV irradiation, 5 minutes post-UV recirculation

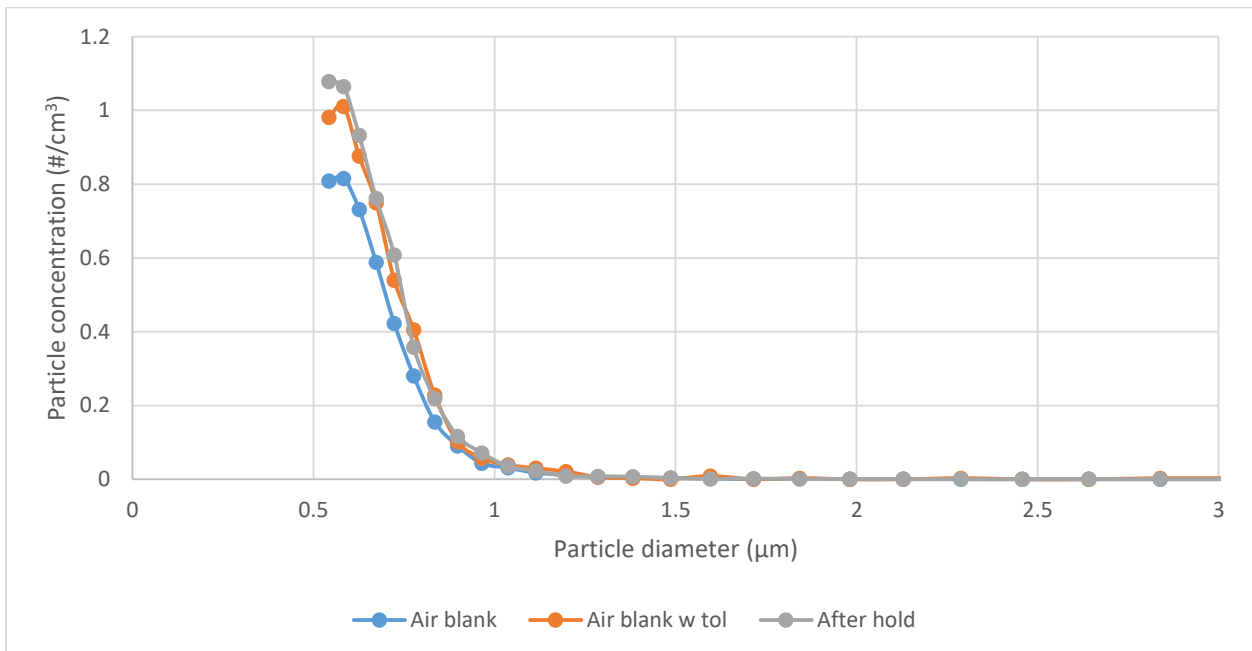


Figure A-2: 55-85 ng/mL toluene, 2 minutes UV irradiation, 5 minutes post-UV recirculation

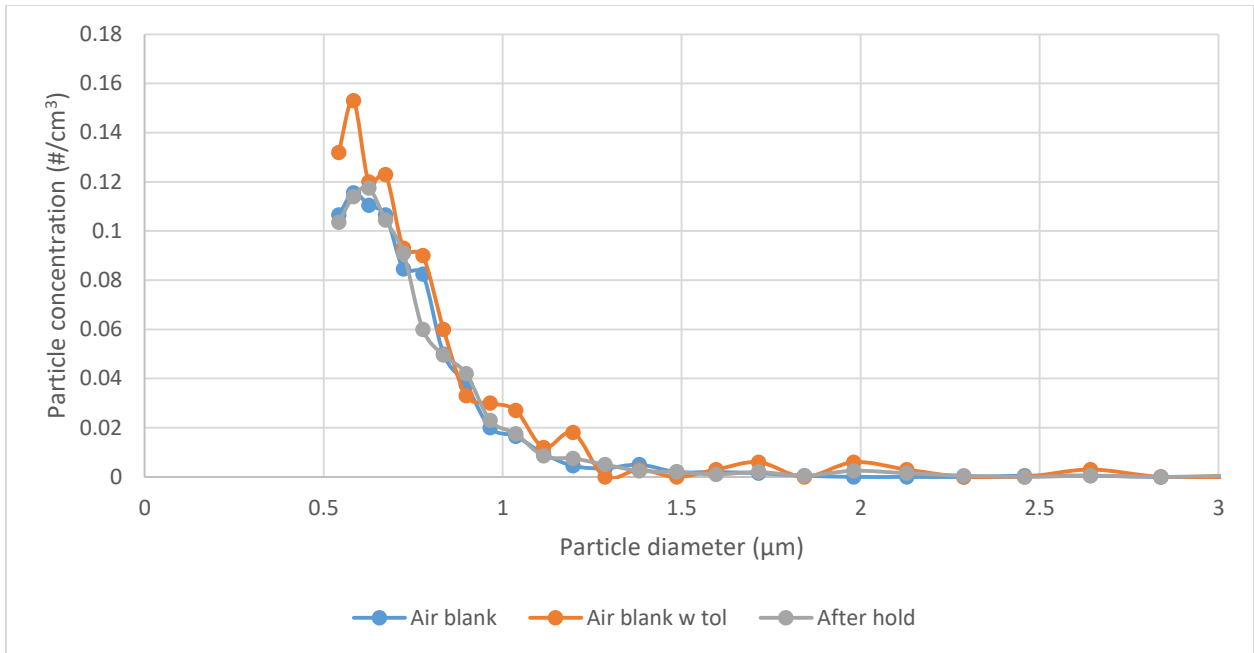


Figure A-3: 55-85 ng/mL toluene, 3 minutes UV irradiation, 5 minutes post-UV recirculation

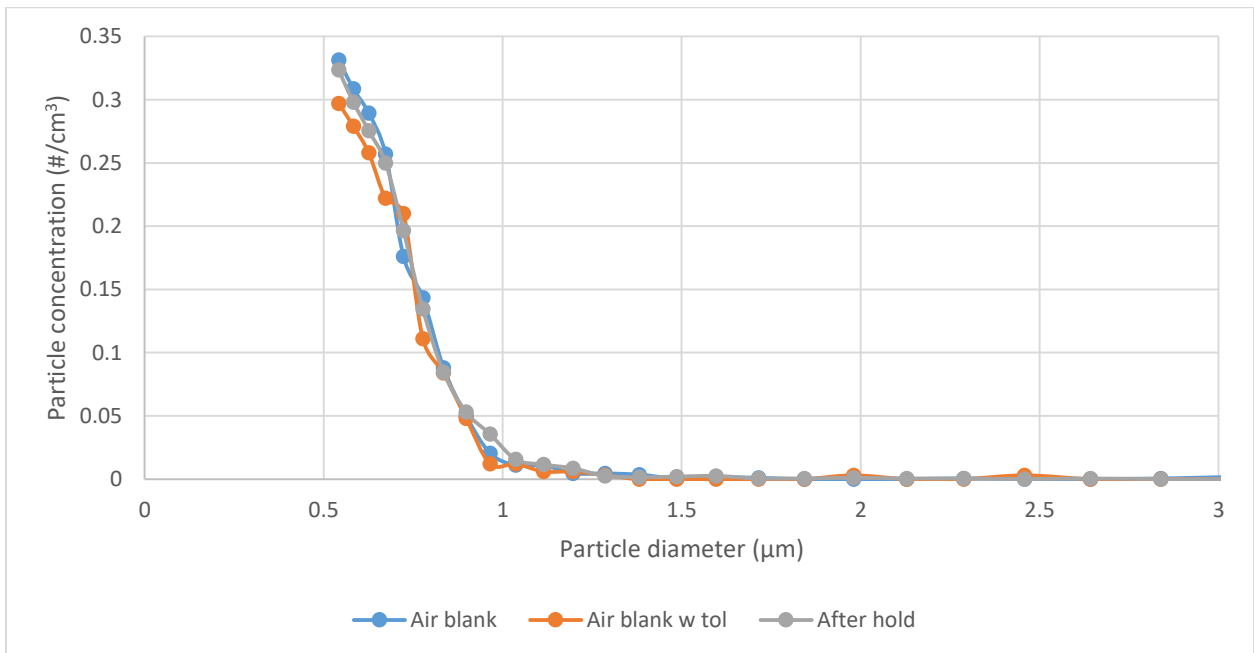


Figure A-4: 55-85 ng/mL toluene, 4 minutes UV irradiation, 5 minutes post-UV recirculation

A-1.3 Determination of Significant Particle Formation Level

Table A-3: Data for analysis of significant particle formation

Sample	Air blank	Air blank with toluene	Difference
1	26.30251	21.28857005	-5.01394
2	2.923442	4.77540389	1.851962
3	8.134838	5.845384163	-2.28945
4	5.900883	6.08337834	0.182495
5	5.657887	4.811402277	-0.84648
6	3.940923	3.781424073	-0.1595
7	7.086356	5.272893023	-1.81346
8	13.98831	13.95073729	-0.03757
9	1.654468	1.280475043	-0.37399
10	5.1269	2.36395534	-2.76295
11	5.127398	6.126376483	0.998979
12	5.951381	5.370392887	-0.58099
13	8.127838	8.678326277	0.550488
14	9.648808	8.073838417	-1.57497
15	0.970981	2.195956083	1.224975
16	4.737404	6.513370817	1.775967
17	3.083438	1.955961767	-1.12748
18	9.399312	11.36127885	1.961967
19	9.415312	8.8703195	-0.54499
20	8.231337	5.860881727	-2.37045
21	5.622387	5.860381633	0.237994
22	7.433352	4.10841627	-3.32494
23	4.778907	8.774326173	3.99542
24	10.0168	10.67578851	0.658989
25	7.13836	7.798844117	0.660484
26	7.677847	7.662349137	-0.0155
27	1.284976	0.877982773	-0.40699
28	2.819946	1.631967153	-1.18798
29	8.512828	8.983320387	0.470492
Mean			-0.34005
Standard deviation			1.779686
Minimum significant particle formation (#/cm ³)			1.439637

A-2 Factorial Experiment

A-2.1 Data Set

Table A-4: Data set for factorial experiments

Initial toluene level	Length of UV exposure (mins)	Length of post-UV recirculation (mins)	Initial fine particulate matter (particles/cm ³)	Final fine particulate matter (particles/cm ³)	Fine particulate matter produced (particles/cm ³)
55-85 ng/mL (55-85 ng/mL)	5	1	6.5134	13.5922	7.0789
		5	13.9507	20.4735	6.5228
		15	2.3640	3.5734	1.2095
	10	1	8.8703	222.8236	213.9533
		5	1.9560	10.1753	8.2193
			4.1084	37.1392	33.0308
	7.6623	23.8670	16.2047		
	15	7.7988	14.6642	6.8654	
	15	1	1.2805	28.4884	27.2079
5		10.6758	173.8245	163.1487	
15		2.1960	45.0381	42.8421	
15 μ L (100-125 ng/mL)	5	1	8.0738	16.4242	8.3504
		5	15.2907	97.8686	82.5780
		15	8.6783	13.0840	4.4056
	10	1	5.8609	24.0625	18.2016
		5	1.6320	262.9523	261.3203
		15	8.9833	68.6551	59.6718
	15	1	5.3704	1455.1303	1449.7600
		5	5.8604	704.7648	698.9044
		15	6.1264	874.5554	868.4290

A-2.2 Particle Size Distributions

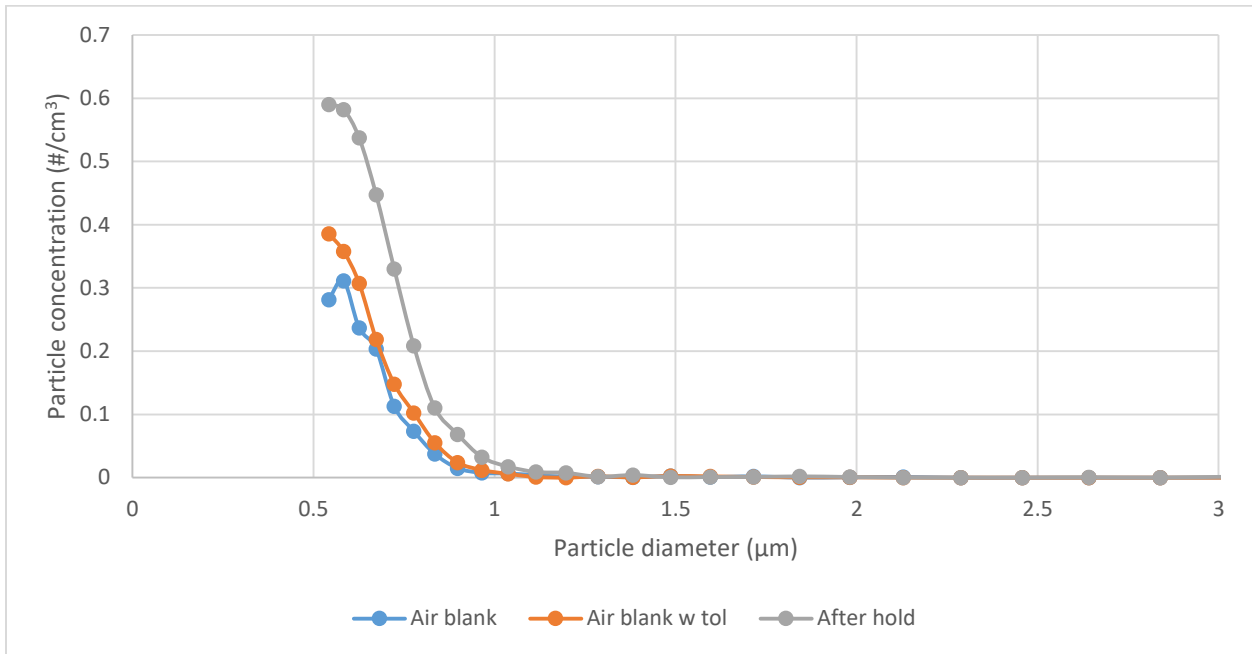


Figure A-5: 55-85 ng/mL toluene, 5 minutes UV irradiation, 1 minute post-UV recirculation

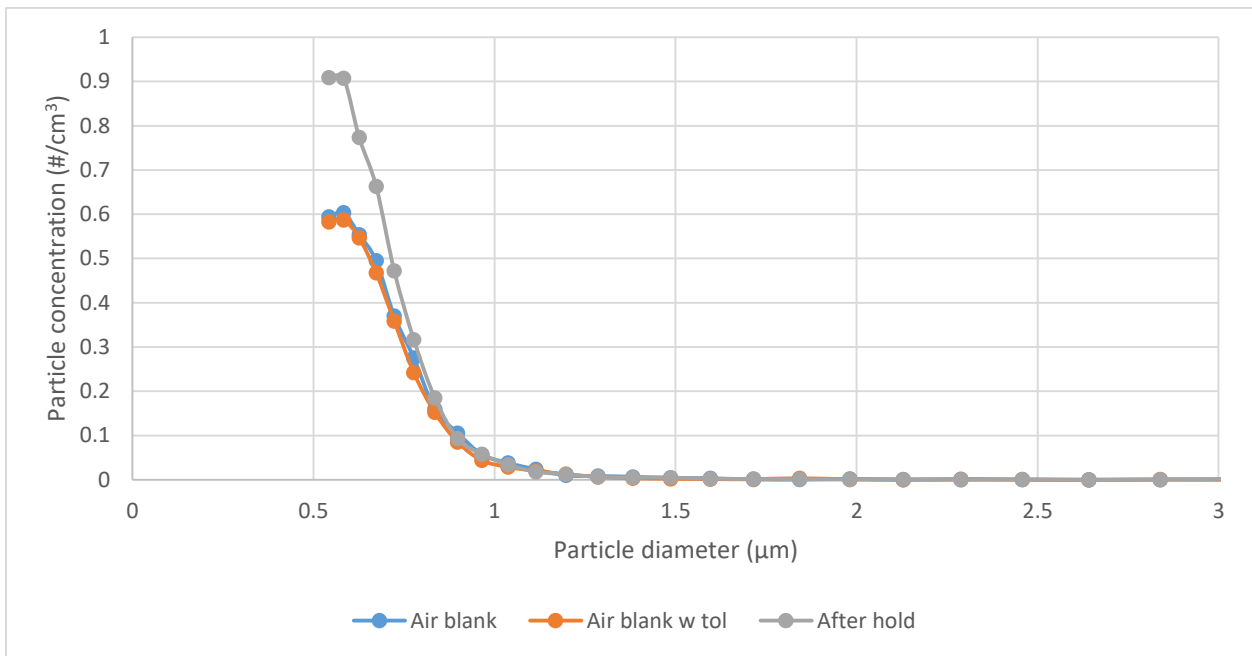


Figure A-6: 55-85 ng/mL toluene, 5 minutes UV irradiation, 5 minutes post-UV recirculation

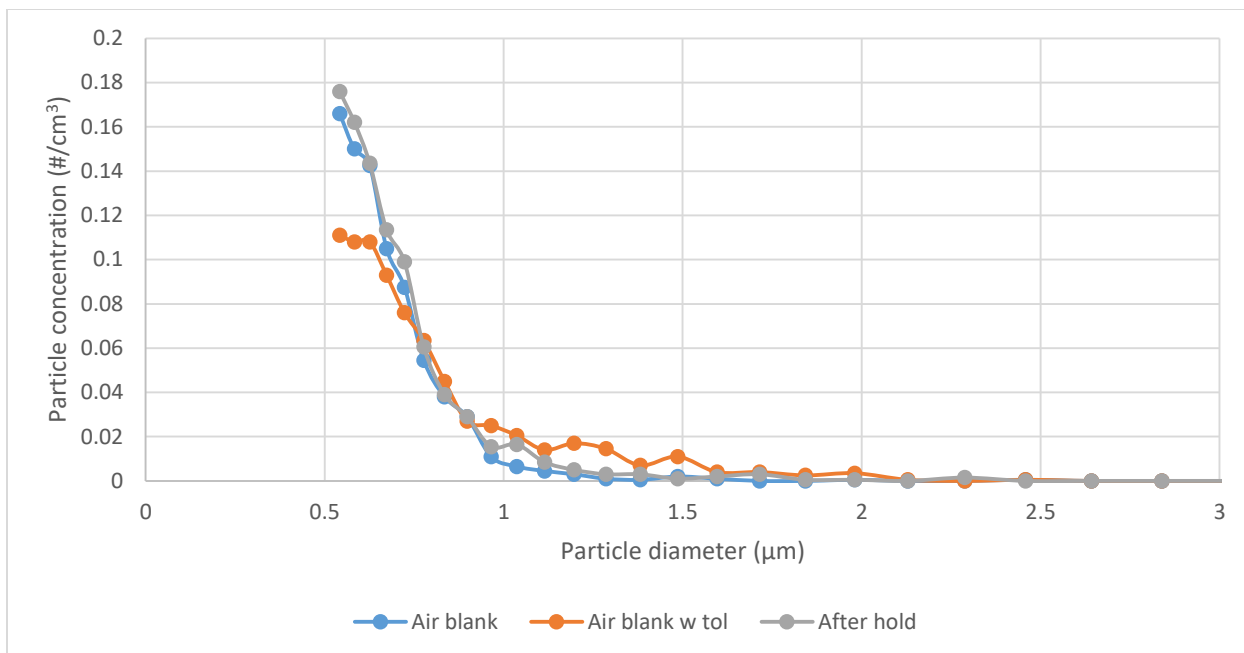


Figure A-7: 55-85 ng/mL toluene, 5 minutes UV irradiation, 15 minutes post-UV recirculation

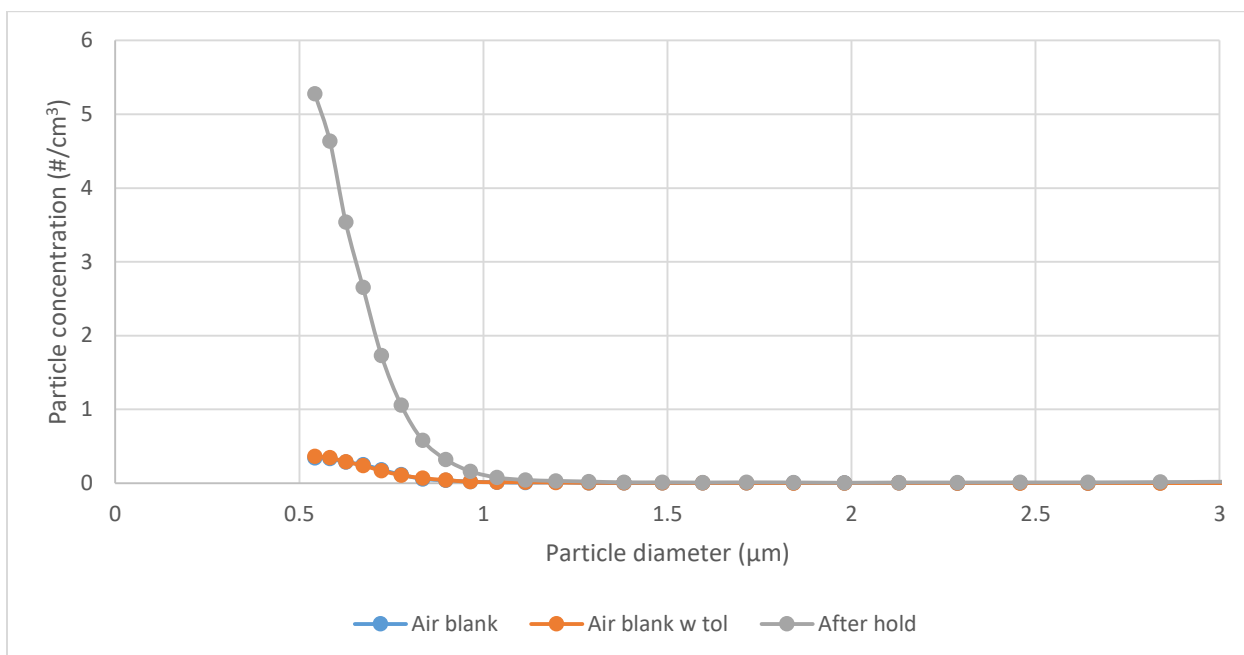


Figure A-8: 55-85 ng/mL toluene, 10 minutes UV irradiation, 1 minute post-UV recirculation

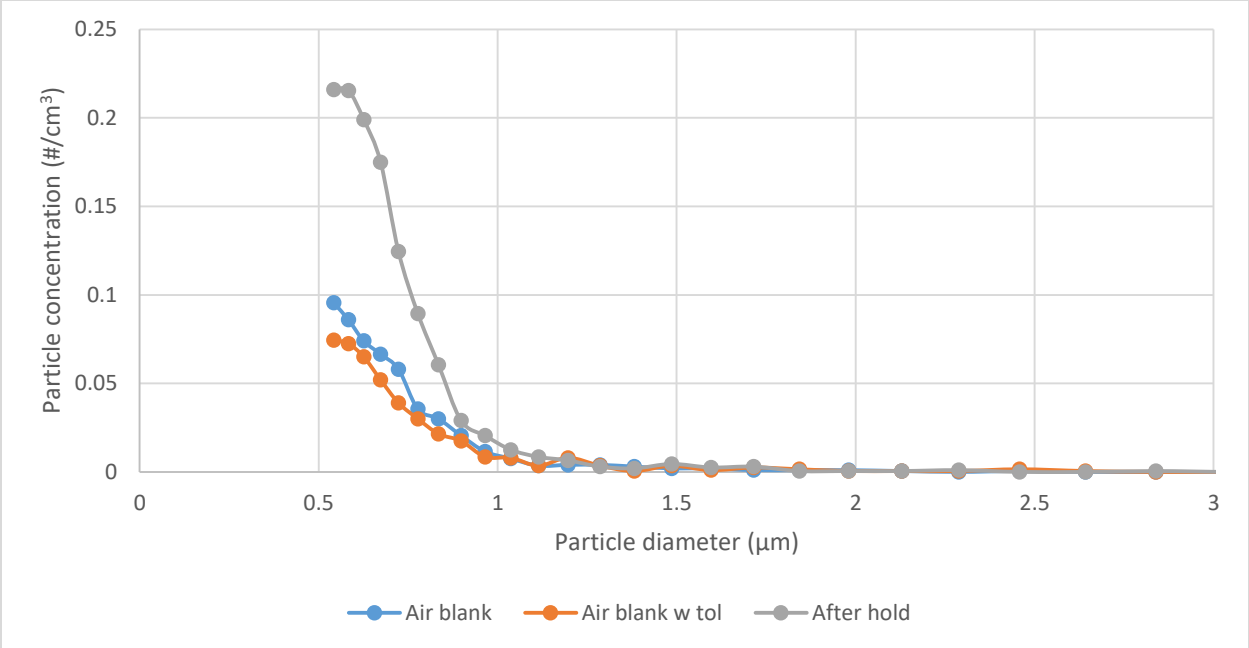


Figure A-9: 55-85 ng/mL toluene, 10 minutes UV irradiation, 5 minutes post-UV recirculation (Experiment 1)

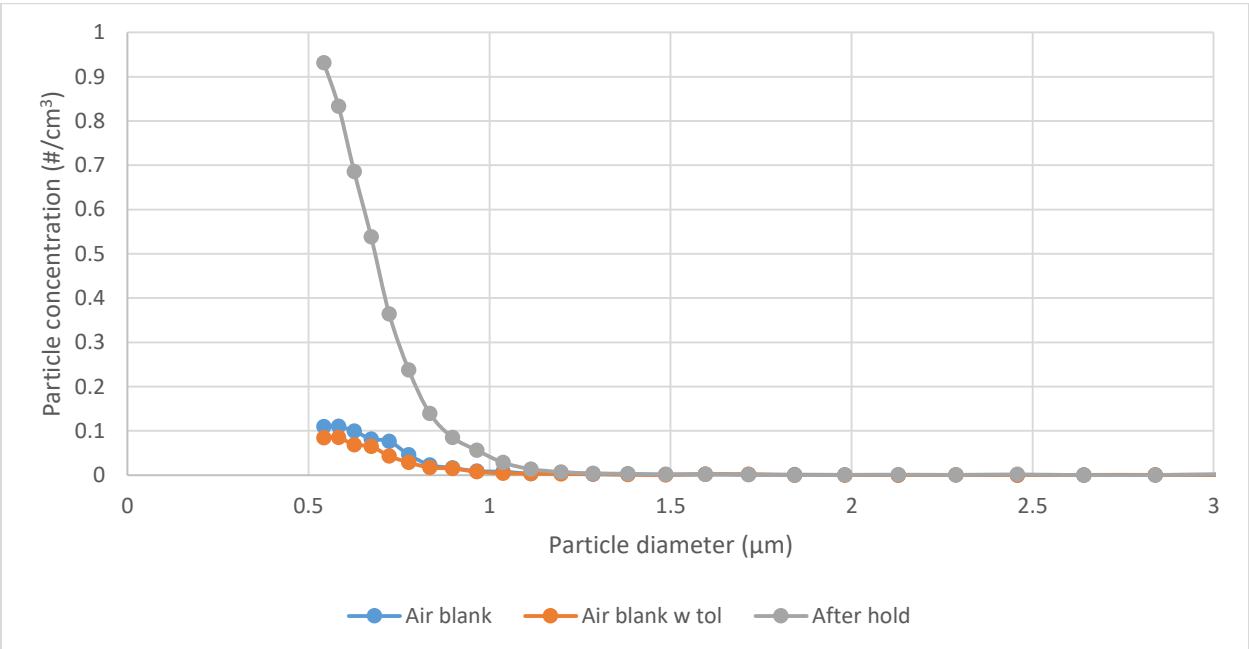


Figure A-10: 55-85 ng/mL toluene, 10 minutes UV irradiation, 5 minutes post-UV recirculation (Experiment 2)

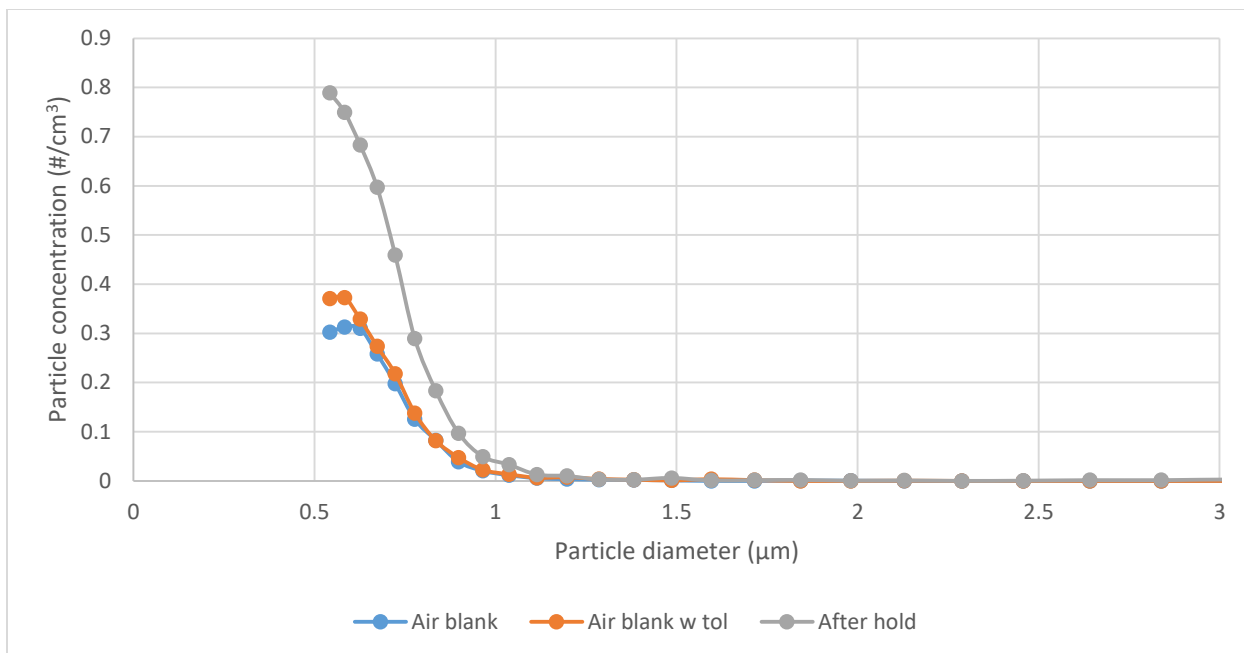


Figure A-11: 55-85 ng/mL toluene, 10 minutes UV irradiation, 5 minutes post-UV recirculation (Experiment 3)

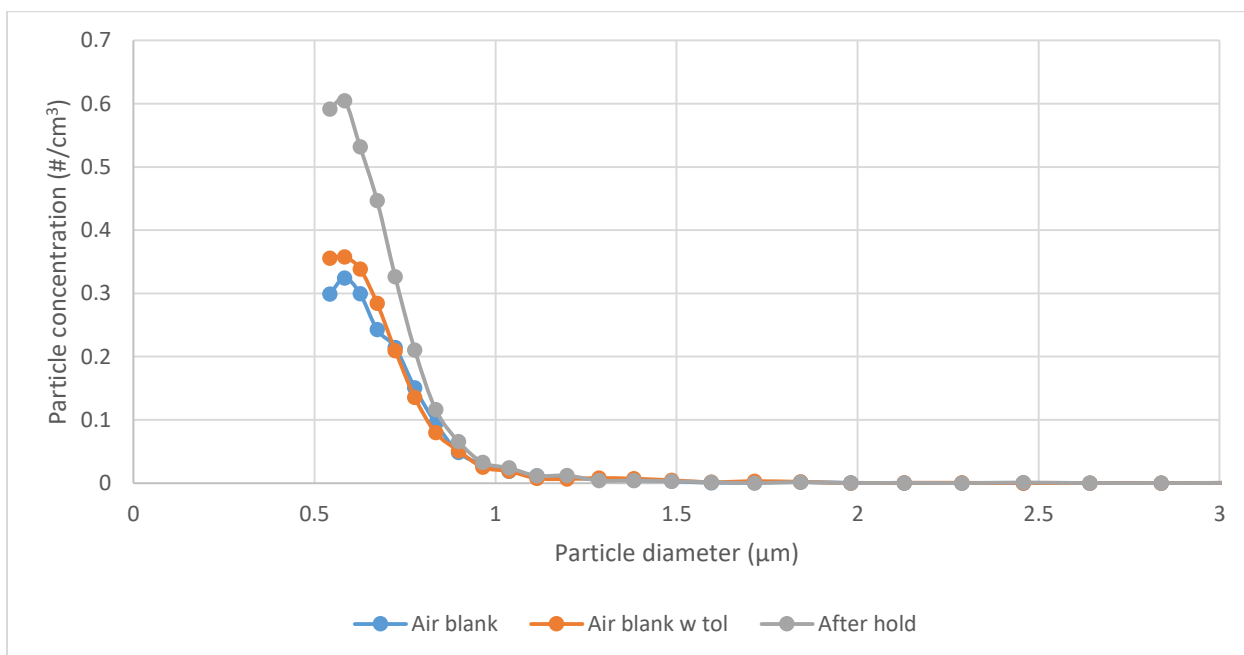


Figure A-12: 55-85 ng/mL toluene, 10 minutes UV irradiation, 15 minutes post-UV recirculation

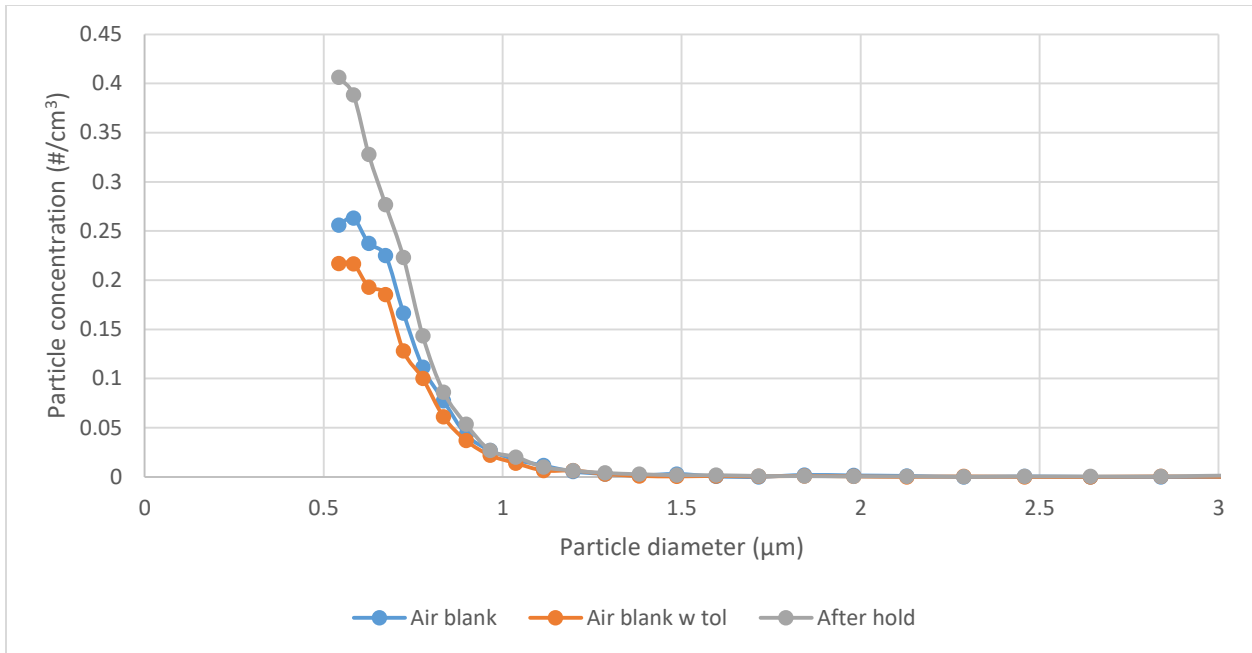


Figure A-13: 55-85 ng/mL toluene, 15 minutes UV irradiation, 1 minute post-UV recirculation

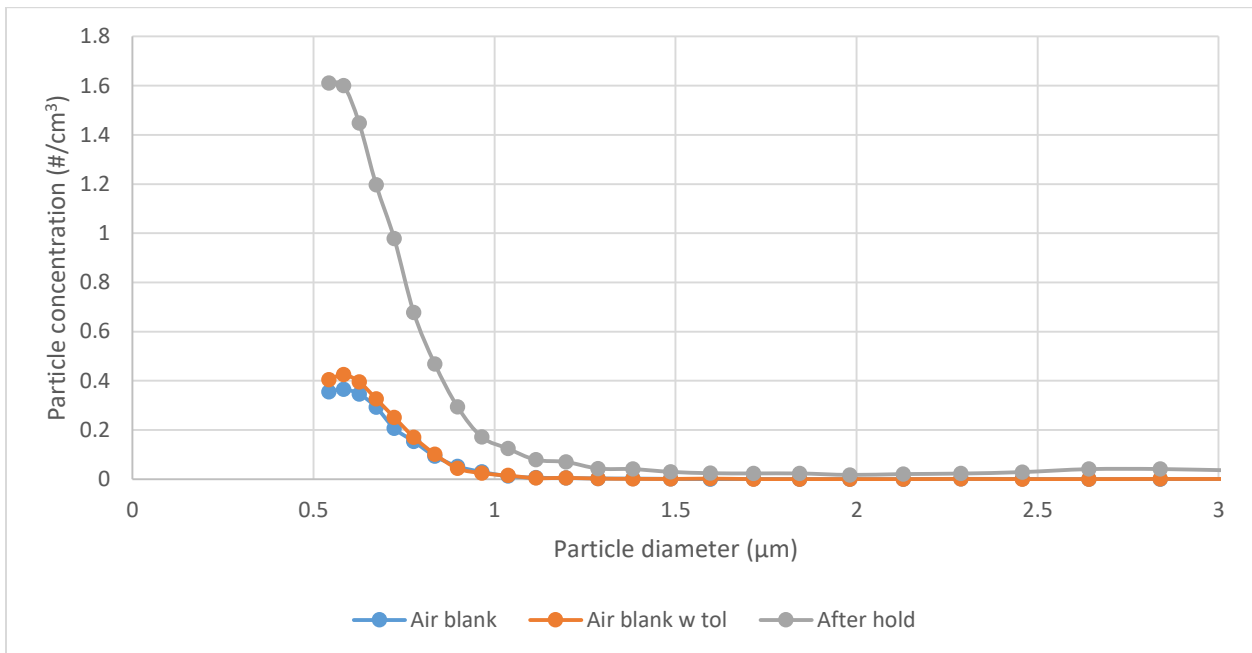


Figure A-14: 55-85 ng/mL toluene, 15 minutes UV irradiation, 5 minutes post-UV recirculation

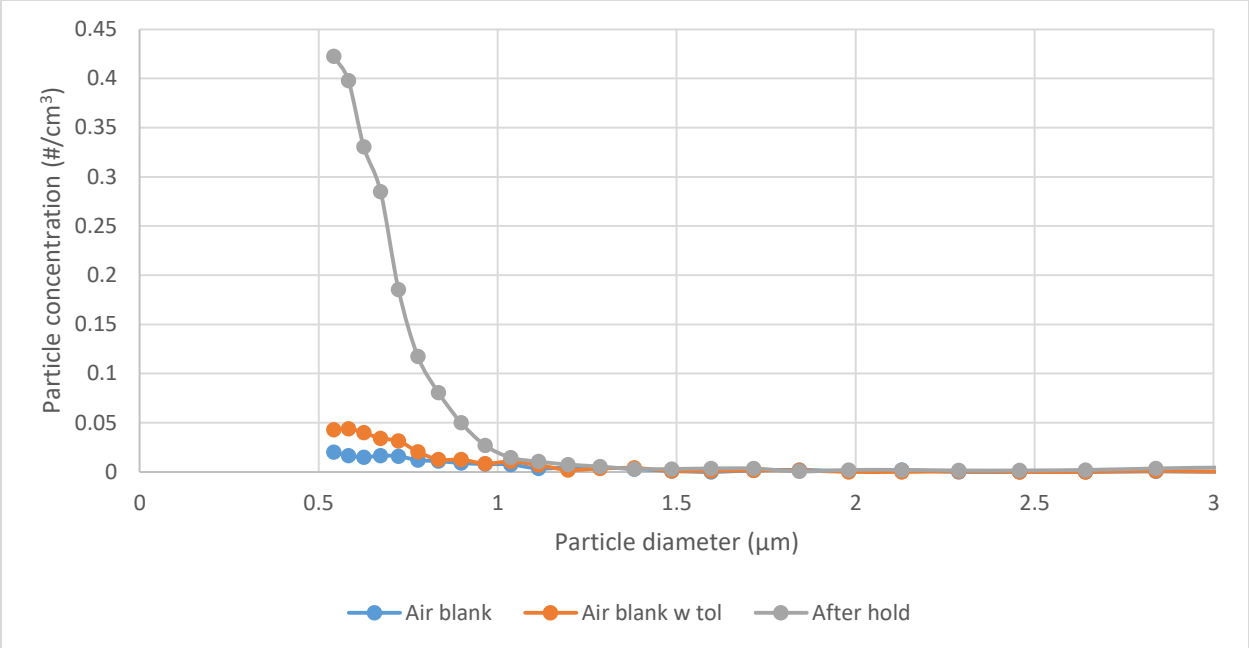


Figure A-15: 55-85 ng/mL toluene, 15 minutes UV irradiation, 15 minutes post-UV recirculation

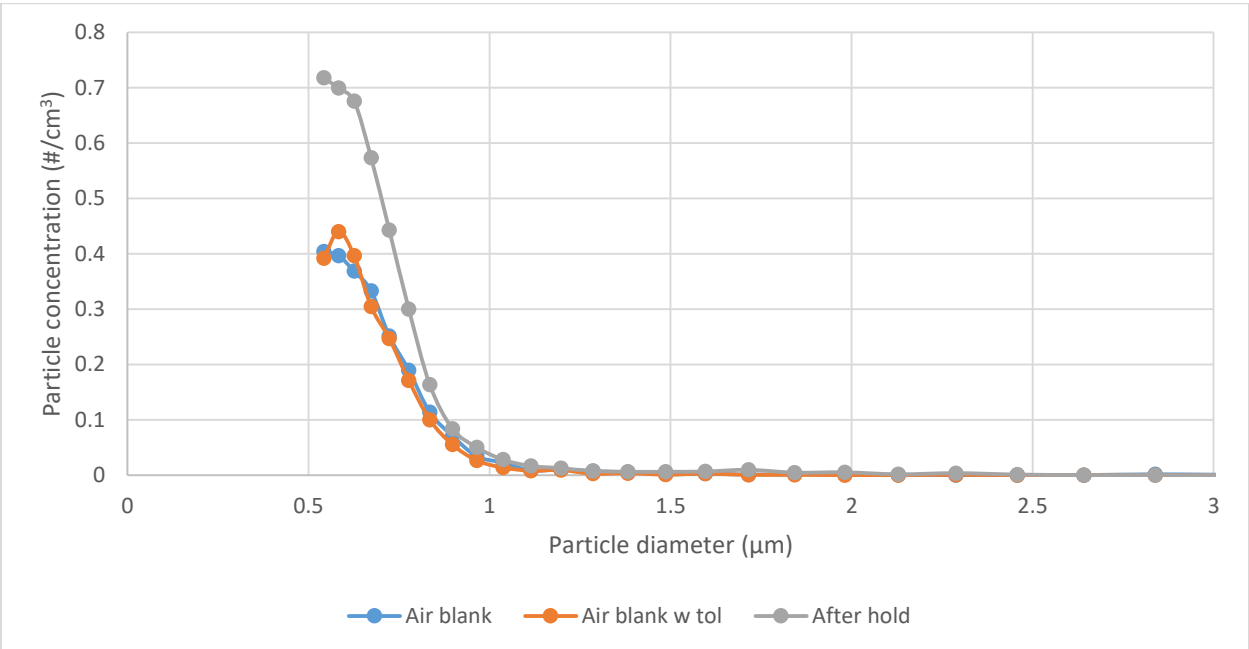


Figure A-16: 100-125 ng/mL toluene, 5 minutes UV irradiation, 1 minute post-UV recirculation

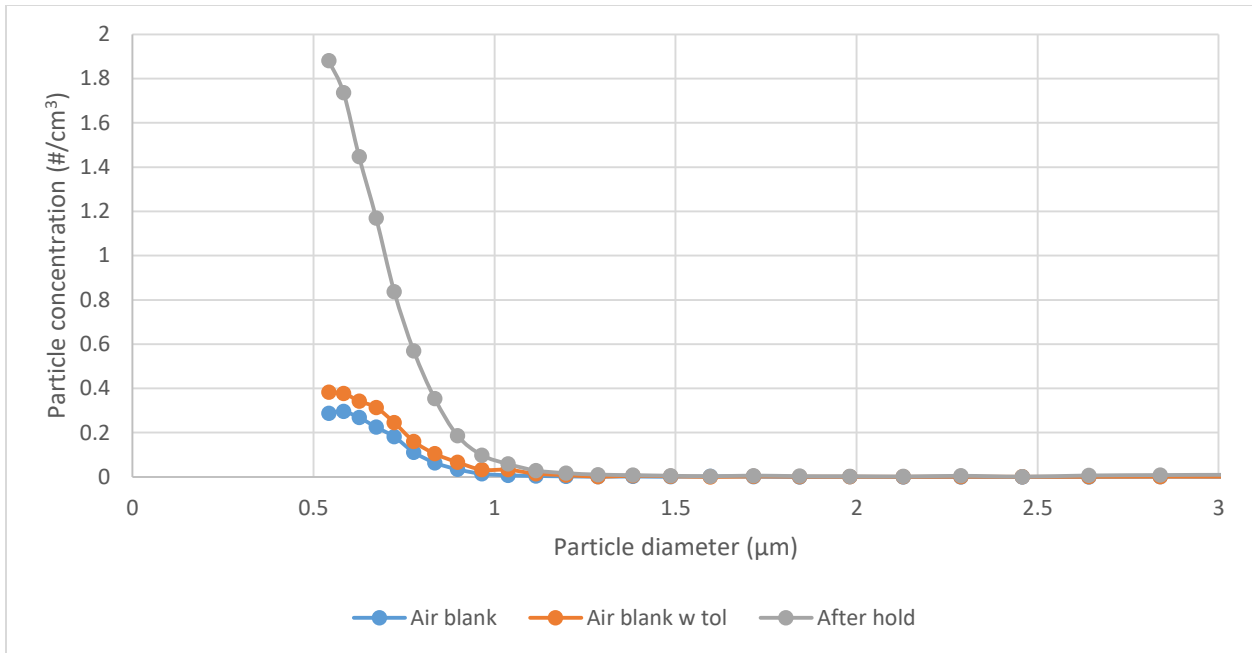


Figure A-17: 100-125 ng/mL toluene, 5 minutes UV irradiation, 5 minutes post-UV recirculation

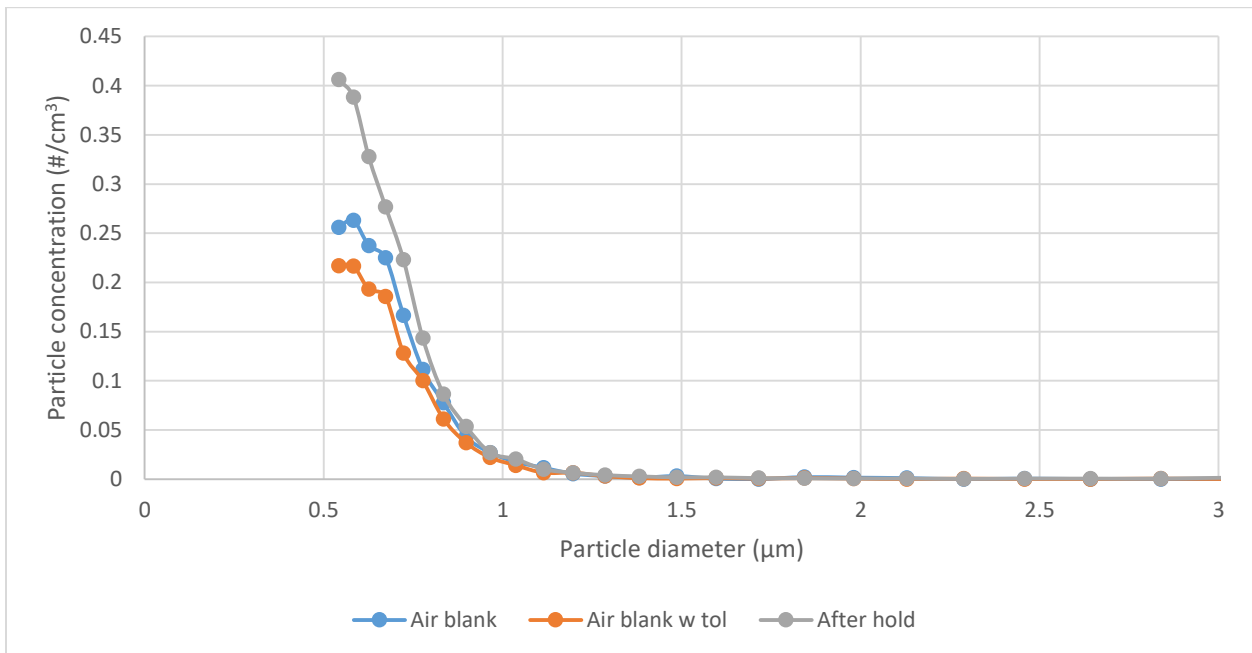


Figure A-18: 100-125 ng/mL toluene, 5 minutes UV irradiation, 15 minutes post-UV recirculation

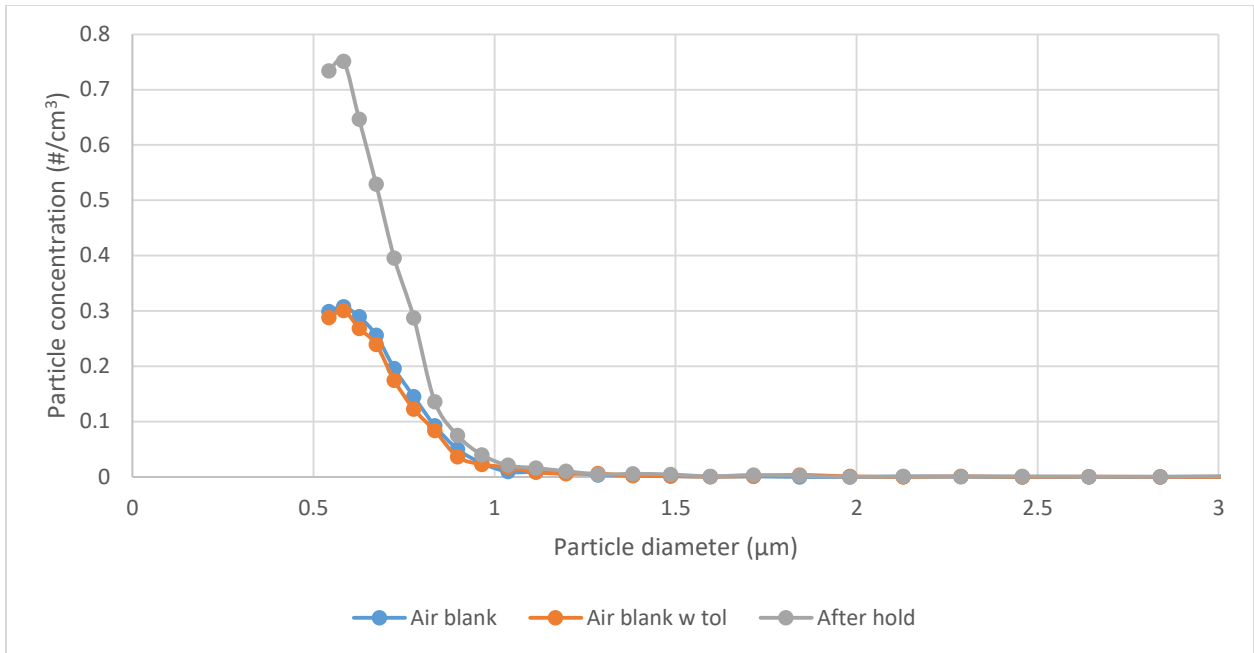


Figure A-19: 100-125 ng/mL toluene, 10 minutes UV irradiation, 1 minute post-UV recirculation

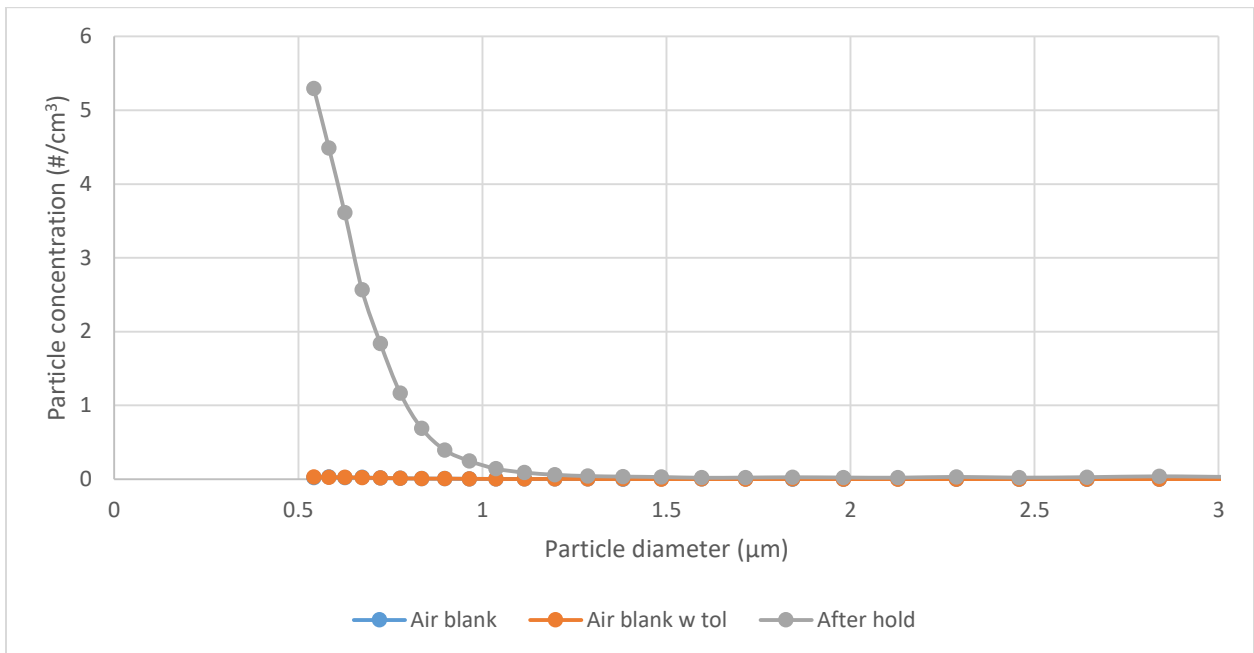


Figure A-20: 100-125 ng/mL toluene, 10 minutes UV irradiation, 5 minutes post-UV recirculation

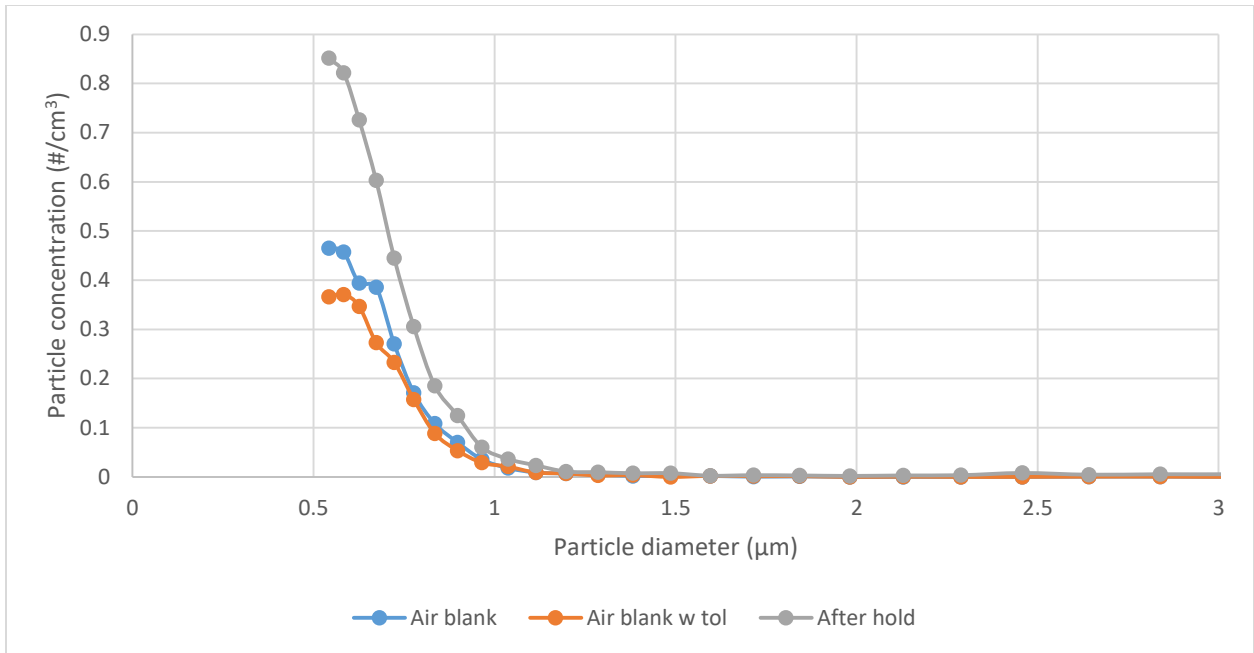


Figure A-21: 100-125 ng/mL toluene, 10 minutes UV irradiation, 15 minutes post-UV recirculation

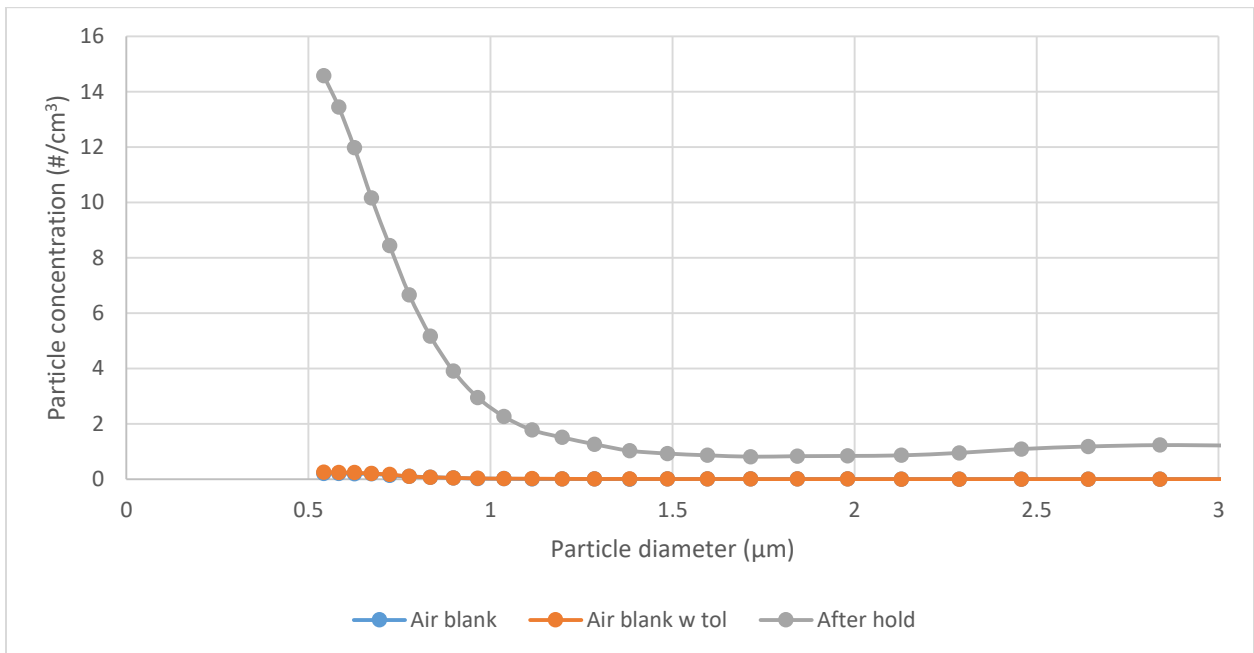


Figure A-22: 100-125 ng/mL toluene, 15 minutes UV irradiation, 1 minute post-UV recirculation

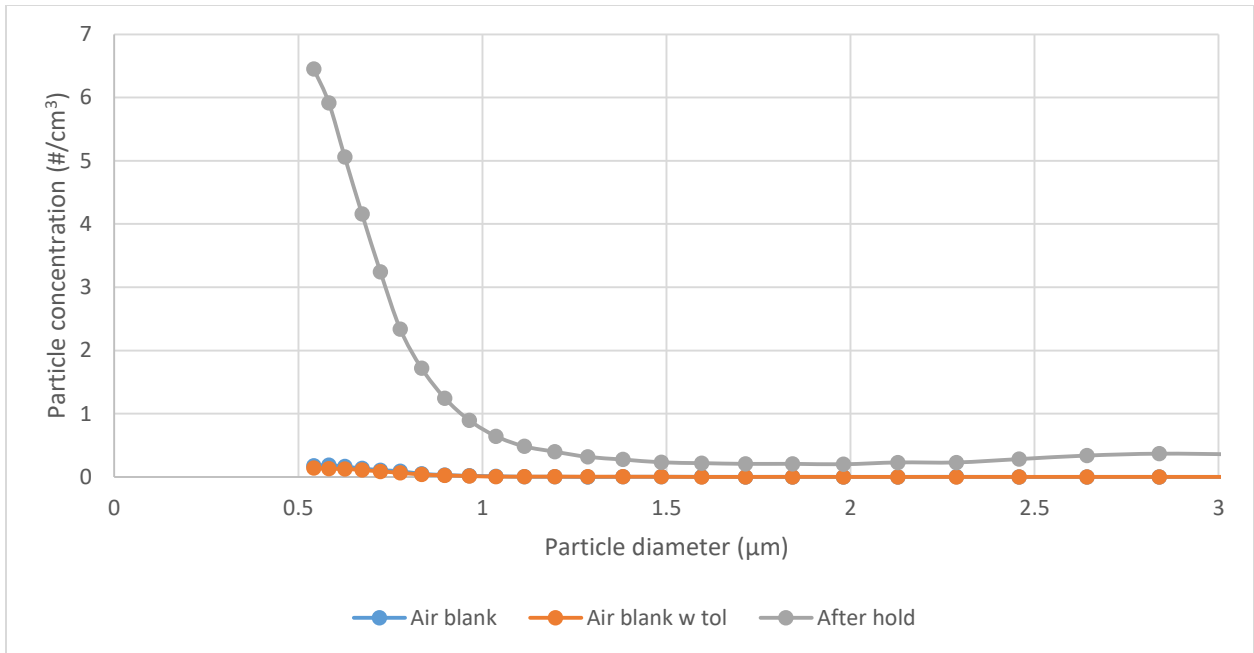


Figure A-23: 100-125 ng/mL toluene, 15 minutes UV irradiation, 5 minutes post-UV recirculation

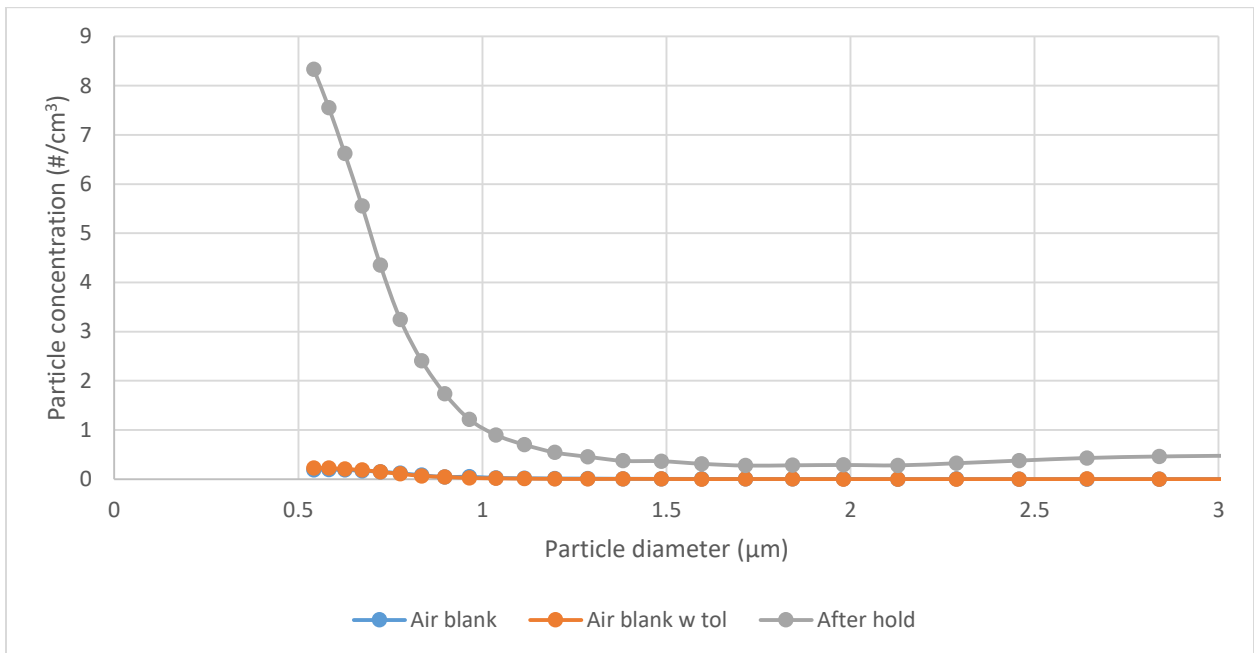


Figure A-24: 100-125 ng/mL toluene, 15 minutes UV irradiation, 15 minutes post-UV recirculation

A-2.3 Data for Statistica 11 Analysis

Table A-5: Data for Analysis in Statistica 11

Toluene added (μL)	UV irradiation (mins)	Recirculation (mins)	Fine particulate matter produced (# of particles/cm^3)
9	5	1	7.07887
9	5	5	6.522765
9	5	15	1.209474
9	10	1	213.9533
9	10	5	8.219337
9	10	5	33.03084
9	10	5	16.20469
9	10	15	6.865379
9	15	1	27.20794
9	15	5	163.1487
9	15	15	42.84214
15	5	1	8.35035
15	5	5	82.57797
15	5	15	4.405653
15	10	1	18.20165
15	10	5	261.3203
15	10	15	59.67182
15	15	1	1449.76
15	15	5	698.9044
15	15	15	868.429

A-3 Unfiltered Air Experiment

A-3.1 Data Sets

Table A-6: Initial toluene concentration and initial fine particulate matter levels for compressed air experiments

	Initial toluene concentration (ng/mL)	Fine particulate matter before UV (#/cm ³)
Filtered	73.37	21.296
	77.81	27.082
	71.63	4.779
	82.43	5.846
	69.92	6.084
	56.7	4.811
	56.43	3.781
	59	5.273
Unfiltered	59.24	9.831

A-3.2 Particle Size Distribution

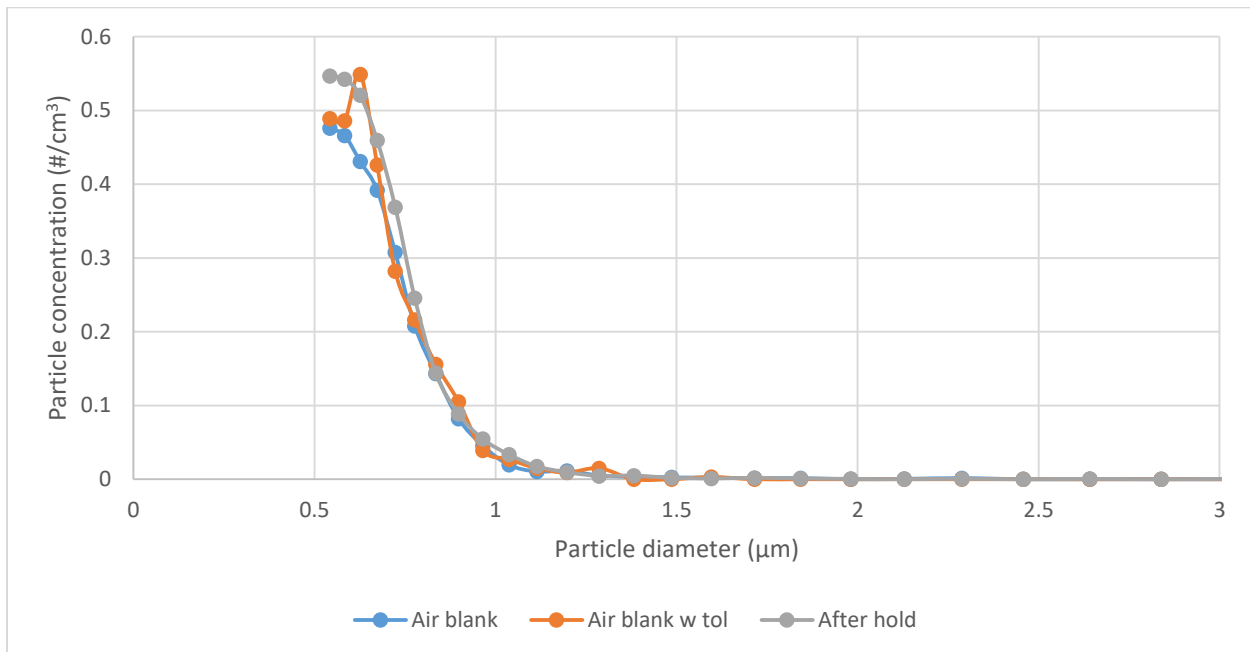


Figure A-25: Unfiltered compressed air, 55-85 ng/mL toluene, 5 minutes UV irradiation, 1 minute post-UV recirculation

A-4 Room Air Experiments

A-4.1 Data Set

Table A-7: Data for Room Air Experiments

Room Air	Relative Humidity (%)	Fine Particulate Matter Before UV (#/cm ³)	Fine Particulate Matter After UV (#/cm ³)	Fine Particulate Matter Formation (#/cm ³)
Unfiltered	23.8	26.07648	35.39631	9.320
Unfiltered	33.4	86.48479	102.4635	15.979
Unfiltered	18.6	42.63566	38.43372	-4.202
Filtered	15.9	4.502408	4.54991	0.048
Filtered	16	9.504313	10.46779	0.963
Filtered	43.2	23.85155	33.45434	9.603
Filtered	22.7	5.99188	5.19039	-0.801

A-4.2 Particle Size Distributions

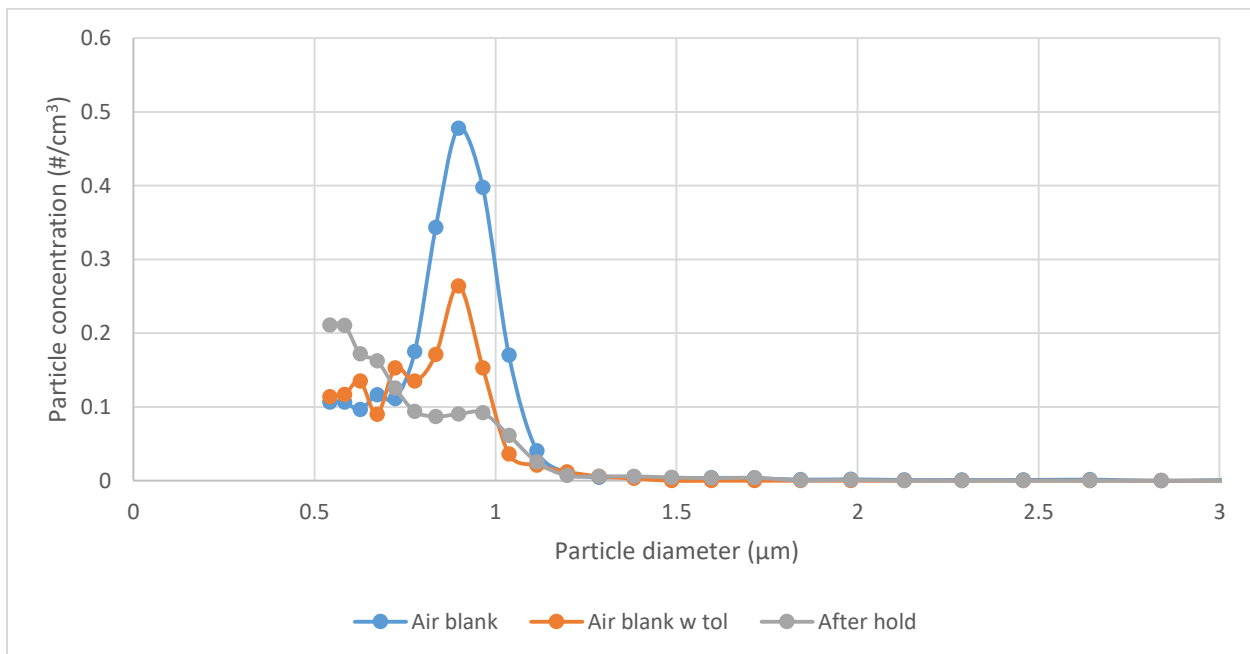


Figure A-26: Filtered room air, 15.9% RH, 55-85 ng/mL toluene, 5 minutes UV irradiation, 1 minute post-UV recirculation

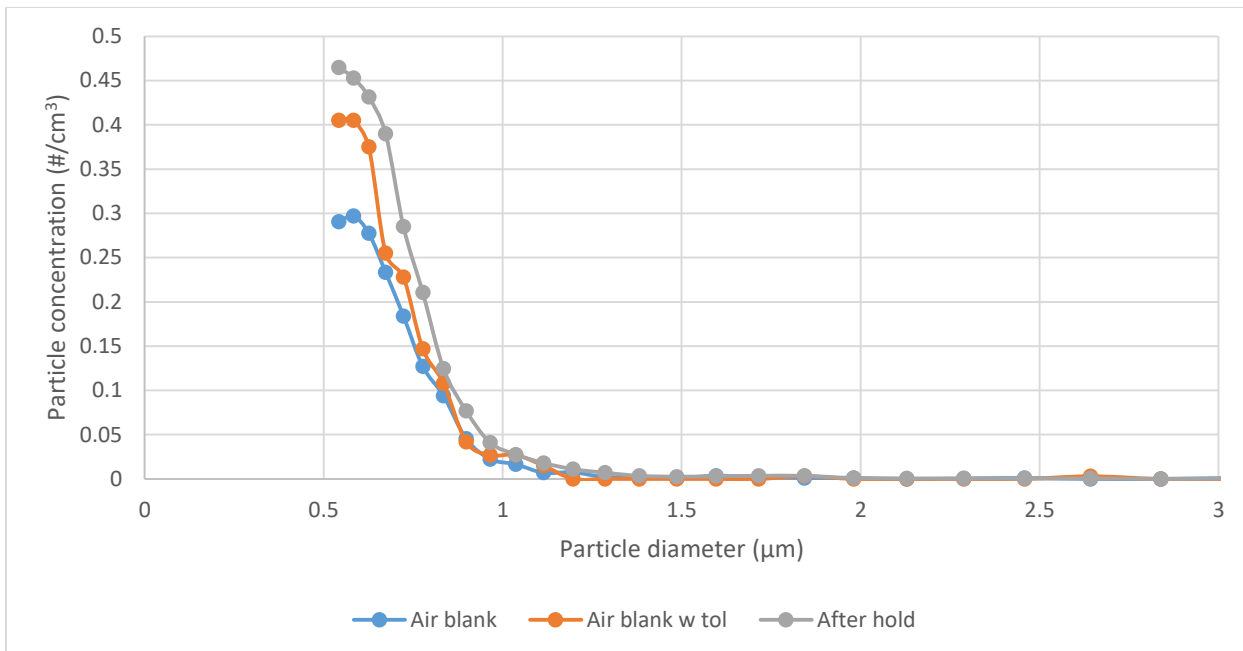


Figure A-27: Filtered room air, 16.0% RH, 55-85 ng/mL toluene, 5 minutes UV irradiation, 1 minute post-UV recirculation

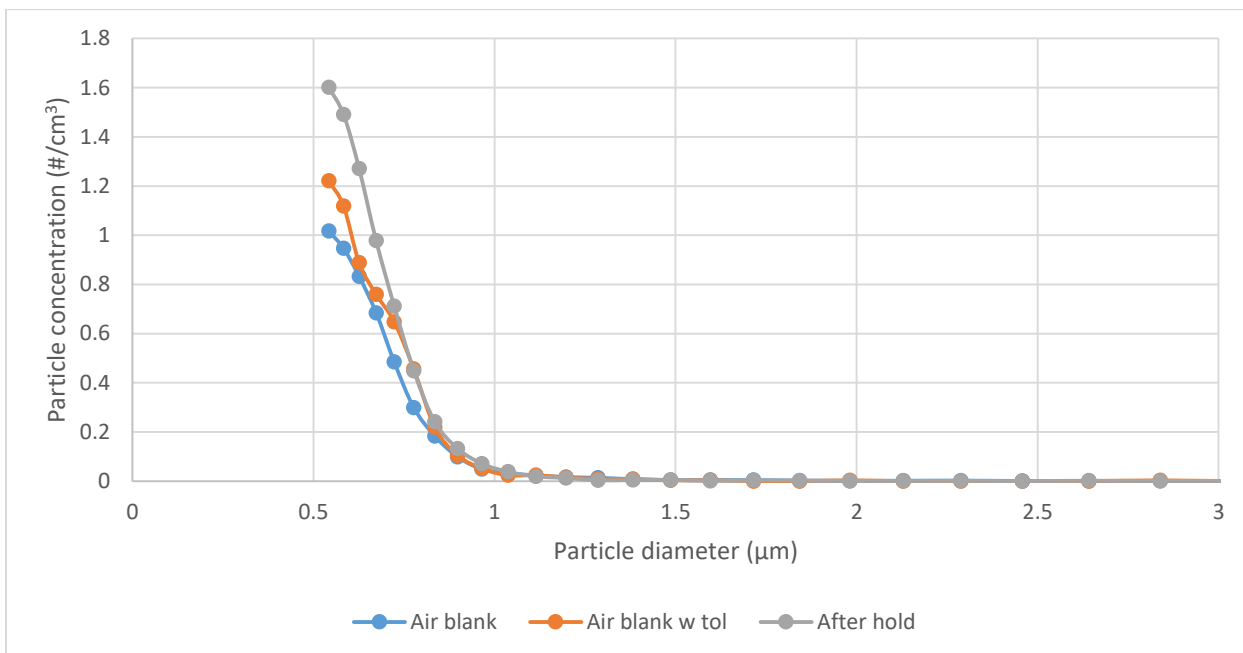


Figure A-28: Filtered room air, 43.2% RH, 55-85 ng/mL toluene, 5 minutes UV irradiation, 1 minute post-UV recirculation

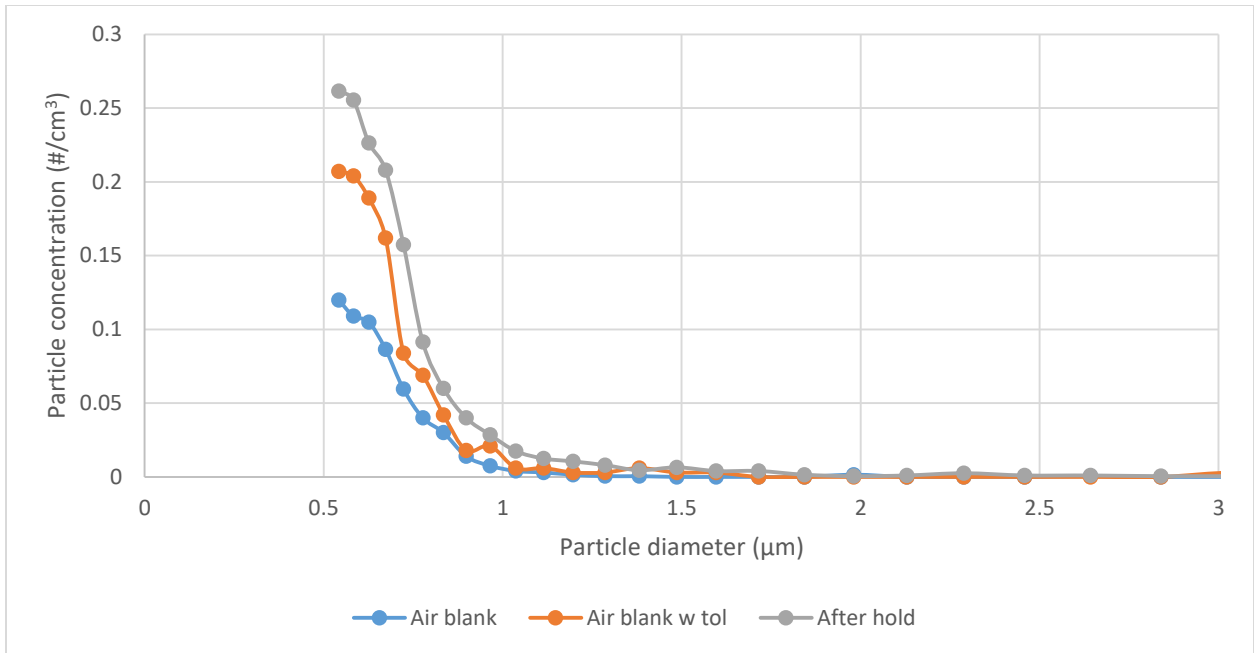


Figure A-29: Filtered room air, 22.7% RH, 55-85 ng/mL toluene, 5 minutes UV irradiation, 1 minute post-UV recirculation

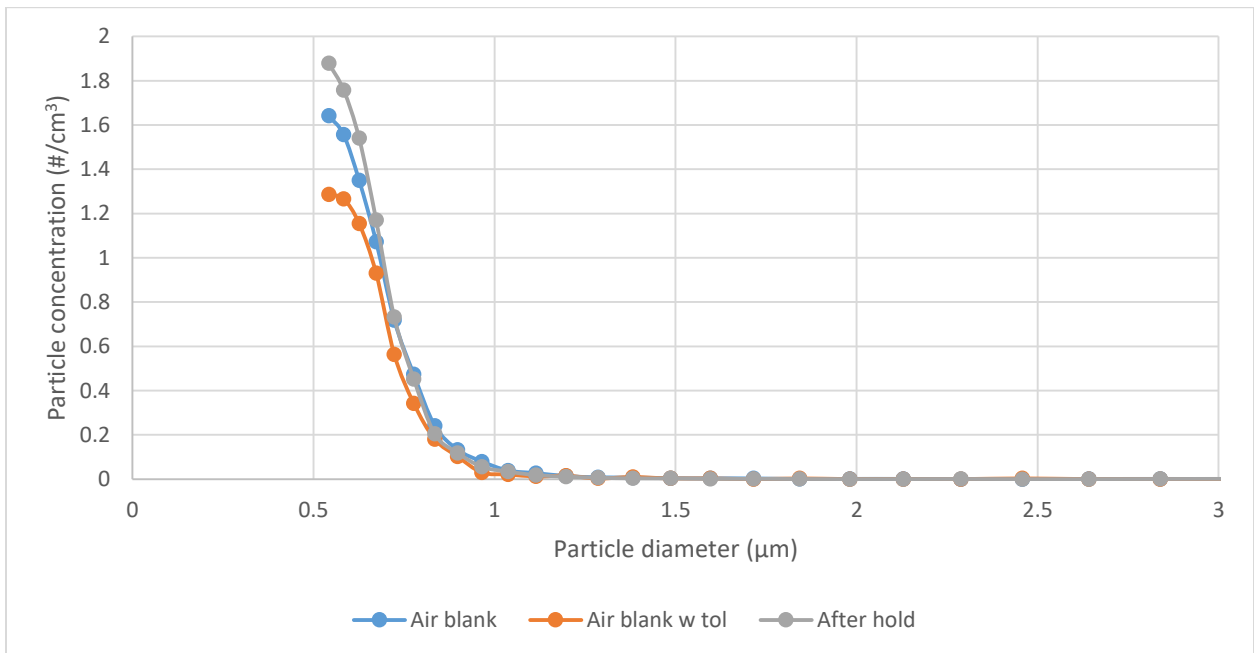


Figure A-30: Unfiltered room air, 23.8% RH, 55-85 ng/mL toluene, 5 minutes UV irradiation, 1 minute post-UV recirculation

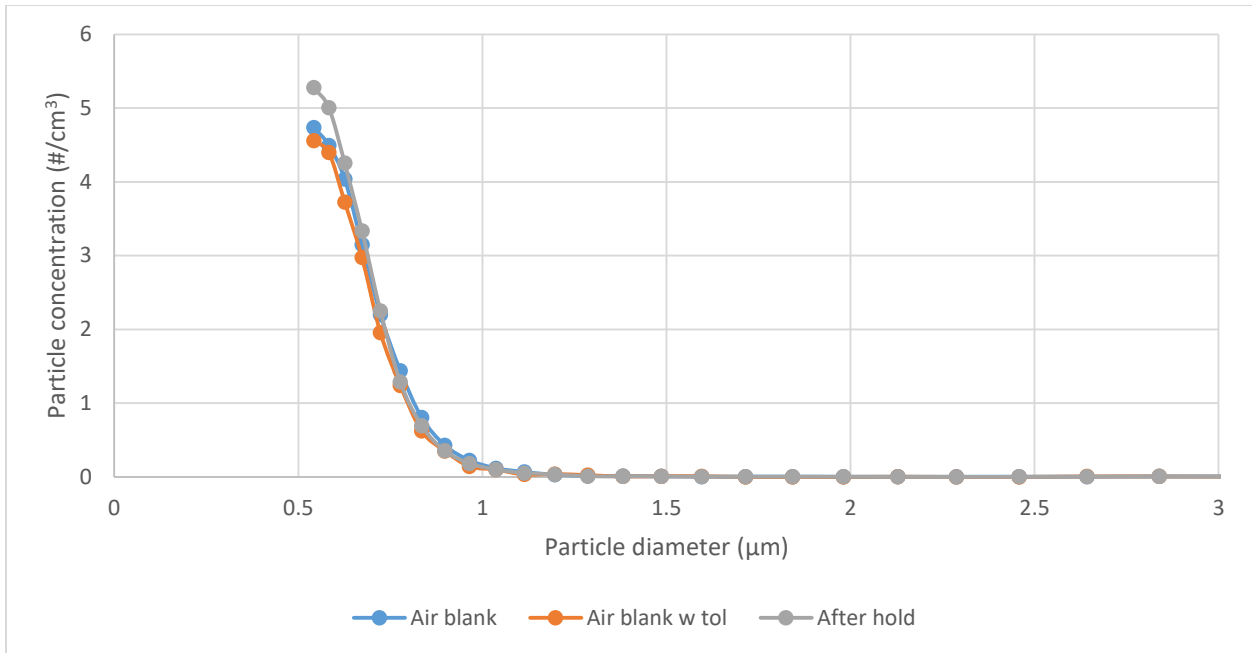


Figure A-31: Unfiltered room air, 33.4% RH, 55-85 ng/mL toluene, 5 minutes UV irradiation, 1 minute post-UV recirculation

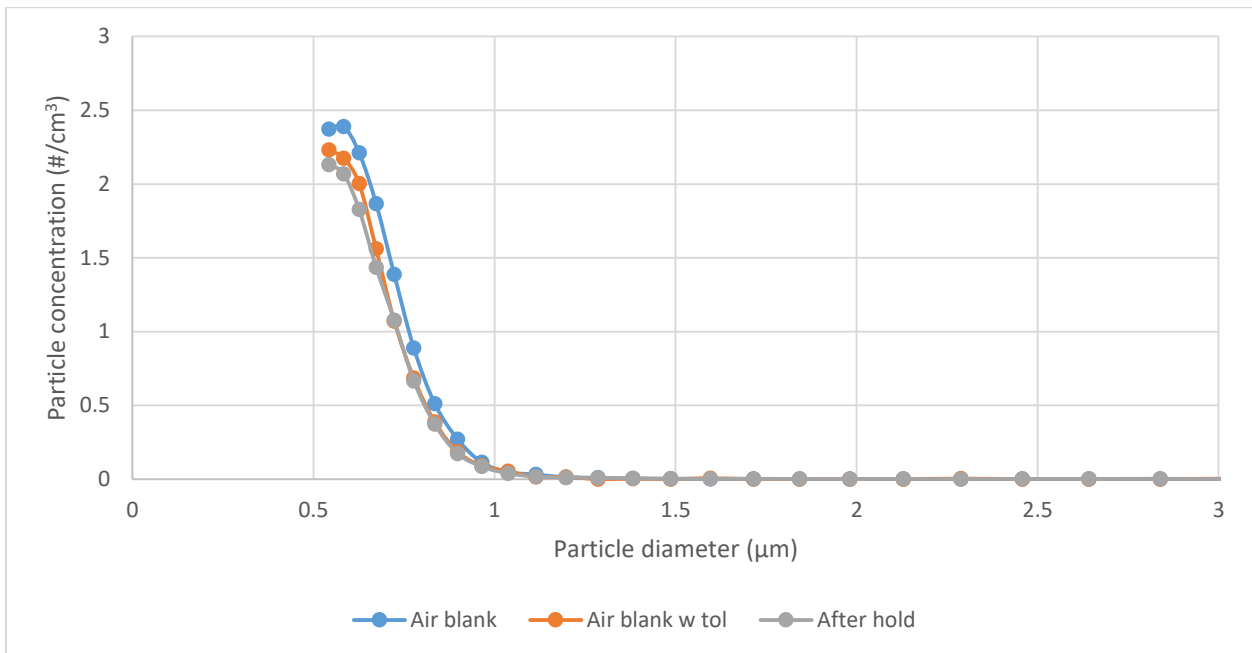


Figure A-32: Unfiltered room air, 18.6% RH, 55-85 ng/mL toluene, 5 minutes UV irradiation, 1 minute post-UV recirculation

A-5 Toluene Mass Balances

Table A-8: Data for toluene mass balances

Experiment specifications	Toluene mass (μg)			Particle mass (μg)			Mass balance (μg) (total initial mass – total final mass)
	Initial	Final	Amount consumed	Initial	Final	Amount formed	
55-85 ng/mL toluene 5 mins UV 1 min post-UV recirculation	2135.079	1712.281	422.798	259.924	258.443	-1.481	424.279
55-85 ng/mL toluene 5 mins UV 5 mins post-UV recirculation	2027.798	1796.893	230.905	278.371	770.816	492.446	-261.541
55-85 ng/mL toluene 5 mins UV 15 mins post-UV recirculation	1921.308	1889.150	32.158	78.910	74.070	-4.840	36.998
55-85 ng/mL toluene 10 mins UV 1 min post-UV recirculation	1830.896	1731.523	99.373	145.240	3601.190	3455.950	-3356.576
55-85 ng/mL toluene 10 mins UV 5 mins post-UV recirculation	1854.092	1574.687	279.405	208.670	746.015	537.344	-257.939
55-85 ng/mL toluene 10 mins UV 5 mins post-UV recirculation	2002.493	1408.625	593.868	101.719	584.082	482.362	111.505
55-85 ng/mL toluene 10 mins UV 5 mins post-UV recirculation	1583.122	1566.779	16.342	679.238	468.132	-211.105	227.448
55-85 ng/mL toluene 10 mins UV 15 mins post-UV recirculation	1483.748	1424.704	59.044	150.542	275.919	125.377	-66.333
55-85 ng/mL toluene 15 mins UV 1 min post-UV recirculation	1730.468	1596.307	134.431	69.241	694.498	625.256	-490.825
55-85 ng/mL toluene 15 mins UV 5 mins post-UV recirculation	1673.533	1598.410	75.123	1069.711	4136.007	3066.296	-2991.173
55-85 ng/mL toluene 15 mins UV	1942.658	1518.015	424.644	230.681	608.790	378.108	46.535

15 mins post-UV recirculation							
100-125 ng/mL toluene 5 mins UV 1 min post-UV recirculation	2876.821	2557.614	319.208	185.010	331.087	146.076	173.131
100-125 ng/mL toluene 5 mins UV 5 mins post-UV recirculation	3261.135	3214.216	46.919	282.741	1921.105	1638.364	-1591.445
100-125 ng/mL toluene 5 mins UV 15 mins post-UV recirculation	3166.770	3120.378	46.392	180.730	245.634	64.903	-18.512
100-125 ng/mL toluene 10 mins UV 1 min post-UV recirculation	2939.292	2794.054	145.238	394.211	418.728	24.517	120.721
100-125 ng/mL toluene 10 mins UV 5 mins post-UV recirculation	2757.942	2582.918	175.024	22.292	5367.915	5345.624	-5170.600
100-125 ng/mL toluene 10 mins UV 15 mins post-UV recirculation	2959.061	2890.528	68.533	229.07	1121.426	892.352	-823.818
100-125 ng/mL toluene 15 mins UV 1 min post-UV recirculation	3116.425	2914.515	201.910	112.963	12672.785	126859.82 1	-126657.912
100-125 ng/mL toluene 15 mins UV 5 mins post-UV recirculation	2781.665	2516.230	265.435	102.084	34114.717	34012.632	-33747.197
100-125 ng/mL toluene 15 mins UV 15 mins post-UV recirculation	2741.072	2499.360	241.712	114.114	45204.645	45090.532	-44848.819

Appendix B: Supplemental Information

B-1 VOC Concentrations in Indoor Environments

Table A-9: Statistics of VOC concentrations in home or school environments (Cometto-Muñiz and Abraham, 2015)

Variable (indoor home/school VOCs)	Minimum	Maximum	Range (max/min)	Mean	Median	Std. deviation	Variance	Std. error
Styrene (n = 23)	0.04	64.0	1600	6.1	0.9	14.2	202.270	2.97
Alpha-pinene (n = 21)	0.20	269.0	1345	32.8	11.0	62.3	3883.600	13.60
Beta-pinene (n = 8)	0.10	49.0	490	9.6	2.8	16.8	283.490	5.95
Benzene (n = 23)	0.09	43.7	486	6.1	2.5	9.8	95.910	2.04
Trichloroethylene (n = 8)	0.02	7.0	350	1.4	0.3	2.5	6.059	0.87
1,4-Dichlorobenzene (p-dichlorobenzene) (n = 19)	0.50	144.6	289	26.5	4.1	39.3	1545.600	9.02
n-Heptane (n = 15)	1.20	295.4	246	34.0	11.0	75.5	5695.800	19.49
Naphthalene (n = 10)	0.29	51.8	179	7.1	1.3	15.8	250.300	5.00
1,2,3-Trichlorobenzene (n = 2)	0.01	1.4	140	0.7	0.7	1.0	0.966	0.70
o-Xylene (n = 15)	0.24	33.5	139	4.6	1.8	8.3	68.986	2.14
Toluene (n = 30)	1.60	170.7	107	21.2	14.8	30.2	909.890	5.51
Ethylbenzene (n = 28)	0.24	20.0	83	4.0	3.0	4.5	20.593	0.86
1,3,5-Trimethylbenzene (n = 2)	0.02	1.6	80	0.8	0.8	1.1	1.248	0.79
Methyl isobutyl ketone (MIBK) (n = 4)	0.46	32.7	71	12.6	8.6	15.2	230.740	7.60
Tetrachloroethylene (n = 6)	0.02	1.3	65	0.5	0.4	0.4	0.191	0.18
1,2,4-Trimethylbenzene (n = 12)	0.14	7.6	54	4.3	4.2	2.2	4.867	0.64
n-Tridecane (n = 8)	0.78	40.0	51	7.3	3.0	13.3	177.510	4.71
2-Butanone (n = 5)	0.24	11.0	46	4.6	3.0	4.3	18.481	1.92
n-Octane (n = 8)	1.30	52.7	41	9.8	2.9	17.5	306.610	6.19
1,3-Dichlorobenzene (m-dichlorobenzene) (n = 2)	0.02	0.7	33	0.3	0.3	0.4	0.198	0.32
Acetic acid (n = 6)	6.80	190.0	28	48.3	21.9	70.1	4920.000	28.64
Methylene chloride (n = 6)	0.30	8.2	27	2.5	0.4	3.4	11.743	1.40
Limonene (n = 24)	1.90	49.3	26	20.6	19.2	13.1	171.680	2.67
n-Hexane (n = 9)	1.50	36.4	24	10.7	7.3	11.0	120.190	3.65
Chloroform (n = 8)	0.09	2.1	23	0.9	0.7	0.7	0.553	0.26
n-Nonane (n = 14)	1.50	33.5	22	14.3	13.2	8.8	78.294	2.36
1,2,4-Trichlorobenzene (n = 2)	0.07	1.4	20	0.7	0.7	0.9	0.884	0.67
n-Decane (n = 17)	2.20	41.8	19	19.1	16.0	11.4	129.040	2.76
n-Butyl acetate (n = 8)	2.50	47.0	19	16.3	9.0	17.5	305.730	6.18
Dodecane (n = 10)	2.22	38.0	17	15.8	7.5	15.0	224.810	4.74
m/p-Xylene (n = 15)	1.20	19.0	16	7.5	6.5	5.5	30.796	1.43
Ethanol (n = 3)	70.00	860.0	12	340.7	92.0	449.9	202400.000	259.74
Phenol (n = 3)	0.61	7.1	12	3.1	1.7	3.5	12.078	2.01

Variable (indoor home/school VOCs)	Minimum	Maximum	Range (max/min)	Mean	Median	Std. deviation	Variance	Std. error
p-Xylene (n = 9)	2.60	30.0	12	11.4	7.6	10.8	116.550	3.60
Tetrahydrofuran (n = 2)	0.16	1.7	11	0.9	0.9	1.1	1.186	0.77
Trichlorofluoromethane (Freon 11) (n = 4)	4.73	50.0	11	25.6	23.8	23.3	544.290	11.67
Formaldehyde (n = 16)	12.70	134.0	11	60.5	53.4	34.8	1208.400	8.69
Ethylacetate (n = 11)	3.30	34.0	10	16.6	16.7	9.9	98.928	3.00
Acetone (n = 8)	9.10	87.1	9.6	35.0	32.8	24.2	587.050	8.57
n-Undecane (n = 9)	3.00	24.1	8.0	9.6	8.8	6.2	38.392	2.07
2-Butoxyethanol (n = 3)	0.75	5.8	7.7	3.1	2.6	2.6	6.528	1.48
Isopentane (n = 2)	1.40	9.5	6.8	5.5	5.5	5.7	32.805	4.05
Pentanal (valeraldehyde) (n = 7)	1.00	5.5	5.5	2.4	1.3	1.8	3.303	0.69
2-Methylpentane (n = 3)	0.37	1.8	4.9	1.2	1.5	0.8	0.569	0.44
Crotonaldehyde (2-butenal) (n = 8)	1.60	7.6	4.8	4.8	4.9	1.8	3.385	0.65
1-Butanol (n = 8)	35.00	147.6	4.2	66.0	51.4	37.4	1400.800	13.23
n-Pentane (n = 2)	1.40	5.8	4.1	3.6	3.6	3.1	9.680	2.20
Tetrachloroethene (n = 2)	0.70	2.9	4.1	1.8	1.8	1.6	2.420	1.10
Xylene (n = 6)	5.00	18.2	3.6	7.8	5.8	5.1	26.327	2.09
Butanal (n = 9)	2.20	8.0	3.6	5.1	4.2	2.2	4.993	0.74
Isobutylketone (diisobutylketone) (n = 4)	8.00	27.0	3.4	15.0	12.5	8.3	68.667	4.14
Benzaldehyde (n = 7)	2.00	6.2	3.1	3.4	3.0	1.4	1.922	0.52
Octanal (n = 2)	4.30	13.0	3.0	8.7	8.7	6.2	37.845	4.35
Camphene (n = 2)	1.90	5.2	2.7	3.6	3.6	2.3	5.445	1.65
Nonanal (n = 3)	8.10	22.0	2.7	16.0	18.0	7.2	51.203	4.13
3-Carene (n = 2)	8.50	23.0	2.7	15.8	15.8	10.3	105.130	7.25
Trichloroethene (n = 2)	2.30	6.0	2.6	4.2	4.2	2.6	6.845	1.85
Hexanal (n = 10)	5.00	13.0	2.6	7.9	7.5	2.8	7.683	0.88
Chlorobenzene (n = 3)	0.68	1.7	2.5	1.3	1.6	0.6	0.316	0.32
4-Ethyltoluene (p-ethyltoluene) (n = 6)	2.26	5.4	2.4	3.3	2.8	1.1	1.302	0.47
3-Ethyltoluene (m-ethyltoluene) (n = 5)	0.97	2.3	2.4	1.5	1.2	0.6	0.347	0.26
Acrolein (n = 2)	1.00	2.3	2.3	1.7	1.7	0.9	0.845	0.65
2-Ethyltoluene (o-ethyltoluene) (n = 5)	1.02	2.3	2.3	1.5	1.3	0.5	0.270	0.23
Acetaldehyde (n = 9)	11.00	24.3	2.2	17.8	20.0	5.1	26.292	1.71
Methyl ethyl ketone (MEK) (n = 2)	3.60	7.4	2.1	5.5	5.5	2.7	7.220	1.90
Cyclohexane (n = 2)	2.90	5.2	1.8	4.1	4.1	1.6	2.645	1.15
Methyl tert-butyl ether (MTBE) (n = 2)	12.00	19.3	1.6	15.7	15.7	5.2	26.645	3.65
Propanal (n = 7)	6.90	10.9	1.6	8.2	8.0	1.3	1.665	0.49
Carbon tetrachloride (n = 5)	0.50	0.7	1.4	0.6	0.6	0.1	0.006	0.03
n-Tetradecane (n = 2)	1.30	1.7	1.3	1.5	1.5	0.3	0.080	0.20
Methylchloride (chloromethane) (n = 2)	1.49	1.8	1.2	1.6	1.6	0.2	0.048	0.16
n-Pentadecane (n = 2)	1.10	1.2	1.1	1.2	1.2	0.1	0.005	0.05
n-Hexadecane (n = 2)	1.10	1.1	1.0	1.1	1.1	0.0	0.000	0.00
Methylbenzaldehyde (tolualdehyde) (n = 4)	1.00	1.0	1.0	1.0	1.0	0.0	0.000	0.00

Table A-10: Statistics of VOC concentrations in commercial environments (Cometto-Muñiz and Abraham, 2015)

Variable (indoor commercial VOCs)	Minimum	Maximum	Range (max/min)	Mean	Median	Std. deviation	Variance	Std. error
Acetone (n = 3)	22.9	5510.0	241	1852.2	23.7	3167.70	10035000.000	1828.90
Alpha-pinene (n = 6)	0.7	163.9	234	28.8	2.1	66.18	4379.400	27.02
Isopropyl alcohol (isopropanol) (n = 2)	2.7	493.0	183	247.9	247.9	346.69	120200.000	245.15
Styrene (n = 10)	0.2	32.9	165	4.8	1.4	9.98	99.638	3.16
Tetrachloroethylene (n = 4)	3.0	432.0	144	115.2	13.0	211.33	44660.000	105.67
Toluene (n = 13)	6.5	776.5	119	112.3	33.3	208.47	43461.000	57.82
Ethylacetate (n = 2)	2.1	135.0	64	68.6	68.6	93.97	8831.200	66.45
1,3,5-Trimethylbenzene (n = 3)	0.2	8.8	44	5.6	7.8	4.70	22.120	2.72
1,4-Dichlorobenzene (p-dichlorobenzene) (n = 5)	0.3	13.0	43	5.5	2.4	5.73	32.847	2.56
Ethylbenzene (n = 10)	0.6	25.1	42	6.8	5.0	7.33	53.798	2.32
Chloroform (n = 5)	0.4	13.5	31	5.6	1.1	6.71	45.023	3.00
4-Ethyltoluene (p-ethyltoluene) (n = 3)	0.3	6.0	20	3.8	5.1	3.06	9.390	1.77
Benzene (n = 12)	1.2	23.6	20	8.0	4.9	7.58	57.435	2.19
Dichlorodifluoromethane (Freon 21) (n = 3)	2.8	42.9	15	16.3	3.3	23.01	529.400	13.28
Naphthalene (n = 3)	0.3	4.3	13	1.7	0.5	2.23	4.990	1.29
o-Xylene (n = 9)	1.5	17.3	12	6.5	4.1	5.85	34.192	1.95
1,2,4-Trimethylbenzene (n = 6)	1.1	12.2	11	6.3	5.7	5.05	25.550	2.06
Trichloroethylene (n = 3)	0.8	8.8	11	5.1	5.6	4.03	16.213	2.32
m/p-Xylene (n = 7)	3.9	41.6	11	14.7	6.2	15.05	226.510	5.69
Carbon tetrachloride (n = 3)	0.1	0.9	9.0	0.6	0.7	0.41	0.168	0.24
n-Heptane (n = 4)	1.8	14.3	7.9	8.0	8.0	5.30	28.087	2.65
Hexaldehyde (hexanal) (n = 3)	2.2	17.0	7.7	8.2	5.4	7.79	60.640	4.50
p-Xylene (n = 3)	6.6	46.9	7.1	20.2	7.2	23.10	533.420	13.33
Nicotine (n = 2)	5.4	38.3	7.1	21.9	21.9	23.26	541.200	16.45
o-Limonene (n = 8)	2.5	17.5	7.0	6.8	5.6	4.64	21.554	1.64
Xylene (n = 2)	2.6	14.3	5.5	8.5	8.5	8.27	68.445	5.85
Propanal (propionaldehyde) (n = 2)	2.5	11.9	4.8	7.2	7.2	6.65	44.180	4.70
Isoprene (n = 2)	4.5	20.6	4.6	12.6	12.6	11.38	129.610	8.05
1,1-Dichloroethane (n = 2)	0.4	1.8	4.5	1.1	1.1	0.99	0.980	0.70
MTBE (methyl tert-butyl ether) (n = 3)	2.3	10.0	4.4	4.9	2.4	4.43	19.615	2.56
m-Xylene (n = 3)	12.3	50.4	4.1	25.4	13.5	21.66	469.110	12.51
1,1,2,2-Tetrachloroethane (n = 2)	1.0	4.0	4.0	2.5	2.5	2.12	4.500	1.50
1,3-Butadiene (n = 2)	1.1	4.3	3.9	2.7	2.7	2.26	5.120	1.60

Variable (indoor commercial VOCs)	Minimum	Maximum	Range (max/min)	Mean	Median	Std. deviation	Variance	Std. error
Methylchloride (chloromethane) (n = 3)	0.9	3.5	3.9	2.5	3.0	1.38	1.903	0.80
Formaldehyde (n = 7)	5.6	21.3	3.8	15.4	17.1	5.55	30.818	2.10
3-Ethenylpyridine (n = 2)	1.2	4.4	3.7	2.8	2.8	2.26	5.120	1.60
Dichloromethane (n = 2)	14.1	50.2	3.6	32.2	32.2	25.53	651.600	18.05
Trichlorofluoromethane (Freon 11) (n = 3)	2.8	9.8	3.5	5.1	2.8	4.04	16.333	2.33
Pyridine (n = 2)	0.8	2.6	3.4	1.7	1.7	1.29	1.674	0.92
Methylene chloride (n = 3)	0.7	2.2	3.3	1.2	0.8	0.87	0.759	0.50
3-Picoline (n = 2)	0.7	2.2	3.3	1.4	1.4	1.09	1.186	0.77
Acetaldehyde (n = 6)	7.5	24.4	3.3	13.7	10.4	7.19	51.663	2.93
Dodecane (n = 2)	12.0	38.5	3.2	25.3	25.3	18.74	351.120	13.25
1,1,2-Trichlorotrifluoroethane (n = 3)	0.9	2.6	2.9	1.6	1.4	0.87	0.763	0.50
Furfuryl aldehyde (n = 2)	1.6	4.4	2.8	3.0	3.0	1.98	3.920	1.40
Phenol (n = 2)	1.1	2.8	2.5	2.0	2.0	1.20	1.445	0.85
n-Undecane (n = 2)	3.0	7.5	2.5	5.3	5.3	3.18	10.125	2.25
3-Ethyltoluene (m-ethyltoluene) (n = 3)	4.5	9.1	2.0	6.4	5.6	2.40	5.770	1.39
1,2,4-Trichlorobenzene (n = 2)	12.8	24.5	1.9	18.7	18.7	8.27	68.445	5.85
Methylcyclohexane (n = 2)	2.0	3.8	1.9	2.9	2.9	1.27	1.620	0.90
Trichloroethene (n = 2)	0.2	0.4	1.9	0.3	0.3	0.14	0.020	0.10
Benzaldehyde (n = 2)	1.5	2.3	1.5	1.9	1.9	0.57	0.320	0.40
Perchloroethylene (n = 2)	1.4	2.1	1.5	1.8	1.8	0.48	0.231	0.34
Bromomethane (n = 2)	1.1	1.6	1.5	1.4	1.4	0.35	0.125	0.25
1,2-Dichlorobenzene (o-dichlorobenzene) (n = 2)	1.6	2.3	1.4	2.0	2.0	0.49	0.245	0.35
1,3-Dichlorobenzene (m-dichlorobenzene) (n = 2)	1.6	2.2	1.4	1.9	1.9	0.42	0.180	0.30
Ethylchloride (n = 2)	0.3	0.4	1.3	0.4	0.4	0.07	0.005	0.05
1,1,1-Trichloroethane (n = 2)	13.4	17.1	1.3	15.3	15.3	2.62	6.845	1.85
n-Octane (n = 2)	3.1	3.9	1.3	3.5	3.5	0.57	0.320	0.40
1,2-Dibromoethane (n = 2)	0.9	1.1	1.2	1.0	1.0	0.14	0.020	0.10
Chlorobenzene (n = 2)	1.4	1.7	1.2	1.6	1.6	0.21	0.045	0.15
1,1-Dichloroethane (n = 2)	0.5	0.6	1.2	0.6	0.6	0.07	0.005	0.05
1-Butanol (n = 2)	2.2	2.6	1.2	2.4	2.4	0.28	0.080	0.20
1,2-Dichloroethane (n = 2)	0.6	0.7	1.2	0.7	0.7	0.07	0.005	0.05
1,1,2-Trichloroethane (n = 2)	0.6	0.7	1.2	0.7	0.7	0.07	0.005	0.05
n-Decane (n = 2)	4.4	4.7	1.1	4.6	4.6	0.21	0.045	0.15
1,2-Dichlorotetrafluoroethane (n = 2)	0.7	0.7	1.0	0.7	0.7	0.00	0.000	0.00
1,2-Dichloroethene (n = 2)	0.4	0.4	1.0	0.4	0.4	0.00	0.000	0.00

B-2 UV Irradiance Rate in Reactor Calculation

Table A-11: Overview of calculations of UV irradiance in reactor

Average Irradiance Rate Calculations for Batch UV reactor, based on Bolton's (2000) report of Blatchley's (1997) closed form equation			
(Ignores reflection and refraction effects)			
Lamp Length	81.3	cm	
Distance minimum	0.5	cm	radial
Distance maximum	10.15	cm	radial
Height/Length	81.3	cm	reactor height or length (depending on orientation)
Max Height	40.65	cm	above lamp middle
Min Height	40.65	cm	below lamp middle
Lamp Power	40	W	at 254 nm
Volume average irradiance rate	19.52	mW/cm ²	

Table A-12: Calculations for UV irradiance in reactor

Height above lamp mid-point (cm)	Radial Distance (cm)																					
	0.50	0.98	1.47	1.95	2.43	2.91	3.40	3.88	4.36	4.84	5.33	5.81	6.29	6.77	7.26	7.74	8.22	8.70	9.19	9.67	10.15	
40.65	0.123	0.062	0.041	0.031	0.025	0.021	0.018	0.015	0.014	0.012	0.011	0.010	0.009	0.009	0.008	0.007	0.007	0.007	0.006	0.006	0.006	0.006
40.15	0.184	0.081	0.050	0.036	0.028	0.023	0.019	0.017	0.015	0.013	0.012	0.011	0.010	0.009	0.008	0.008	0.007	0.007	0.006	0.006	0.006	0.006
39.65	0.209	0.094	0.057	0.041	0.031	0.025	0.021	0.018	0.016	0.014	0.012	0.011	0.010	0.009	0.009	0.008	0.008	0.007	0.007	0.006	0.006	0.006
39.15	0.220	0.102	0.063	0.044	0.034	0.027	0.022	0.019	0.017	0.015	0.013	0.012	0.011	0.010	0.009	0.008	0.008	0.007	0.007	0.006	0.006	0.006
38.65	0.226	0.107	0.067	0.047	0.036	0.029	0.024	0.020	0.017	0.015	0.014	0.012	0.011	0.010	0.009	0.009	0.008	0.008	0.007	0.007	0.007	0.006
38.15	0.230	0.110	0.069	0.049	0.038	0.030	0.025	0.021	0.018	0.016	0.014	0.013	0.012	0.011	0.010	0.009	0.008	0.008	0.007	0.007	0.007	0.006
37.65	0.233	0.112	0.071	0.051	0.039	0.031	0.026	0.022	0.019	0.017	0.015	0.013	0.012	0.011	0.010	0.009	0.009	0.008	0.008	0.007	0.007	0.007
37.15	0.234	0.114	0.073	0.052	0.040	0.032	0.027	0.023	0.020	0.017	0.015	0.014	0.012	0.011	0.010	0.010	0.009	0.008	0.008	0.007	0.007	0.007
36.65	0.236	0.115	0.074	0.054	0.041	0.033	0.028	0.023	0.020	0.018	0.016	0.014	0.013	0.012	0.011	0.010	0.009	0.009	0.008	0.007	0.007	0.007
36.15	0.237	0.116	0.075	0.054	0.042	0.034	0.028	0.024	0.021	0.018	0.016	0.015	0.013	0.012	0.011	0.010	0.009	0.009	0.008	0.008	0.008	0.007
35.65	0.238	0.117	0.076	0.055	0.043	0.035	0.029	0.025	0.021	0.019	0.017	0.015	0.013	0.012	0.011	0.010	0.010	0.009	0.008	0.008	0.008	0.007
35.15	0.238	0.118	0.076	0.056	0.043	0.035	0.029	0.025	0.022	0.019	0.017	0.015	0.014	0.013	0.011	0.011	0.010	0.009	0.008	0.008	0.008	0.007

3.65	0.244	0.123	0.082	0.061	0.049	0.040	0.034	0.030	0.026	0.023	0.021	0.019	0.018	0.016	0.015	0.014	0.013	0.012	0.011	0.011	0.010
3.15	0.244	0.123	0.082	0.061	0.049	0.040	0.034	0.030	0.026	0.023	0.021	0.019	0.018	0.016	0.015	0.014	0.013	0.012	0.011	0.011	0.010
2.65	0.244	0.123	0.082	0.061	0.049	0.040	0.034	0.030	0.026	0.023	0.021	0.019	0.018	0.016	0.015	0.014	0.013	0.012	0.011	0.011	0.010
Average	0.239	0.119	0.079	0.058	0.046	0.038	0.032	0.028	0.024	0.022	0.019	0.018	0.016	0.015	0.014	0.013	0.012	0.011	0.010	0.010	0.009
Radius x Average	0.12	0.117	0.115	0.113	0.112	0.11	0.109	0.107	0.106	0.104	0.103	0.102	0.101	0.099	0.098	0.097	0.096	0.095	0.094	0.093	0.092